DESIGN, FABRICATION, TESTING, AND DELIVERY OF A SOLAR ENERGY COLLECTOR SYSTEM FOR RESIDENTIAL HEATING AND COOLING

By T. H. Holland and J. T. Borzoni

Prepared under Contract No. NAS8-31327 by
HONEYWELL INC.
Energy Resources Center
Minneapolis, Minnesota

for

NATIONAL AERONAUTICS AND SPACE ADMINISTRATION

ABSTRACT

This report describes the development of a low-cost flat-plate solar energy collector for the heating and cooling of residential buildings.

The objective of the collector design effort was to produce a solar collector capable of meeting specified performance requirements, at the desired system operating levels, for a useful life of 15 to 20 years, and to do it at the minimum cost, given state-of-the-art materials and technology. The primary consideration was to minimize costs rather than to provide performance in excess of the minimum system requirements.

The rationale for the design method was based on identifying possible material candidates for various collector components and then selecting the components which best meet the solar collector design requirements. The criteria used to eliminate certain materials were: performance and durability test results, cost analysis, and prior solar collector fabrication experience.

The collector determined to be the best design candidate was a two-sheet spot-and-seam welded steel absorber housed in a molded paper product box. The collector cover could have either one or two sheets of double strength glass mounted in an extruded aluminum frame. The absorber surface had an iron oxide selective coating with an organic overcoat.

This collector was built and tested, showing both ease of assembly and acceptable performance. It was discovered, however, that the overcoat material and the inner glass cover would not withstand the high stagnation temperature due to the superior insulation qualities of the housing. Two changes in the design are therefore recommended. The selective coating should be changed to black chrome and the cover glass should be tempered.

The total materials cost of the collector incorporating these recommended changes ranges from \$43.93/m^2 (4.08/ft^2) to \$30.69/m^2 (2.86/ft2), depending on production volume. Assembly costs should be fairly low due to collector simplicity.

Two recommendations are made regarding further development of the collector design. First, other overcoat materials for the iron oxide coating should be investigated to develop a coating which will increase absorptance into the .90 plus range while not raising the emittance to unacceptable levels, and yet still not degrade at high temperature. Secondly, in light of the insulating and cost advantages to be derived from the use of the processed paper housing, further development activity is recommended, particularly in the areas of determining useful life and additives for extending useful life.

TABLE OF CONTENTS

PRECEDING PAGE BLANK NOT FILMED

TABLE OF CONTENTS (CONCLUDED)

LIST OF ILLUSTRATIONS

LIST OF ILLUSTRATIONS (CONTINUED)

LIST OF ILLUSTRATIONS (CONCLUDED)

LIST OF TABLES

DESIGN, FABRICATION, TESTING AND DELIVERY OF A SOLAR ENERGY COLLECTOR SYSTEM FOR RESIDENTIAL HEATING AND COOLING

By T. H. Holland and J. T. Borzoni

Energy Resources Center
Honeywell, Inc.

SUMMARY

This is the final report describing the work performed for the NASA George C. Marshall Space Flight Center, Huntsville, Alabama, under Contract Number NAS8-31327, "Design, Fabrication, Testing, and Delivery of a Solar Energy Collector System for Residential Heating and Cooling."

This report describes the development of a low-cost flat-plate solar energy collector for the heating and cooling of residential buildings.

STATEMENT OF THE PROBLEM

Scope

All collector designs described in the literature seem to suffer from the same two major problems: cost, and reliability or life expectancy. Most all collectors on the market and projected for the market have questionable life expectancies. Corrosion between the absorber plate and heat transfer fluid, degradation of the absorber coating, housing durability, and degradation and breakage of the transparent covers are the most frequent life problems.

Performance, currently not a problem to obtain, is extremely important in that it, too, affects costs; that is, cost of the heat collected. For example, adding a selective black absorber coating and an anti-reflection coating to a two-glass-cover collector will increase the projected costs by 24 percent, but the collector will collect some 45 percent more energy.

Maintenance, aesthetics, and ease of installation and repair also greatly affect the use of solar systems. The task of this program has been to design a collector which satisfies the above criteria and is also cost-effective.

Requirements Analysis

The system requirements for the collector are those of the experimental solar conditioned "house" presently in operation at Marshall Space Flight Center. Briefly, the system is an equivalent 232 m^2 (2500 ft^2) conventional, single family residential load using a collector array of 120 m^2 (1300 ft^2) to provide space heating and cooling. Cooling is provided by a water fired 10.5 -kW (3 ton) ARKLA absorption air conditioner that requires an input flow of approximately 3.8 ℓpm (1 gpm) of water at a temperature of 99°C to 110°C (210°F to 230°F). Operation of both heating and cooling modes is from a 13600 - liter (3600 gallon) storage tank, with make-up heat provided by auxiliary conventional heaters. The present system is a single fluid (deionized water), two loop operation with the collectors coupled to the system by stratification levels in the storage tank.

The operating requirements, as applied to the collector, are to provide a nominal 122 kg/hr m^2 (25 lbm/hr ft^2) flow of outlet water at 94-110°C (201° - 230°F), with a 120 m^2 (1300 ft^2) array. The design conditions are to collect 1293 W/day m^2 (410 Btu/day ft^2) given an input of clear sky insolation on 21 June at 34° 45' N latitude, assuming a 45° collector tilt angle, a 16 kph (10 mph) wind, and an insolation level of 946 cosineα W/m^2 (300 cosineα Btu/hr ft^2), where α is the angle of incidence. The design ambient temperature is 27°C (80°F). This represents a collection efficiency, η, of 21.6 percent, integrated over the design day.

Design Objective

The objective of the collector design effort is to produce a solar collector capable of meeting the performance requirements, at the desired system operating levels, for a useful life of 15 to 20 years, and to do it at the minimum cost, given state of the art materials and technology. The primary consideration is to minimize costs rather than to provide performance in excess of the minimum system requirements. However, the contractor interprets this to mean life cycle costs, rather than first costs, and designed the collector to minimize the costs per unit of heat flux delivered over the life of the collector.

DESIGN PROGRAM

Introduction

The rationale for the design method is based on identifying possible material candidates for various collector components and then selecting the components which will best meet the solar collector design requirements. The criteria used to eliminate certain materials were: performance and durability test results, cost analysis, and prior solar collector fabrication experience.

Initial Design Activity

Based on our existing collector design experience and a re-examination of available literature regarding various collector types, it is our contention that the design objectives can best be met by a conventional flat plate collector design of a configuration similar to that shown in Figure 1; that is, a parallel-flow channel absorber with insulation behind and around the edges of the absorber, a box-like housing to hold the absorber and insulation, and a cover or covers suspended above the absorber.

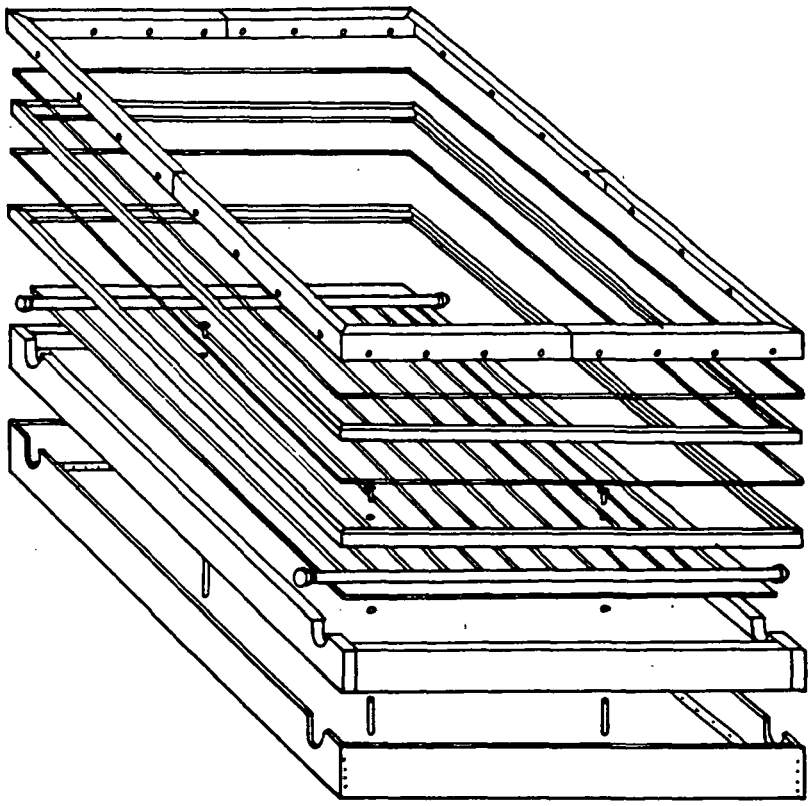

Figure 1. Flat-Plate Solar Collector Assembly

To generate a collector design of this type, the following component sections were isolated:

- Absorber panel
- Absorber coating
- Insulation

- Housing
- Cover system
- Interconnects

Design requirements, design considerations, and accompanying initial candidate materials or configurations for these six components are detailed in the following sections.

Absorber Panel

Design Requirements

The design requirements for the absorber panel are as follows:

- Operating temperature range up to 110°C (230°F)
- Maximum stagnation temperature of 232°C (450°F)
- Operating flow of 122 kg/hr-m^2 (25 lbm/hr-ft^2)
- Operating pressure of 1.7 x 10^5 nt/m^2 (25 psi)
- Temperature-cycling endurance between -29°C and 121°C (-20°F and 250° F)

Design Considerations

Absorber plate designs should consider the following minimum factors for an effective collector configuration:

- Absorber plate thermal performance
- Life
- Operating pressures, flow distribution in large arrays, and pumping power
- Fabrication and material costs

These factors are not mutually compatible, and trade-off studies in design have been necessary.

The initial preferred absorber panel candidates are presented below, followed by a discussion of each minimum factor for an effective configuration, covering what design approaches were taken to optimize the absorber plate design.

The initial absorber candidates were:

- Single steel sheet with triangular parallel flow (Figure 2)
- Single steel or aluminum sheet with staked circular steel or copper tubes (Figure 3)
- Current flat-plate collector design with larger flow passages (Figure 4)

The thermal performance analysis, as presented later in Appendix A, considers such design criteria as cross-tube size and spacing, absorber material and thickness, cross-tube flow rate and geometry, and header size.

Life. - To develop a reliable absorber (20 year life), consideration must be given to structural integrity, corrosion resistance in various environments, quality control during fabrication and installation, and general operating conditions such as pressure and pressure fluctuations, type of circulating fluid, and operating temperature. In addition, any coatings which must be applied should be economical to apply repeatably and have a long life span.

Steel, copper, and aluminum are likely candidates for absorber plate material. These plates can be homogeneous or formed from combinations of these materials. Each material has special properties which are optimum for some design parameters.

Fabrication processes determine to some extent the service life of a given absorber. Welding (spot or seam) of steel structures may leave carbide precipitation in the weld area. This would magnify corrosion effects, especially in "crevice" areas. Flexing of material due to the system's pressure fluctuations, coupled with the thinness of the material, may break the welded or bonded sections. Consideration has been given to fabricating collector plates on an assembly line basis with a minimum of individual components to minimize interconnects within the collector plate and reduce fabrication errors. Fabrication of copper, steel, and aluminum tubing is a well defined process and is highly reliable from a tolerance viewpoint.

Corrosion resistance of copper, aluminum, and steel to the operating environments of absorber plates must be considered. The use of water as a circulating fluid with the addition of ethylene glycol containing various inhibitors and buffers at elevated temperatures must be recognized for its corrosion protection properties. Ethylene glycol degrades in such service and forms organic acids. The accompanying reduction in pH tends to make the mixture more corrosive.

All components in the collector plate assembly were studied for galvanic corrosion between absorber plate components and between the absorber and other system components. Aluminum components should be galvanically isolated from components made of other metals, which tend to produce "heavy metal" ions. Otherwise the aluminum corrodes. This weighs heavily against using this metal as a fluid carrying element.

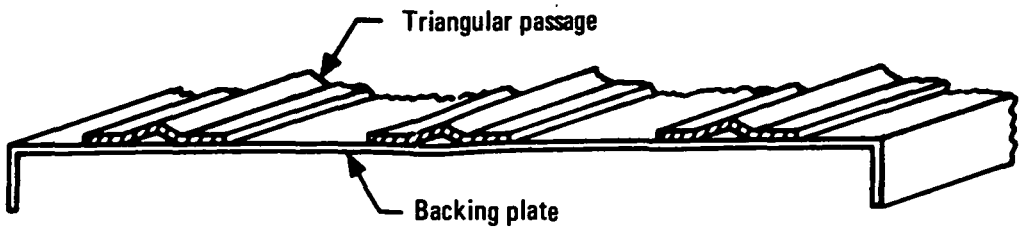

Typical cross section

Figure 2. Single Steel Sheet with Triangular Parallel Flow

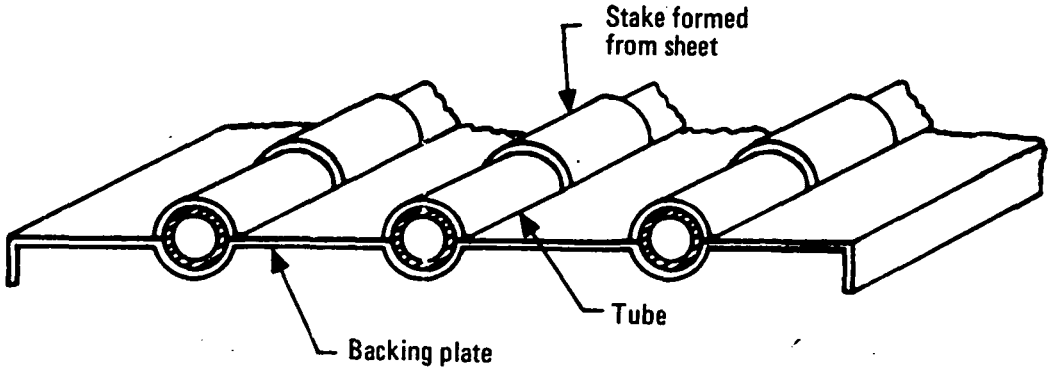

Typical cross section

Figure 3. Single Steel Sheet or Aluminum Sheet with Staked Circular Steel or Copper Tubes

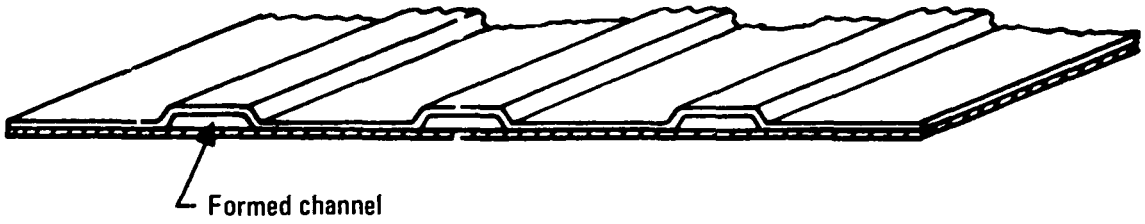

Typical cross section

Figure 4. Current Flat-Plate Collector Design with Larger Flow Passages

Operating Pressures and Flow Distribution. - Absorber plates operating at temperatures in excess of 104°C (220°F) with water as the circulating fluid will require greater than atmospheric pressures. Adding ethylene glycol raises the boiling point to 110°C (230°F) at atmospheric pressure, with a 50-50 water/glycol mixture.

Various flow channel configurations were analyzed for uniform flow distribution in arrays of series and parallel connections with regard to pumping energy and thermal efficiency. The collector system (thermal design) analysis described in Appendix A illustrates the analysis conducted on the steel panels designed and manufactured by the contractor. This analysis determined that channels of 1.3 mm x 6.4 mm (0.050 x 0.250-inch) were optimum from thermal and flow distribution standpoints; but, they appear not to be optimum for corrosion and particulate contamination when used.

Fabrication and Material Costs. - Fabrication costs were a major factor in the absorber plate design. Attention was given to designs which lend themselves to automatic fabrication and testing. Material costs vary, but it is obvious that as little copper and aluminum should be used as is consistent with good thermal design. The design should also consider the ease of installing the absorber plate into the collector assembly.

Material Candidates

The candidate materials evaluated include:

a. Internal-flow-tube type

   1. Aluminum roll bond
   2. Copper roll bond
   3. Steel sheets spot- and seam-welded together

b. Tube-and-plate type

   1. Copper tubes on copper plate
   2. Copper tubes staked, welded, soldered, or adhesively bonded to steel plate
   3. Steel channels copper-brazed to steel plate
   4. Stainless steel strips welded to steel plate

Nonmetallic absorber materials were considered. Various plastics appeared particularly attractive from a cost standpoint, but were generally unable to withstand the operating temperatures, particularly the expected stagnation temperature. Operating pressures are also a difficulty. It is felt that an extensive study program would be required to define a material, and several additional costly design techniques would have to be employed to enable the use of a plastic absorber for the program's application.

Design Trade-offs

Material choices for the absorber panel were limited to steel, aluminum/copper and steel/copper combinations due primarily to temperature constraints. Olin Brass presently manufactures both aluminum and copper Roll-Bond absorber panels. The copper, while attractive from a corrosion standpoint, is quite costly: $\$43.06/m^2$ ($\$4.00/ft^2$) for 0.10-cm (0.040-in) wall. The aluminum, while less costly, $\$7.86/m^2$ ($\$0.73/ft^2$) for 0.07-cm (0.030-in) wall, is expensive to electroplate for a selective absorber coating. It also can corrode, which has not yet been adequately explored. The spot- and seam- welded steel absorber panels are relatively inexpensive, and also permit using iron oxide for an absorber coating. The primary problem associated with the steel absorber panel designs is the development of a reasonable production process. There is also a mild corrosion problem between the plate surfaces that must be addressed. Fastening copper tubes to a steel plate is attractive because it practically eliminates the corrosion problem and still offers the use of iron oxide. It does, however, present a definite process development problem.

Recommended Design

The best choice for absorber material is steel, and the best associated design incorporates spot and seam welds. This assumes that a satisfactory production process can be developed. The design will make use of the thermal analysis in Appendix A to assure optimal absorber performance.

Absorber Coating

Design Requirements

The design requirements for the absorber coating may be summarized as follows:

- High solar absorptance
- Durability over collector life
- Temperature cycling endurance between $-29^{\circ}C$ and $121^{\circ}C$ ($-20^{\circ}F$ and $250^{\circ}F$)
- Low emittance (desired but not required)

Design Considerations

The absorber coating for a flat plate collector may be either selective or nonselective. If the collector application is solely for heating, then a nonselective coating might be preferable. Collector performance would be about the same with either type coating at low temperatures, but the nonselective coating may be less costly and more durable. If the collector is used for heating and cooling, then a selective coating would be preferable. Increased collector performance will more than offset the higher cost of high performance selective coatings.

The net amount of solar energy absorption depends on the optical surface properties of the absorber panel. Solar absorptance values of up to 95 percent can be achieved by simply blackening the absorber panel by painting, oxidizing, or anodizing; however, these surfaces also tend to have equally high emittance levels in the infrared, the wave length region where energy is emitted from the plate.

An improved type of surface preparation is the selective black solar absorber coating. This surface has a relatively high solar absorptance and a low infrared emittance. Most bare metals show roughly the behavior desired. They are all quite reflective in the infrared near 10μ, but much less so in the solar region. However, their solar absorptance is not strong enough to be used alone. The absorption of the metal can be greatly increased by overcoating it with a material with high absorption in the solar region, but transparent in the infrared. The metal substrate "shows through" in the infrared, so the emittance is not greatly increased.

One technique used to produce a selective coating is to coat the metal surface with an optical interference coating. If a single layer coating is so used, the coating thickness is such that light in the solar region of the spectrum which is transmitted through the coating and reflected off the metallic substrate interferes destructively with light reflected off the front surface of the coating. The coating thickness is minimal, approximately 0.1μ, so that infrared light does not "see" the coating, and the highly reflecting character of the metal substrate is retained.

Coating Candidates

Table 1 is a tabulation of selective coatings considered, including the absorptance and emittance of the various coatings and some estimation of the coating durability. The cost figures are an estimate of potential mass production costs, and do not represent firm data. (The various coatings are discussed in Appendix B.)

TABLE 1.- PROPERTIES OF COATING SUBSTRATES INVESTIGATED

Coating	Substrate	Absorptivity, α	Emissivity, ϵ	Durability		Estimated cost per ft^2 (see text)
				Breakdown temperature	Humidity degradation per MIL-STD-810B	
Black nickel on nickel	Steel or copper	.96	.07	>288°C (>550°F)	Variable	$ .30
	Aluminum	.96	.07	>288°C (>550°F)	Variable	.40 to 1.00
Black chrome on nickel	Steel or copper	.95	.09	>427°C (>800°F)	No effect	.15 to .35
	Aluminum	.96	.12	>427°C (>800°F)	No effect	.45 to 1.00
Black chrome	Steel	.91	.07	>427°C (>800°F)	Completely rusted	.10
	Copper	.95	.14	316°C (600°F)	Little effect	.10
	Galvanized steel	.95	.16	427°C (800°F)	Complete removal	.10
Black copper	Copper	.88	.15	316°C (600°F)	Complete removal	.10
Iron oxide	Iron	.85	.08	427°C (800°F)	Little effect	.05
Black paint	Any	.97	.97	---	---	.05
Honeywell selective paint	Any	.90	.30	---	---	.05
Permanganate treatment	Aluminum	.70	.08	---	---	.10
Organic overcoat on iron oxide	Iron with silicone	.89	.32	---	Poor adhering capability	.15
	Iron with EPM	.90	.20	149°C (300°F)	Little effect	.15
Organic overcoat on black chrome	Steel	.94	.20	149°C (300°F)	Little effect	.15

Design Trade-offs

In evaluating whether to use the more costly selective coating in preference to a cheap, nonselective coating, such as black paint, it is important to consider overall cost effectiveness in terms of total heat flux collected per dollar of coating cost.

Solar energy may well be collected more cost effectively if selective absorber coatings are used. Because cooling applications require high (110°C (230°F)) absorber plate temperatures, the infra-red energy emittance levels from black paint absorbers significantly impair collector effiency. The increase in collector performance due to the selective coating is shown in Figure 5.[1] The selective coating presented here is black nickel, with an absorptivity, α, of .95 and an emissivity, ϵ, of .06. The nonselective black absorber has an α of .97 and an ϵ of .95. As can be seen from Figure 5, if the collector operating parameters, t_{in}, t_{amb}, and Q_{inc}, are such that the collector operating point is out toward the right hand side of the operating curve, significant increases in collector effiency may be realized from using the selective coating. By integrating collector performance over an extended period, such as a full calendar year, it is possible to determine the average percentage improvement available from adding the selective coating. As long as the percent cost increase of adding the selective coating is less than the percent performance increase, the selective collector is more cost effective. Data taken from prior programs indicate that for most space heating and cooling applications, the selective coating is definitely cost effective. The tradeoff study presented in Appendix C, further illustrates the cost effectiveness of selective coatings.

Recommended Candidates

A selective iron/oxide coating, when augmented by an organic overcoat, has a solar performance capability nearly equal to that of selective black nickel, with significantly greater apparent durability and humidity resistance and half the expected cost. Iron oxide with an EPM organic overcoat is therefore the prime candidate for the absorber coating.

---

[1] Experimental Evaluation of Flat-Plate Collector Configurations. J.W. Ramsey, Honeywell Inc. Presented at NSF/RAAN Workshop of Solar Collectors for Heating and Cooling of Buildings, Nov. 21-23, 1974, New York, N.Y.

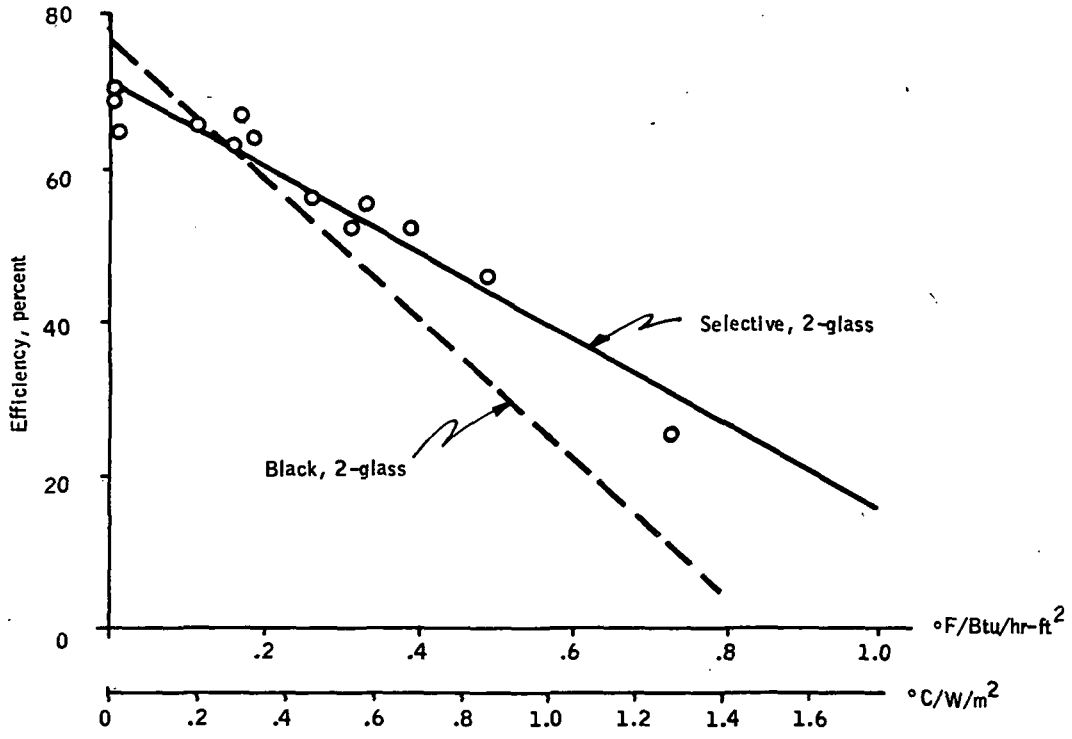

Figure 5. Selective Absorber - Two Glass Covers

Insulation

Design Requirements

The back surface of the collector absorber plate must be thermally insulated to minimize the amount of heat lost to the collector housing. The design requirements for the collector insulation are:

- Maximum temperature of 204°C (400°F)
- Temperature cycling endurance between -29°C and 121°C (-20°F and 250°F)
- Thermal conductance less than 0.57 W/m^2-°C (0.1 Btu/hr-ft^2-°F)
- Moisture-resistant

Design Considerations

In the construction industry, many insulation materials are available that can be used in the collector assembly for reducing heat losses. There are four basic types of insulation to consider:

- Mineral fiber
- Ceramic fiber
- Foamed glass and plastic
- Fiberglass

The mineral fibers and ceramic fibers are generally used for much higher temperatures and their costs are also generally much higher than fiberglass, which has comparable thermal conductivity. The exception would be mineral wool, which is a loose fill material giving a reasonably low thermal conductivity. However, this material tends to settle under its own weight, which eventually leaves an air gap behind the absorber panel and decreases the efficiency of the collector by increasing the heat loss from the absorber plates. Mineral wool also loses its insulation qualities if it is subjected to humidity cycling. This requires that the collector housing be hermetically sealed to prevent such cycling. A loose insulation would also be undesirable during repair or maintenance operations.

The lowest cost insulation available today is fiberglass, which is produced in a variety of densities (affecting thermal conductance) and a variety of binder conditions depending on the application. Manufacturers of regular building fiberglass insulation with a bakelite binder specify an upper use temperature of 177°C (350°F). When first heated above 177°C, the binder burns, giving off odor and fumes. If the fumes encountered in this burning of the binder are not objectionable, the material can be used to 371°C (700°F). The insulating value is not degraded at the higher temperatures, provided the material does not become compressed.

Fiberglass insulation with little or no binder is made specifically for higher temperature applications. Usually there is a small amount of binder which is allowed to burn off during the first heating of the insulated device.

The binder residue could collect on the collector covers, which would degrade the collector performance. To alleviate this possible problem area, a design consisting of two types of insulation could be used. Immediately behind the absorber plate, a high temperature, thin sheet of insulation would be used. An additional layer of low cost insulation would complete the design to give the desired thermal resistance to heat flow.

Material Candidates

Table 2 summarizes the insulations considered; the eventual choice was made from among these materials.

Design Trade-offs

The basis for selection was cost effectiveness, which was determined by the insulation thickness required for a desired minimum heat loss, and also cost per inch of additional box depth needed to hold this thickness of insulation.

In addition to reducing the heat loss during normal operations, the insulation must withstand the high temperatures when no heat is removed (e.g., no flow of the heat transfer fluid). The absorber plates of well-designed collectors can reach temperatures in excess of 204°C (400°F) when no heat is removed. This high temperature imposes severe restrictions on the use of some insulations. For example, the maximum temperatures allowable for urethane and polystyrene are 107°C (225°F) and 74°C (165°F), respectively.

Fiberglass best fits the design requirements in that most fiberglass blankets and boards have a maximum operating temperature of 232°C (450°F), and good durability with regard to temperature and humidity cycling.

Recommended Material

Based on cost and performance data, the fiberglass board insulations appear to offer the best combination of performance and cost. The loose fill types of insulation are significantly lower in cost; however, their tendency to settle, particularly when wet, is considered a significant deterrent to their use. Accordingly, we selected Certainteed Products K-231 and Owens-Corning 701 as the two alternate insulations.

Housing

Design Requirements

The physical and mechanical requirements for the collector housing are readily satisfied by several different types of materials. The maximum operating temperature anticipated is in the neighborhood of 121°C (250°F). The housing must be structurally sound, weather-tight, and fire resistant. It must also provide for mechanical connection to some sub-structure in order to be fastened into an array.

TABLE 2.- INSULATION CANDIDATES

Type	Name	Mfg.	$W/m^2-°C$	At mean temp. °C	Max. temp. °C	Structure	Required thickness for loss of 31.5 W/m^2 at T=71°C	$/$m^2$, 2.5 cm thick[c]	$/$m^2$ for 31.5 W/m^2 loss[c]	Weight, kg/m^3	K$/$m^2$, 2.5 cm thick[c]	K$ Ref.[c]
Fiberglass blanket	Pf-3340	O-C-	.0414	---	121	Blanket	11.7	.462	5.4	9.65	---	---
	PF-382	O-C	.0317	---	121	Blanket	8.9	---	---	48.2	---	---
	K-295	C-TP	.0577	93	232	Blanket	16.2	.440	7.13	12.8	2.54	.50
	K-242	C-TP	.0461	93	232	Blanket	13.0	.712	9.26	25.7	3.28	.65
	K-231	C-TP	.0418	93	232	Blanket	11.7	1.01	11.8	40.2	4.22	.84
Fiberglass board	730	O-C	.0533	93	232	Semirigid	15.0	---	---	---	---	---
	735	O-C	.0389	93	232	Semirigid	10.9	---	---	---	---	---
	701	O-C	.0490	93	232	Semirigid	13.7	.645	8.84	24.1	3.16	---
	703	O-C	.0432	93	232	Semirigid	12.2	1.21	14.8	48.2	5.23	---
	705	O-C	.0404	93	232	Semirigid	11.4	2.17	24.7	96.4	---	---
	812	JM	.0505	93	171[a] 121[b]	Semirigid	14.2	.732	10.4	25.7	3.69	.7
	814	JM	.0418	93	171[a] 121[b]	Semirigid	11.7	1.2	14.0	48.2	5.0	1.0
	817	JM	.0389	93	171[a] 121[b]	Semirigid	10.9	2.29	24.9	96.4	8.9	1.8
	Microlite	JM	.0692	93	171[a] 121[b]	Semirigid	20.0	.462	9.24	9.69	3.19	.6
	Microlite	JM	.0562	93	171[a] 121[b]	Semirigid	15.7	.7906	12.4	16.1	4.49	.9
	Microlite	JM	.0447	93	171[a] 121[b]	Semirigid	12.7	1.58	20.0	32.2	7.1	1.4
	850	C-TP	.0432	93	454	Semirigid	12.2	---	---	---	---	---
	IB-300	C-TP	.0432	93	232	Semirigid	12.2	.949	11.6	98.2	4.09	.8
	IB-600	C-TP	.0404	93	232	Semirigid	11.4	1.81	20.6	96.4	7.31	1.5
	Duct liner ultralite	C-TP	.0548	93	232	Semirigid	15.5	1.69	26.2	---	9.26	1.8
	B-005	JM	.0447	93	537.7	Blanket	12.7	2.09	26.5	24.1	9.34	1.9
	B-010	JM	.0403	93	537.7	Blanket	11.4	2.09	23.8	98.2	8.42	1.7
	Unbonded "B" fiber	JM	.0389	93	537.7	Blanket	10.9	2.09	22.8	72.9	8.13	1.6
	1000	JM	.0403	93	454	Semirigid	11.4	1.38	15.7	48.2	5.56	1.1
	Fesco board	JM	.0519	23.8	---	Rigid	14.7	1.30	19.1	160.8	6.75	1.3
Glass foam	Foam glass	P-C	.0548	23.8	492	Rigid	15.5	2.37	36.7	---	12.98	2.6
Mineral fibers												
Blanket	Mineral fiber	Eagle Picher	.0386	93	760	Blanket	10.9	---	---	128.6	---	---
Board	MT4	E-P	.0418	93	288	Semirigid	11.7	---	---	64.3	---	---
Board	MT10	E-P	.036	93	288	Semirigid	10.2	---	---	160.8	---	---
Board	Superglas	E-P	.0339	93	982	Semirigid	9.7	---	---	209	---	---
Block	PV super temp block	E-P	.0403	93	1037	Rigid	11.4	---	---	257.3	---	---
Block	HT block	48 Insul	.0548	148.8	982	Semirigid	15.5	7.86	121.8	385.9	43.1	8.5
Block	IV 1200	48 Insul	.0382	93	649	Semirigid	10.7	4.56	48.8	176.9	17.4	3.5
Block	Super caltemp	Pabco	.0494	93	649	Rigid	13.4	3.34	44.8	193	16.5	3.4
Loose	Mineral wool	Conwed	.0461	23.8	649	Loose fill	12.95	.161	2.08	32.2	.742	.15
Loose	Kaowool bulk	Babcock-Wilcox	---	---	---	---	---	---	---	---	---	---
Ceramic fibers (high-temp)												
Blanket	Blanket	B-W	.0577	204.4	1260	Blanket	16.3	6.35	103.5	48.2	36.6	7.3
Blanket	Blanket	B-W	.0404	204.4	1260	Blanket	11.4	17.0	103.8	128.6	68.7	13.6
Board	Kaowool M board	B-W	.0634	204.4	1315	Rigid	17.8	23.7	421.8	193 to 257	150.3	29.8
Block	Kaowool block	B-W	.0577	204.4	1260	Rigid	16.3	25.8	420.4	225 to 289	148.9	29.5
Block	Superglas	E-P	.0562	204.4	1260	Rigid	15.7	---	---	209 to 273	---	---
Foam	Ceramic foam	Dow	.0634	148.8	649	Rigid	17.8	---	---	128.6	---	---
Molded												
Min-K	503	JM	.0259	93	260	Rigid	7.37	---	---	241	---	---
	1301	JM	.0303	148.8	704	Rigid	8.64	---	---	321.6	---	---
Urethane		Owens Corning	.0216	23.8	107	Rigid	6.9	19.8	14.8	---	5.23	1.0

[a]Unfaced; [b]faced; [c]March 1975 prices

Design Considerations

The initial design consideration for a choice of solar collector housing is, in fact, whether or not to have a housing for each collector. The two candidate approaches are (1) to create collector modules, each containing one or more absorber panels, with each module completely enclosed by a housing and cover, and with discrete inlet and outlet plumbing either internal or external to the box; and (2) to create a collector array, consisting of a large backing plate covered with insulation, with all absorber panels mounted on the plate and insulation and plumbed together, and with a frame enclosing the edges of the backing plate and supporting a cover system that covers the entire collector array. Both approaches have distinctly salient features, yet both also have drawbacks significant enough to warrant a detailed examination of their impact on each specific collector application and its installation requirements.

In previously conducted experiments on the modular collector approach, heat loss through the sides of the housing were a major factor in poor collector performance. This loss component may be limited by reducing the heat path from the absorber to the housing (i.e., by increasing the insulation thickness, eliminating mechanical absorber supports that connect to the housing, or moving the sides of the housing away from the absorber panel).

Reflecting this experience back to the two housing approaches, the collector array approach has an advantage in large collector installations, since only the outside rows of the array have housing edges in close proximity, so edge loss should be reduced. Of course, if the collector module approach is used, edge losses could be reduced by designing the housing sufficiently larger than the enclosed absorber panel to accomodate several inches of insulation. This however, reduces the effective absorber area of the collector unit.

Apart from heat loss, the other major concern for evaluation of the candidate approaches is installation and maintainability, once installed. The collector array lends itself readily to integration into the roofline buildings, perhaps using the existing roof as a backing plate and thus requiring only a frame to support the cover system. A modular collector installation, however, would probably use a separate supporting frame work. This makes it well suited for ground installations and building installations where it is either not feasible or simply undesirable to use an existing roof.

During installation and subsequent collector maintenance is where the collector module approach shows a significant advantage. The collector array must be mounted from above, necessitating cranes or scaffolding; maintenance to the installed system must also be accomplished from above, unless ports are made in the backing plate, and that severely challenges the weatherproof integrity of the roof. Furthermore, if the cover sections are reasonably large, a disproportionate amount of effort must be expended to uncover and reach minor repair items, such as a leaking connection.

Material Candidates

The candidate materials considered to be viable alternatives include:

- Steel (folded sheet stock)
- Aluminum (folded sheet stock and also extruded wall)
- Various plastics (eigher molded or extruded)
- Composite wood products, including paper products (molded or pieced)

Material Trade-offs

Regardless of which housing system is chosen, the materials problem remains the same. The housing must be physically sound, durable, weatherproof, relatively light, nonflammable, and aesthetically appealing (or at least neutral), and reasonably priced. Wood or wood composites were considered. While they appear to have marginal durability, wood housing have the sufficient strength, heat resistance, and the cost effectiveness required of a reasonable design. A more likely candidate housing material, however, is sheet steel. It possesses the necessary strength, durability (particularly when galvanized), workability, and is cheaper than other potential metals. Its primary disadvantage is weight. Overall, however, mild steel appears, at present, to have the best potential as housing material, although formable wood composites will require further investigation.

Recommended Candidates

The baseline candidate for the collector housing was a sheet metal breadpan style box. The present cost estimates for a sheet metal box are less than $\$10.76/m^2$, ($\$1/ft^2$), including chromide treatment and painting. The principal disadvantages of the sheet metal box are its weight and potential corrosion problems, aluminum, plastic extrusion, and composites have been considered as housing candidates. Figure 6 presents one concept for a plastic extruded wall housing, adaptable for either one or two covers. This design concept requires a bottom plate, which could be of some cheaper materials, such as particle board. Supplier quotations were received for this particular design. The lowest bid was \$12.20/m (\$1.13/ft), not including the bottom plate. However, the plastic extrusion does include an ultraviolet inhibitor and fire retardant, and would require no external finishing. A similar extrusion of aluminum would also be possible, but at a significantly higher cost. A folded aluminum side with a wood bottom may be cost effective, however.

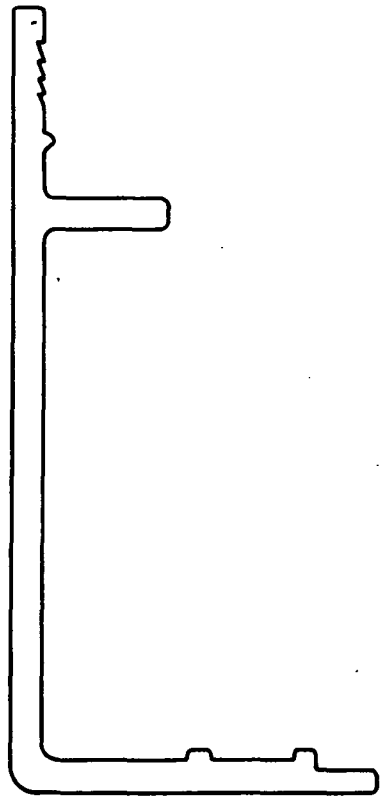

Figure 6. Cross-Sectional View of Extrusion

In addition to the sheet steel and extruded plastic housing examined, a molded processed paper product, similar to paper mache, was examined for use as a collector housing material. A potential supplier indicated that one piece housings could be molded for approximately $\$ 3.77/m^2$ ($\$.35/ft^2$). The advantages of this type of collector housing are obvious; not only is the material light in weight, but it also has fairly good insulating properties. The major concern is its ability to withstand weathering. The manufacturer of this product believes that a 15 year operational life is possible if the material is allowed to dry out periodically. This is a reasonable requirement for a roof-mounted collector array, providing air is allowed to circulate between the roof and collector. A low cost resin may be used to waterproof the housing if necessary. (A detailed structural analysis of the material is provided in Appendix D). Four housing designs were considered:

- Folded sheet steel
- Plastic pultruded sides, wood composite bottom
- Folded aluminum sides, wood composite bottom
- Molded paper product

Cover System

Design Requirements

The requirements of the cover system are summarized below:

- Self-supporting
- Transmission greater than 85 percent
- Minimum degradation from exposure to weather and vandals
- Abrasion-resistant
- Temperature-cycling endurance for -29°C to 121°C (-20°F to 250°F)

Design Considerations

The fundamental question in the design of the cover system is whether to use a single cover or multiple covers. Figure 7 compares the performance of a collector with a selective absorber and either one or two covers. For some operating points, the second cover produces significantly improved collector performance. The one cover, two cover, choice can best be made by once again comparing the performance equations over an extended operating period and examining the cost effectiveness of that second cover. (A detailed analysis of this trade-off can be found in Appendix C).

If a two cover system is selected, the choice of materials used for the two covers may be varied for each cover. The outer cover must provide structural strength, transmit a maximum amount of the incident solar energy, and limit re-radiation and convection losses. It should not be subject to degradation due to ultraviolet radiation; in fact, it is desirable that it be at least partially opaque to the ultraviolet component. The inner cover should also transmit as much of the incident radiation as possible, and limit convection and re-radiation losses. However, it needs only enough structural strength to be self-supporting, and if the outer cover serves as an ultraviolet filter, the inner cover does not have to be highly resistant to ultraviolet degradation.

Material Candidates

Three categories of materials were considered for a cover:

- Glass
- Self supporting plastic sheets
- Plastic films

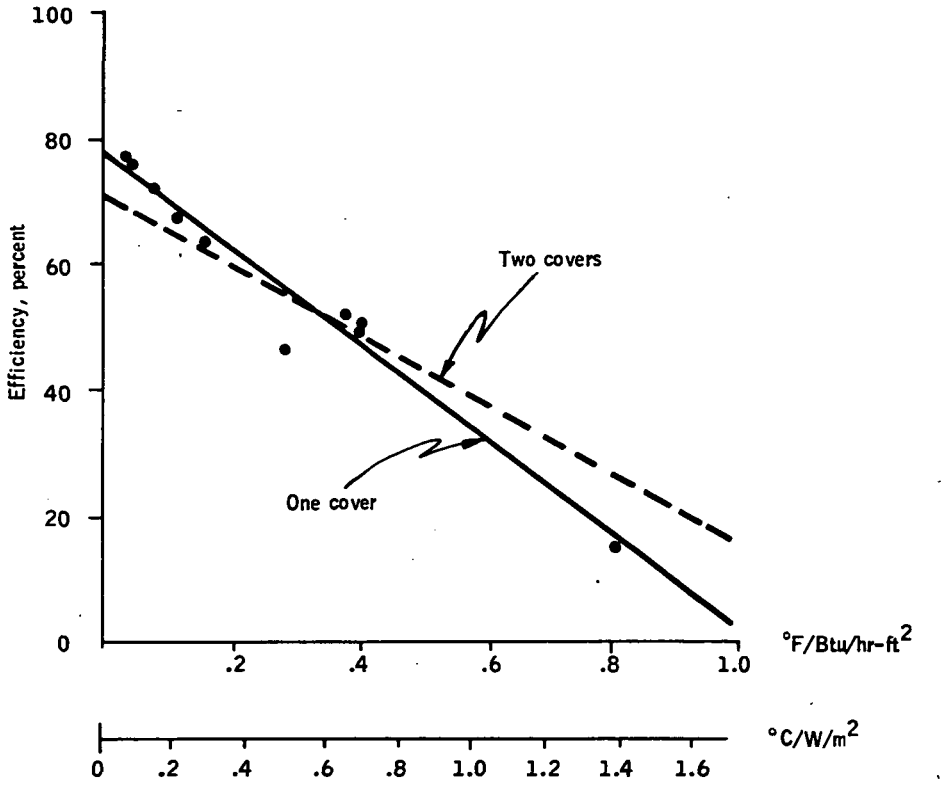

Figure 7. Black Nickel Coated Aluminum Absorber - One and Two Glass Covers

A glass cover achieves good transmission, generally in the range 85 to 88 percent, and in the case of thin, low iron glass, as high as 91 percent. Also, it is self supporting, weathers well, and is moderately priced. Glass is reasonably opaque in the infrared, thereby absorbing the long-wave reradiation emitted from the absorber panel. It is also resistant to ultraviolet radiation. In addition, glass is structurally strong and able to carry wind, rain and snow loads. It has two primary disadvantages: it is heavy and tends to shatter under the force of a well aimed projectile. Shatter resistance can be improved by using tempered glass, but this again increases costs. Another refinement is the use of the new glass etching process to minimize reflections. Etched glass can produce a transmission factor of 97 percent, but surface etching increases the collector's cost. Plastics are generally cheaper and not as heavy and breakable as glass, but most plastics tend to degrade with exposure to the ultraviolet, and, when ultraviolet inhibitors are used, the transmission is degraded. Also, most plastics are more expensive than glass, except in very thin sheets. Lexan, a polycarbonate, is highly shatter resistant and has fairly good transmission in the range of 84.5 to 88 percent. The surface is fairly soft, however, and will lose this transmission level due to both surface weathering and ultraviolet degradation.

Plexiglass has fairly high transmission in the solar wave length region; however, plexiglass is not very opaque in the infrared region. This effectively cancels the transmission advantage of plexiglass. Its softness reduces its desirability as an outer cover; however, it is self-supporting and may therefore be used as an inner cover. Caution must still be used, even if it is selected for an inner cover; when heated to 75°C (162°F), distortion can occur.

The plastic films are potentially attractive because of their low cost. They are, in general, not very durable when exposed to ultraviolet radiation; however, if used as an inner cover, ultraviolet durability may not be required. One major disadvantage in using plastic films is the need for supplementary support systems to stretch and hold the material in position. These support devices increase the costs of this type of cover. Properties of the plastic films, such as Mylar (a polyester) and Tedlar (a polyvinyl flouride), are included in Table 3 with the other candidate cover materials.

Design Trade-offs

Previous reports have suggested that glass substitutes, such as plexiglass or Lexan, may be desirable cover materials for collector use. Their primary appeal is in their shatter resistance, breakage being recognized as the most significant drawback to glass covers. Weight considerations also make non-glass covers a desirable choice. On the negative side, however, most of glass substitutes exhibit lower transmission in the solar spectrum than do glass covers and are also subject to both physical and optical degradation, due to ultraviolet exposure and normal weathering.

To evaluate the trade-off between the positive and negative attributes of the glass substitutes, it was necessary to quantify the optical and physical differences between the various potential cover materials. The solar transmission was examined by taking direct insolation readings with an Eppley Pyrheliometer, both with and without a window, of each candidate cover material and comparing the millivolt output of each measurement. Table 4 presents the results of this test for 16 potential cover materials, including glass and Tedlar. An opaque black surface was also measured to provide a reference level. The data indicates several materials that have solar transmission levels within 5 percent of FOURCO low-iron glass. Three of these plastic materials were tested for direct solar transmission before and after a two month solar exposure test using an Eppley Normal Incidence Pyrheliometer. The test was made at Desert Sunshine Laboratory in Phoenix, Arizona. (The materials and test results are given in Table 5.) These results show that the plastic materials degraded significantly during the two month test.

TABLE 3.- PROPERTIES OF COVER MATERIALS

Material	Solar transmittance, %	Cost $/m^2	Thickness, cm	Weight, kg/m^2	Temperature endurance, °C	Bearing strength, kg/cm^2	Manufacturer
Ordinary glass	90	2.91	.23	5.8	177	NA	FOURCO
Tempered glass	88	4.31	.43	11.6	177	NA	FOURCO
Tempered and etched glass	94	8.61	.43	11.6	177	NA	FOURCO, Honeywell
Tedlar	92	1.08	.005	0.3	204	703	DuPont
Plexiglass DR	89	10.76	.64	7.32	82	380	Rohm & Haas
Lexan	85 to 88	9.15	.32	3.81	60	703	General Electric
Lascolite	86	4.31	.15	1.22	NA	2109	LASCO
Sunlite premium	86	4.09	.10	1.53	60	1195	Kalwall Corp.
Lumasite	NA[a]	6.46	.15	1.98	110	879	American Acrylic
Mylar S	NA	0.11	.005	0.08	121	NA	DuPont
Polyethylene, high-density	NA	2.15	.051	0.5	66	352	---

[a]NA = Not available.

TABLE 4. - SOLAR TRANSMISSION OF SELECTED COVER MATERIALS

Sample No.	Material	Transmission, %	Reading, mV			Remarks
			Sample window	No window, before	No window, after	
1	Fiberglass	83.8	6.8 to 6.9	8.1 to 8.2	8.2	
2	Kal-lite premium	89.3	7.1	7.9	8.0	
3	Kal-lite regular	89.4	7.4	8.3	8.2 to 8.3	
4	Lascolite	86.4	7.1 to 7.2	8.3	8.2 to 8.3	
5	Duo-wall	81.9	6.8	8.3 to 8.4		Vertical
		84.3	7.0		8.2 to 8.3	Horizontal
6	Fiberglass	80.5	6.8	8.5	8.4	
7	Plexiglass	89.8	7.5	8.4	8.3	
8	Cyanamid acrylic	92.3	7.8	8.4	8.4 to 8.5	
9	Plexiglass II UVA	88.8	7.5 to 7.6	8.2 to 8.3	8.2 to 8.3	
10	Lexan	86.1	7.1 to 7.2	8.3 to 8.4	8.2	
11	0.035-in. Lumasite	88.5	7.3	8.2	8.2 to 8.3	
12	0.050-in. Lumasite	92.1	7.5 to 7.6	8.3	8.1 to 8.2	
13	Corrugated Lascolite/Tedlar	83.6	6.6 to 6.7	7.9	8.0	Vertical T↓
		88.4	6.8 to 6.9	8.0	7.7 to 7.8	Horizontal
		85.0	6.6 to 6.7	7.7 to 7.8	7.9	Vertical T↑
		87.7	6.9 to 7.0	7.9	7.9 to 8.0	Horizontal
14	FOURCO glass	96.0	7.2 to 7.3	7.5 to 7.6	7.5 to 7.6	
15	Tedlar	95.0	7.5 to 7.6	7.9 to 8.0	7.9 to 8.0	
16	Sunlite	90.7	6.8 to 6.9	7.5 to 7.6	7.5 to 7.6	
17	Black surface	2.6	0.2	7.6	7.6 to 7.7	

TABLE 5.- PLASTIC SOLAR EXPOSURE TESTS[a]

Sample no.	Material	Before test					After test			Average degradation, %
		Direct solar transmission, %	Reading, mV			Direct solar transmission, %	Reading, mV			
			Sample window	No window			Sample window	No window		
				Before	After			Before	After	
2	Kal-lite premium	89.3	7.1	7.9	8.0	72.5	3.7	5.1	5.1	22.8
						67.2	4.5	6.7	6.7	
8	Cyanamid acrylic	92.3	7.8	8.4	8.4 to 8.5	81.9	4.2	5.1	5.1 to 5.2	11.2
						82.1	5.5	6.7	6.7	
12	1.3-mm (0.050-in.) lumasite	12.7	0.8 to 0.9	6.7	6.7	11.8	0.6	5.1	5.1	15.4
						9.7	0.7 to 0.6	6.7	6.7	

[a] *All measurements taken with Eppley Normal-Incidence Pyrheliometer.*

Material Candidate

The transmission tests on various cover materials indicated that none of the plastics had as high a transmission as the low iron glass. Further tests verify that plastic materials degrade under solar exposure and could never be expected to last the entire design life of the collector. Glass is therefore the chosen cover material, to ensure continued environmental protection without loss of transmission quality.

Interconnects

Design Requirements

Collector design efforts should consider the following problem areas in addressing collector interconnects:

- Fluid connections/leakage
- Repair or removal of collectors

The design criterion for a fluid connection is of course that it will not leak. It should be made of materials which will not be affected by thermal cycling, the collector fluid, or weather conditions, including ultraviolet exposure.

Design Considerations

The collector design should emphasize the capability of removing a faulty collector and replacing it with a new unit, as well as the ability to repair collector covers on site. Environmental effects and accessibility of collectors in large arrays make on site repairs difficult and costly. Removal of the entire collector unit would simplify collector design in that emphasis could be placed on sealed collectors without the constraints of on site repair.

Material Candidates

Possible material candidates are:

- Rubber hose and clamp
- Hard copper tubing plumbing connections
- Flexible metal hose with hard connections
- Hard soldered connections

Material Trade-offs

Regardless of the internal/external header configuration selected, one observation is relevant. The connections between collector and system should be hard connections. They may be welded, sweated, or flexible metal hose with swivel fittings, but they should not be rubber hose and clamp fittings. The hose tends to take a set and, at the operating temperatures and pressures encountered in a solar installation, constant clamp tightening is required to prevent leaks.

Fluid connections to a main header should be outside of the collector box. This would permit easier installation and removal of an individual collector, and any leak would be easier to detect.

Recommended Design

Individual connections should be semi-permanent screw type fittings or silicone "O" -ring and screw type fittings of noncorrosive material.

Candidate Collector Designs

Final Material Options

The various collector component materials were evaluated in detail and the selected materials are summarized below:

a. Absorber Options

1. Spot and seam welded steel sheets
2. Steel channel strips copper-brazed to a steel sheet

b. Absorber Coating Options

1. Black chrome over bright nickel on a steel absorber
2. Black chrome directly on steel
3. Iron oxide and an organic overcoat on a steel absorber

c. Insulation Options

1. Semi-rigid fiberglass board

d. Collector Housing Options

1. A one-piece molded paper product pan with an extruded aluminum cover frame.

2. Folded aluminum sheet sides bonded to a chipboard base with an extruded aluminum cover frame

3. Pultruded 70 percent glass-filled polyester (fiberglass) sides bonded to a chipboard base with a pultruded 70 percent glass filled polyester cover frame

4. A folded sheet steel pan with a three-piece folded sheet steel cover frame assembly

e. Glazing Options

1. Low-iron, double-strength glass, either one or two sheets

2. Kalwall Sunlite Premium

3. Tedlar

The list represents the starting point from which the candidate collector designs were generated. During the course of the design process, several of the above listed material options were also eliminated. The collector component areas affected by this further reduction of material choices were the absorber coating and the glazing.

In evaluating whether to use black chrome or iron oxide as the selective absorber coating in the candidate collector designs, the long term production potential was chosen as the primary consideration. Although black chrome performs somewhat better than iron oxide, it is believed that the electroless dip and organic coating required in the iron oxide process will be sufficiently cheaper than the black chrome electroplate process such that iron oxide will be more cost effective, despite its lower performance. This is particularly true if it continues to be necessary to use a nickel undercoat for rust protection with the black chrome.

Using either Kalwall Sunlite or Tedlar for collector glazing involves some definite cost and/or performance penalties. The Kalwall Sunlite is significantly lower in solar transmission than low iron glass. Tedlar has a good solar transmission, but is not self supporting. Special design considerations must be made for either a support structure or some type of stretching frame; both of these approaches add costs to the collector design. Low iron glass collector glazing has good solar transmission and is self supporting, at least in short spans required for a collector. It is also heavy and subject to breakage; however, it still represents the best compromise presently available for collector glazing.

Candidate Collector Designs

Given the material options listed above, four different collector designs were generated, each design using a different collector housing option. Figures 8 through 11 illustrate the four candidate designs. A description of each design follows.

Design I -- This design consists of a folded sheet metal box with U-channel glass spacer and aluminum cover bracket. The sheet metal collector box is folded up and spot welded in the corners. The absorber is mounted on phenolic rod stand-offs and fastened to the box bottom. The inner glass cover is placed on the bracket lip and then a U-channel spacer is placed on the glass. A second glass cover is placed on the spacer frame and the entire assembly held down by the top aluminum cover bracket which is attached with sheet metal screws to the box walls. Butyl rubber tape is used on all glass/metal interfaces. Semi-rigid fiberglass is placed behind and around the absorber plate for insulation (A cross section is shown in Figure 8).

Design II -- This design has an aluminum box with an extruded aluminum cover frame and chipboard bottom. The box consists of folded sheet aluminum sides heli-arced together in the corners and glued to a chipboard bottom. The cover assembly has an extruded aluminum frame with two sheets of 0.39 cm (5/32 in.) low iron glass pressed into the frame using polyvinyl chloride (PVC) U-shaped glazing material. The frame is secured at the corners with self tapping sheet metal screws. The absorber is structurally fastened to the base with phenolic rod standoffs and machine screws. The insulation is semi-rigid fiberglass, which surrounds the absorber panel on the back and sides. The cover assembly snaps into the box by using a resilient PVC weather stripping bead and stamped out aluminum teeth in the box side which fit into a channel in the cover frame extrusion. (A cross section of this design is shown in Figure 9.)

Design III -- This design features a pultruded plastic box and cover frame with a chipboard bottom. Pultruded 70 percent glass filled polyester sides are glued together and to a chipboard base. The cover frame is also a pultrusion which holds two sheets of glass with U-shaped PVC glazing material. The absorber panel is mounted on the chipboard backing with phenolic rod stand-offs using machine screws. Semi-rigid fiberglass insulation is used behind and on the sides of the absorber panel. The top cover assembly is placed in the box and secured with pop rivets. A butyl rubber sealing strip is used between the pultruded plastic sub-assemblies for weather stripping. (A cross section of this design is shown in Figure 10.)

Design IV -- This design consists of a processed paper box with an extruded aluminum cover frame. A molded paper product is used as the collector box. The cover frame is extruded aluminum and carries all of the structural loads. The box only holds insulation around the absorber panel and provides a weather and thermal barrier. PVC glazing strips

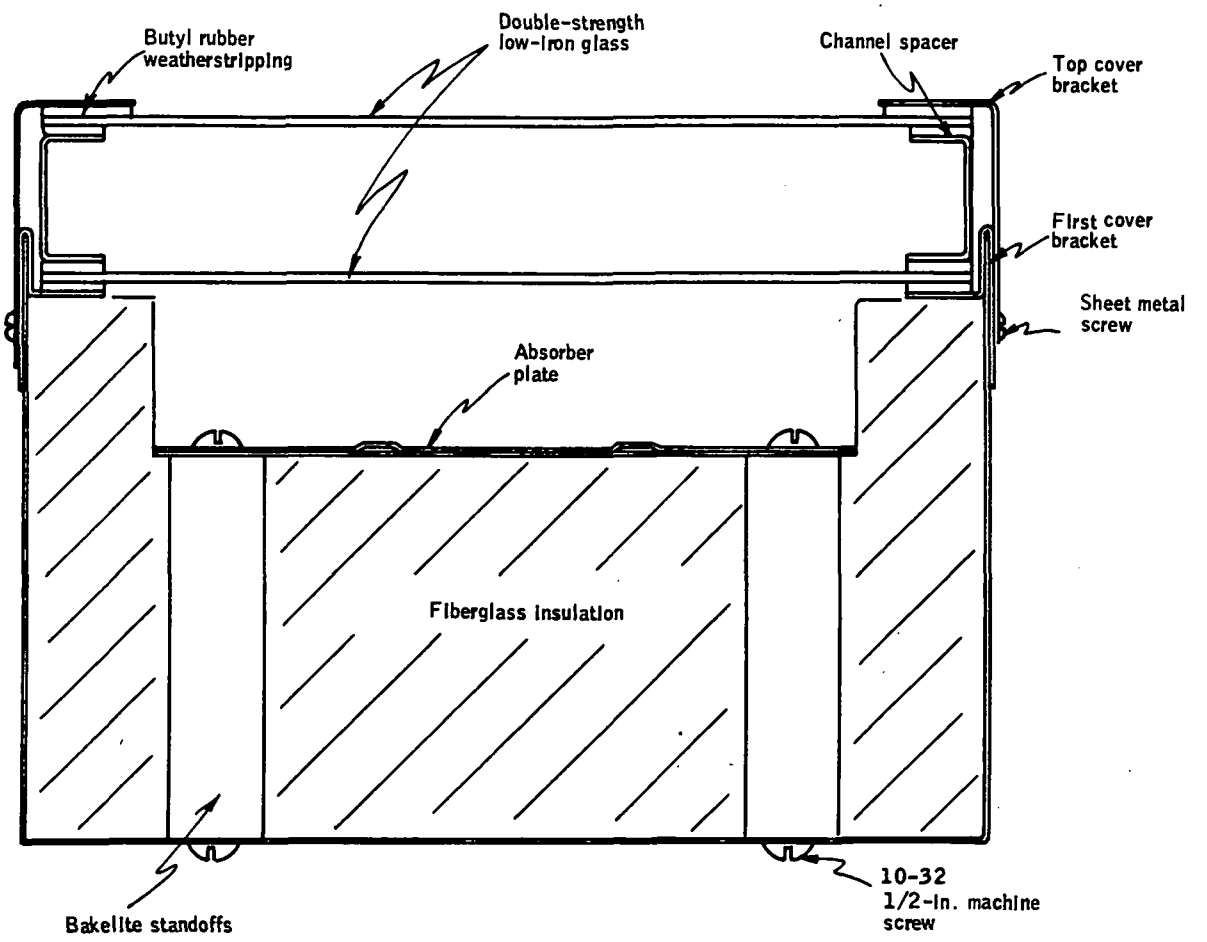

Figure 8. Design I. - Folded Sheet Metal Box with U-Channel Glass Spacer and Aluminum Cover Bracket

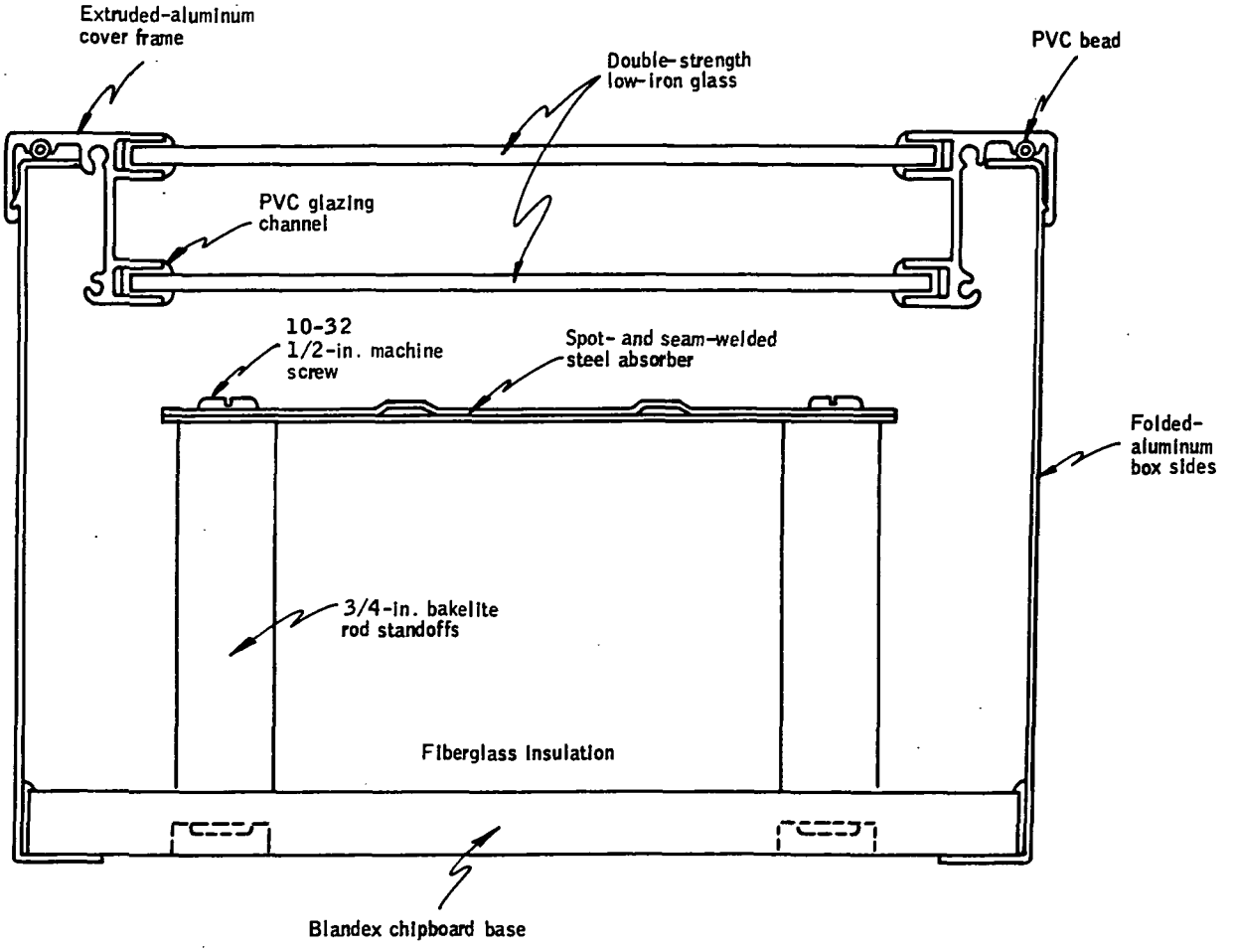

Figure 9. Design II. - Folded Aluminum Box Sides with Extruded Aluminum Cover Frame and Chipboard Bottom

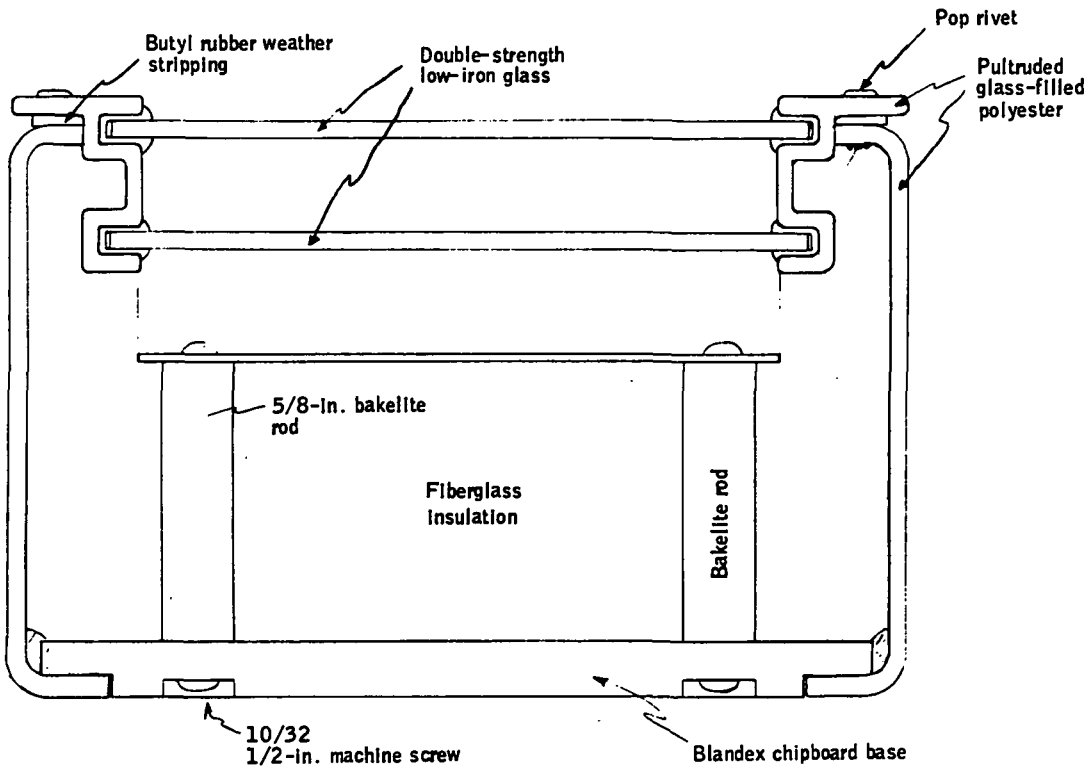

Figure 10. Design III. - Pultruded Plastic Box and Cover Frame with Chipboard Bottom

hold the two glass lites in the aluminum frame, and the assembled cover is secured at the corners with self tapping sheet metal screws. Insulating absorber stand-offs are either held by the aluminum cover frame, or the absorber mounting clips are run between the paper box and aluminum cover assembly and fastened to the collector mounting structure. (This design cross section is shown in Figure 11.)

Each of the four designs has some distinct advantages and disadvantages. Design I, the sheet steel collector, is similar in design to those built previously. There is fabrication and assembly experience reflected in the design. However, experience also indicates that the assembly costs will be high because of the multitude of piece parts. Design II, the sheet aluminum/chipboard collector, is more readily fabricated than Design I, but the technique for fastening the cover to the pan is still unproven. Design III, the fiberglass collector, is light weight and durable, but is the costliest material. Design IV, the molded paper product collector, has the lowest material cost, but may have durability problems.

Cost Analysis of Candidate Designs

Costs should be an important factor in deciding on the design. The costs of each collector design can be broken into two categories: material and assembly labor. Fabrication labor can be considered a part of the cost of materials. Tables 6 through 9 indicate the bill of materials and the associated costs per collector for each of four production levels. The four production levels considered are 929 m^2 (10 000 ft^2), 9290 m^2 (100 000 ft^2), 92 900 m^2 (1 000 000 ft^2) and 464 500 m^2 (5 000 000 ft^2). The collector size considered here is 0.01 m x 1.22 m (3 ft x 4 ft), and all costs quoted in the tables are for sufficient quantity of each item to complete one collector. The total cost of materials per collector is listed below the last item on each material list.

The material costs vary somewhat between designs, depending upon which production level is used. However, in general, the range is only $ 6 to $ 7 on a $30 to $40 per unit cost. This amount of material cost variation is not sufficient to recommend one of the four designs on material costs alone. The assembly labor content of each design must also be considered. It is difficult to place a dollar value on the labor in the assembly of each design, but in relative terms, as determined by counting the number of assembly operations required for each design, it appears the Design IV, the molded paper product collector, will have the least assembly labor content. Since Design IV also has the lowest cost for materials, it appears reasonable that this will be the lowest cost collector. Furthermore, since all four designs are essentially equal from the standpoint of thermal performance, Design IV should also be the most cost effective collector.

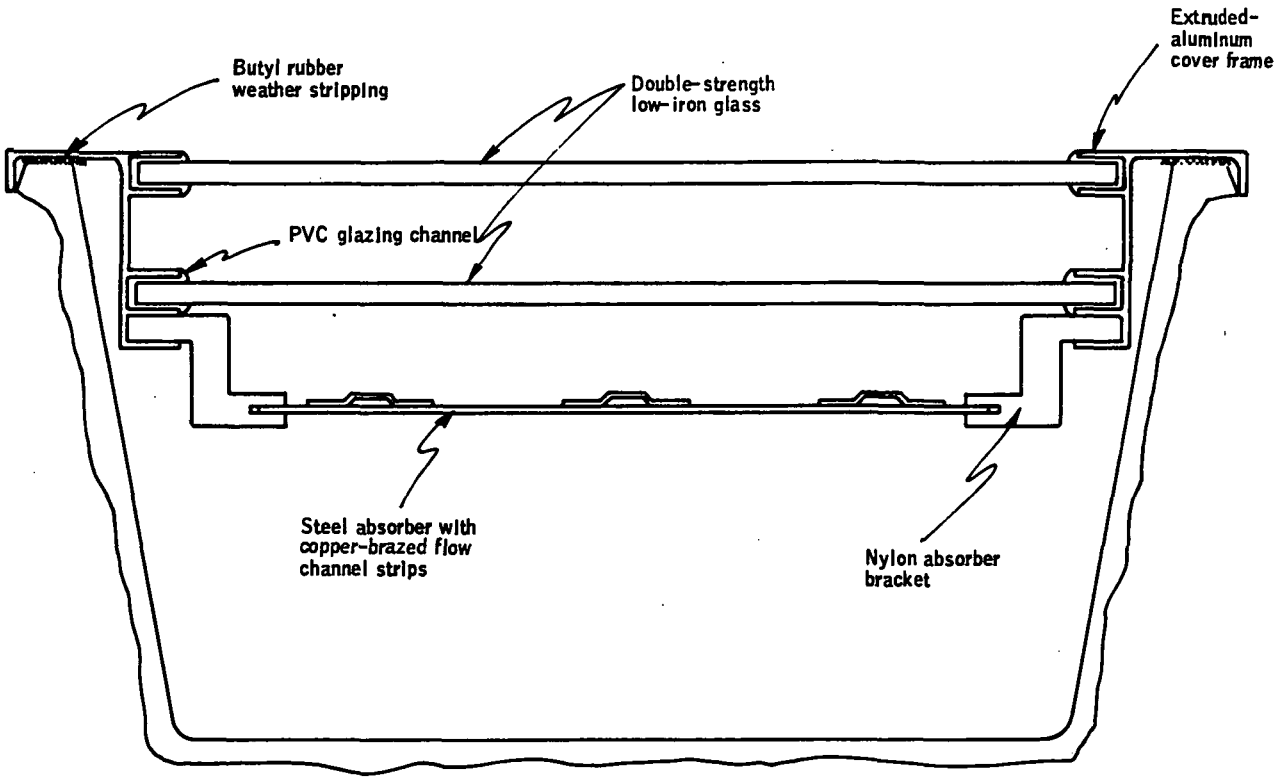

Figure 11. Design IV. - Processed Paper Box with Extruded Aluminum Cover Frame

TABLE 6. - DESIGN I COST SUMMARY

Item	Quantity	Part	Extension, $/unit)			
			929 m^2 (10 000 ft^2)	9290 m^2 (100 000 ft^2)	92 900 m^2 (1 000 000 ft^2	464 500 m^2 (5 000 000 ft^2
1	1 ea.	Box	$ 7.63	$ 6.36	$ 4.20	$ 4.20
2	14 ft	Inner cover bracket	2.88	2.40	1.20	1.20
3	14 ft	Glass spacer	2.88	2.40	1.20	1.20
4	14 ft	Outer cover bracket	2.88	2.40	1.20	1.20
5	2 lites	Glass*	6.60	6.60	6.60	6.60
6	56 ft	Weather stripping	0.49	0.48	0.46	0.46
7	32 ea	Cover screws	0.10	0.10	0.10	0.10
8	4 ea	Absorber standoffs	0.63	0.57	0.51	0.46
9	8 ea	Absorber standoff screws	0.03	0.03	0.03	0.03
10	37.1 bd ft	Insulation	0.41	0.41	0.33	0.33
11	---	Absorber plate	16.14	13.56	11.47	9.60
12	---	Box undercoat and paint	1.80	1.80	1.20	1.20
13	---	Absorber* coating	3.00	2.76	1.92	1.92
Total cost of materials per collector			$45.47	$39.87	$30.35	$28.50

*Substitution of black chrome/bright nickel coating for iron oxide and tempering the cover glass will result in a net increase in total material cost per collector according to the following schedule:

Yearly volume	10 000 ft^2	100 000 ft^2	1 000 000 ft^2	5 000 000 ft^2
Additional cost of coating	8.40	8.64	4.08	4.08
Additional cost of tempering glass	1.68	1.68	1.68	1.68

TABLE 7. - DESIGN II COST SUMMARY

Item	Quantity	Part	Extension, $/unit			
			929 m^2 (10 000 ft^2)	9290 m^2 (100 000 ft^2)	92 900 m^2 (1 000 000 ft^2)	464 500 m^2 (5 000 000 ft^2)
1	14 ft	Box sides	$4.57	$4.38	$4.19	$4.01
2	14 ft	Cover frame extrusion	1.68 2.24	1.68 2.24	1.68 2.24	1.68 2.24
3	14 ft	Weather stripping	0.72	0.59	0.46	0.33
4	28 ft	Window glazing	0.49	0.48	0.48	0.48
5	4 ea	Absorber standoffs	0.63	0.57	0.51	0.46
6	8 ea	Cover frame screws	0.03	0.03	0.03	0.03
7	8 ea	Absorber standoff screws	0.03	0.03	0.03	0.03
8	1 ea	Absorber plate	19.90	16.72	14.06	11.84
9	2 lites	Glass	6.60	6.60	6.60	6.60
10	37.1 bd ft	Insulation	0.41	0.41	0.33	0.33
11	1 ea	Box bottom	1.20	1.20	0.96	0.96
12	---	Absorber* coating	3.00	2.76	1.92	1.92
Total cost of materials per collector			$41.50	$37.69	$33.49	$30.91

*Substitution of black chrome/bright nickel coating for iron oxide and tempering the cover glass will result in a net increase in total material cost per collector according to the following schedule:

Yearly volume	10 000 ft^2	100 000 ft^2	1 000 000 ft^2	5 000 000 ft^2
Additional cost of coating	8.40	8.64	4.08	4.08
Additional cost of tempering glass	1.68	1.68	1.68	1.68

TABLE 8. - DESIGN III COST SUMMARY

Item	Quantity	Part		Extension, $/unit		
			929 m^2 (10 000 ft^2)	9290 m^2 (100 000 ft^2)	92 900 m^2 (1 000 000 ft^2)	464 500 m^2 (5 000 000 ft^2)
1	14 ft	Box side	$8.96	$8.96	$7.84	$7.84
2	14 ft	Cover frame pultrusion	6.44	6.44	5.46	5.46
3	14 ft	Weather stripping	0.58	0.48	0.46	0.46
4	28 ft	Window glazing	0.49	0.48	0.48	0.48
5	4 ea	Absorber standoff	0.63	0.57	0.51	0.46
6	1 ea	Box bottom	1.20	1.20	0.96	0.96
7	8 ea	Absorber standoff screws	0.03	0.03	0.03	0.03
8	1 ea	Absorber plate	16.14	13.56	11.40	9.60
9	37.1 bd ft	Insulation	0.41	0.41	0.33	0.33
10	2 lites	Glass	6.60	6.60	6.60	6.60
11	---	Absorber* coating	3.00	2.76	1.92	1.92
Total cost of materials per collector			$44.83	$41.84	$36.29	$34.44

*Substitution of black chrome/bright nickel coating for iron oxide and tempering the cover glass will result in a net increase in total material cost per collector according to the following schedule:

Yearly volume	10 000 ft^2	100 000 ft^2	1 000 000 ft^2	5 000 000 ft^2
Additional cost of coating	8.40	8.64	4.08	4.08
Additional cost of tempering glass	1.68	1.68	1.68	1.68

TABLE 9. - DESIGN IV COST SUMMARY

Item	Quantity	Part	Extension, $/unit			
			929 m^2 (10 000 ft^2)	9290 m^2 (100 000 ft^2)	92 900 m^2 (1 000 000 ft^2)	464 500 m^2 (5 000 000 ft^2)
1	1 ea	Processed paper box	$3.66	$3.18	$2.96	$2.85
2	14.2 ft	Cover frame extrusion	1.68 2.24	1.68 2.24	1.68 2.24	1.68 2.24
3	14 ft	Weather-stripping	0.58	0.48	0.46	0.46
4	28 ft	Window glazing	0.49	0.48	0.48	0.48
5	6 ea	Absorber brackets	0.30	0.24	0.18	0.18
6	8 ea	Cover frame screws	0.03	0.03	0.03	0.03
7	1 ea.	Absorber plate	19.90	16.72	14.06	11.84
8	2 lites	Glass	6.60	6.60	6.60	6.60
9	33.4 bd ft	Insulation	0.38	0.38	0.30	0.30
10	---	Absorber* coating	3.00	2.76	1.92	1.92
Total cost of materials per collector			$38.86	$34.79	$30.91	$28.58

*Substitution of black chrome/bright nickel coating for iron oxide and tempering the cover glass will result in a net increase in total material cost per collector according to the following schedule:

Yearly volume	10 000 ft^2	100 000 ft^2	1 000 000 ft^2	5 000 000 ft^2
Additional cost of coating	8.40	8.64	4.08	4.08
Additional cost of tempering glass	1.68	1.68	1.68	1.68

Recommended Collector Design

The recommended collector design was a steel absorber with copper brazed flow channel strips supported from an extruded aluminum cover frame by nylon brackets. The cover frame contained two sheets of 0.39 cm (5/32 in.) low iron glass, sealed with a PVC glazing channel. The absorber was backed by 7.5 cm (3 in.) of semi-rigid fiberglass insulation, and the complete absorber/cover assembly was housed in a one piece, molded paper product pan. This design had a fairly low material cost, ranging from \$34.88/m^2 (\$3.24/ft^2) to \$25.64/m^2 (\$2.38/ft^2) depending upon the production level, and appeared to have a fairly low assembly labor cost.

The recommended design was accepted by NASA project personnel with some suggested modifications: (1) redesign of the absorber brackets to enable cover assembly to be removed without disturbing the absorber; (2) routing of the absorber plumbing out the ends of the collector rather than the back; (3) changing the absorber to a two-sheet, spot and seam welded steel design.

The question of whether to use a one cover or two cover system for the collector was not satisfactorily resolved. Consequently, both a one cover and a two cover version of the collector were fabricated and tested within the course of the program. The final designs for the one and two cover collectors are shown in Figures 12 and 13, respectively.

The glazing material to be used in Design IV is double strength FOURCO Clearlite glass. Other glazings may be used in the same aluminum cover frame by using different spline sizes. The following summarizes the glazing material which have been tried in the cover frames with different spline sizes:

- Plastics up to 1.3 mm (0.050 in.) thick
- Single-strength glass 3.3 mm (0.130 in.) thick
- Double-strength glass 3.3 mm (0.130 in.) thick
- Glazings 3.8 mm to 4.4 mm (0.150 to 0.175 in.) thick

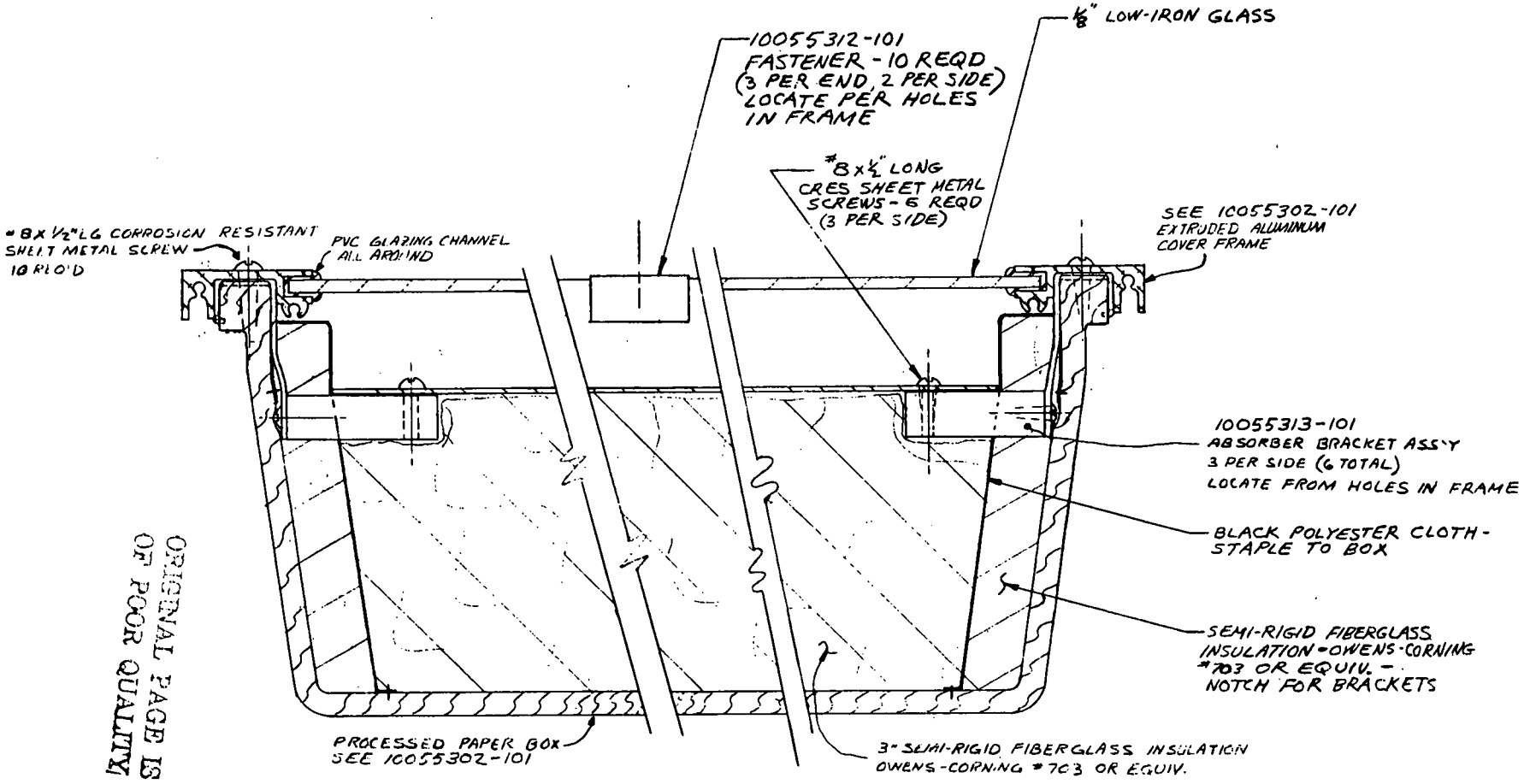

TYPICAL CROSS SECTION

Figure 12. MSFC Single-Glass Collector Assembly

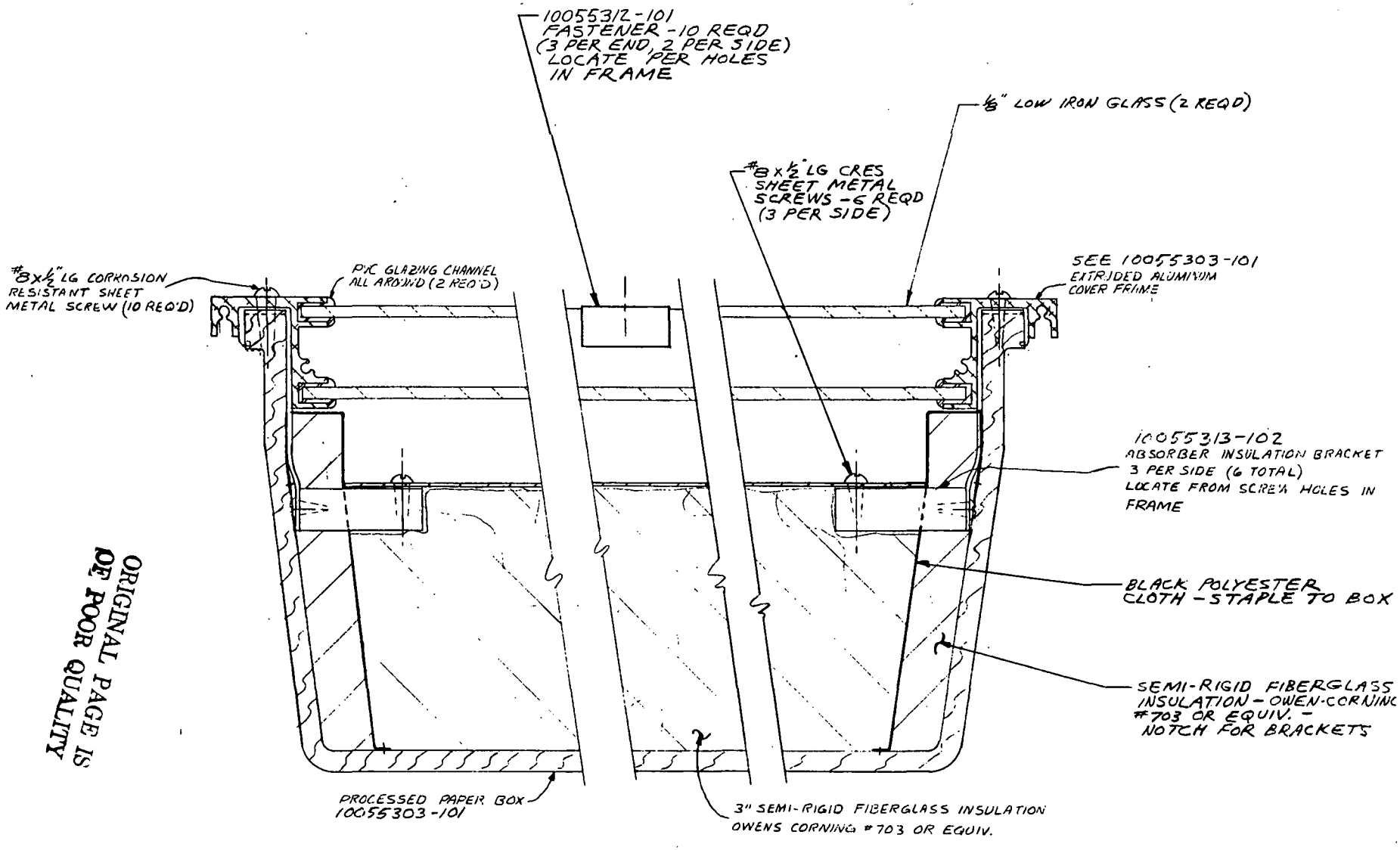

TYPICAL CROSS SECTION

Figure 13. MSFC Double-Glass Collector Assembly

FINAL COLLECTOR DESIGN DRAWINGS

The final designs for the two solar collectors are detailed in this section. The collector assembly for the one and two cover collector versions are shown in Figures 14 and 15, respectively. Figures 16 through 18 describe box, cover frame, and absorber bracket extender for the one cover collector, and Figures 19 through 21 for the two-cover collector. Figures 22 through 24 detail the absorber which is equivalent for both collectors and Figures 25 through 29 provide details of piece parts and subassemblies used in both collector designs.

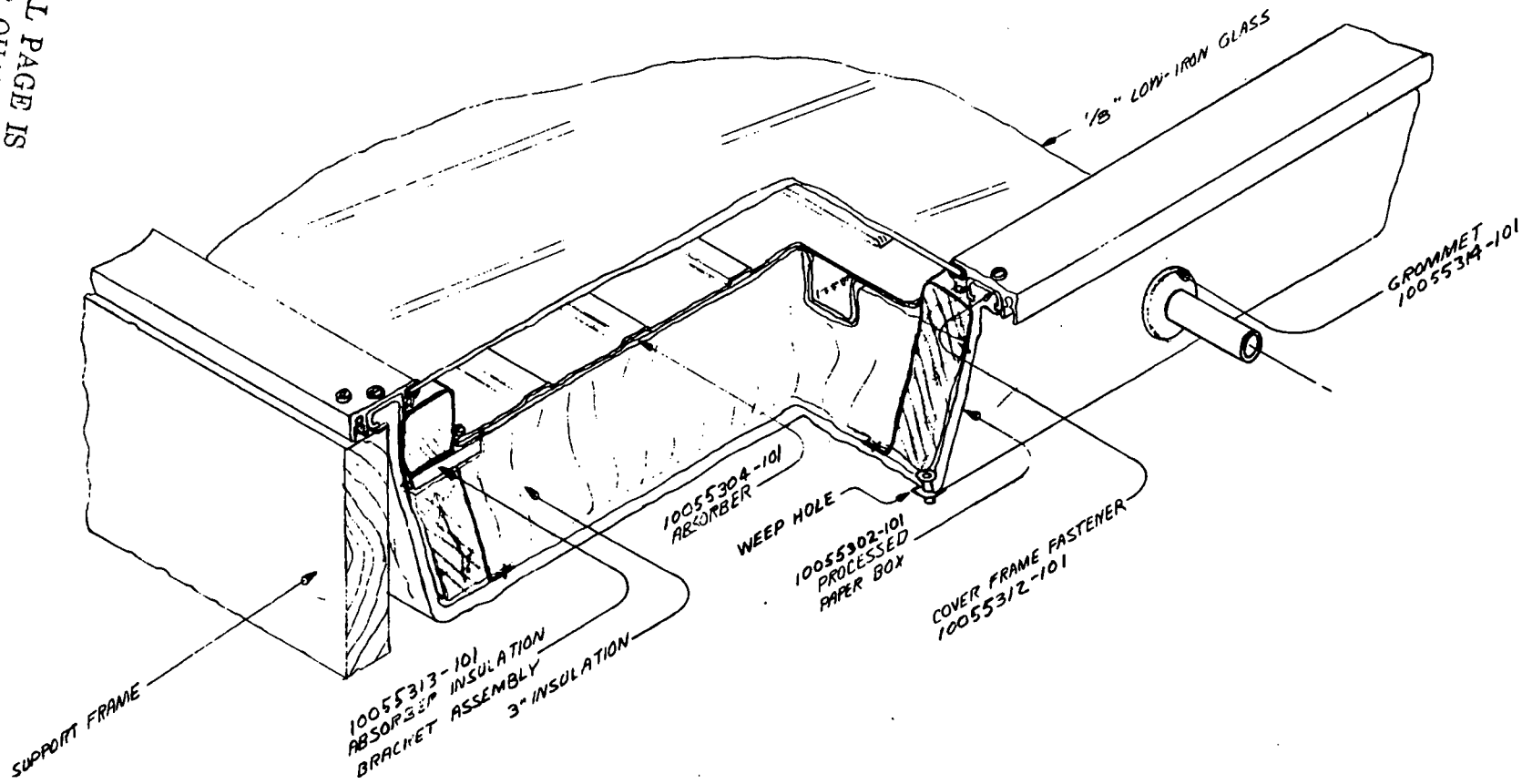

Figure 14. MSFC Single-Glass Collector Assembly

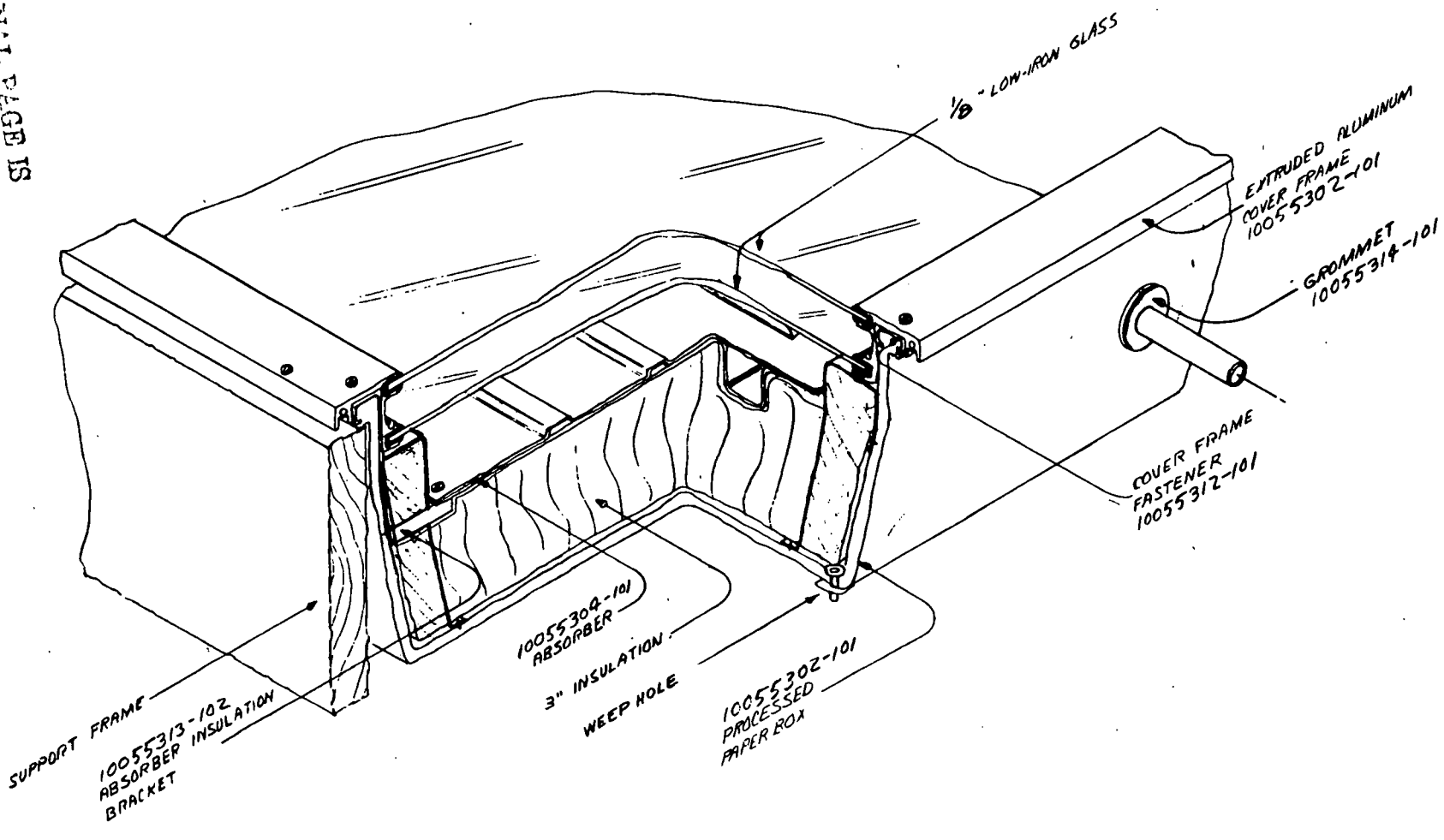

Figure 15. MSFC Double-Glass Collector Assembly

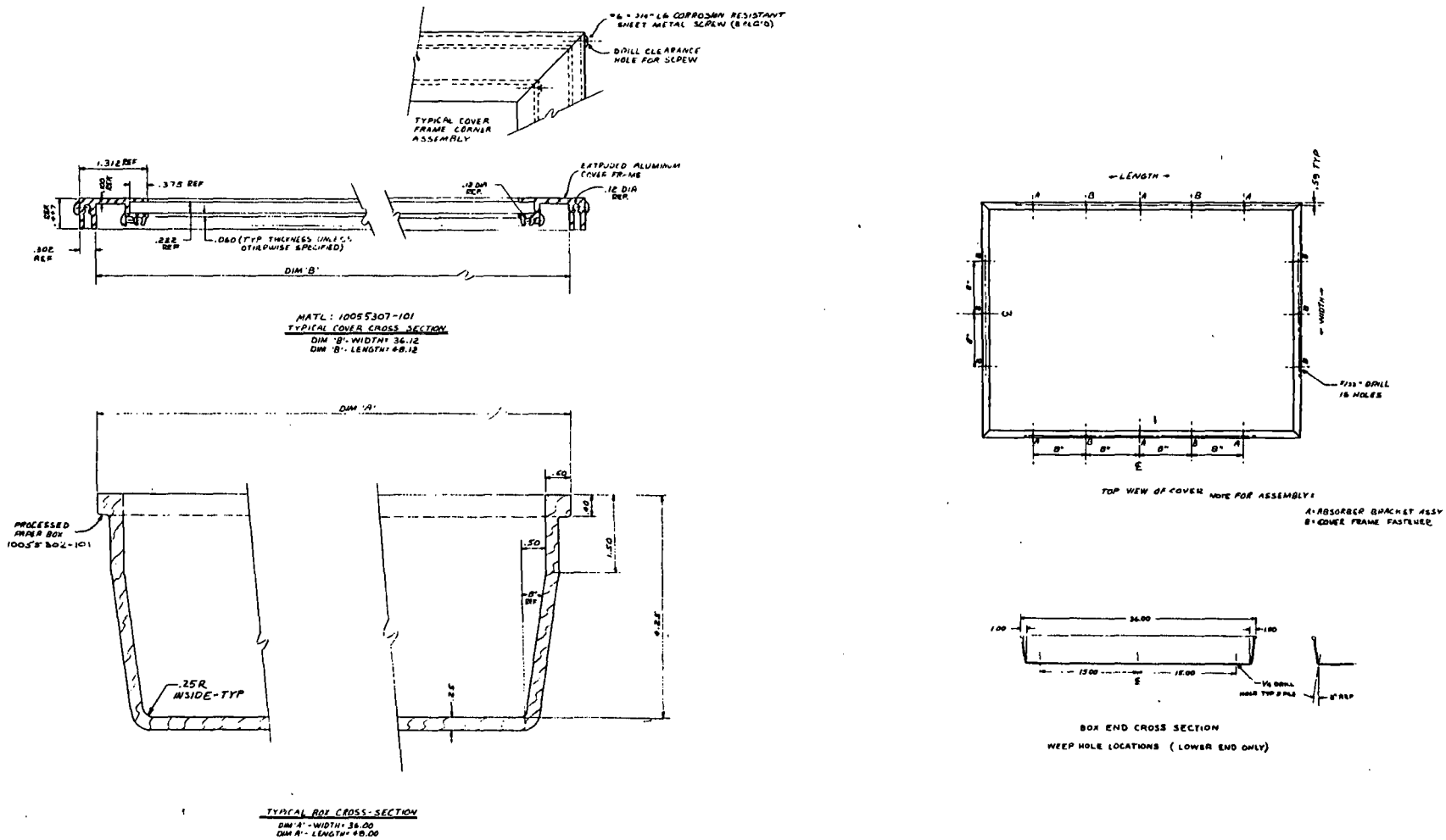

Figure 16. Box and Extruded Frame -- Single-Glass

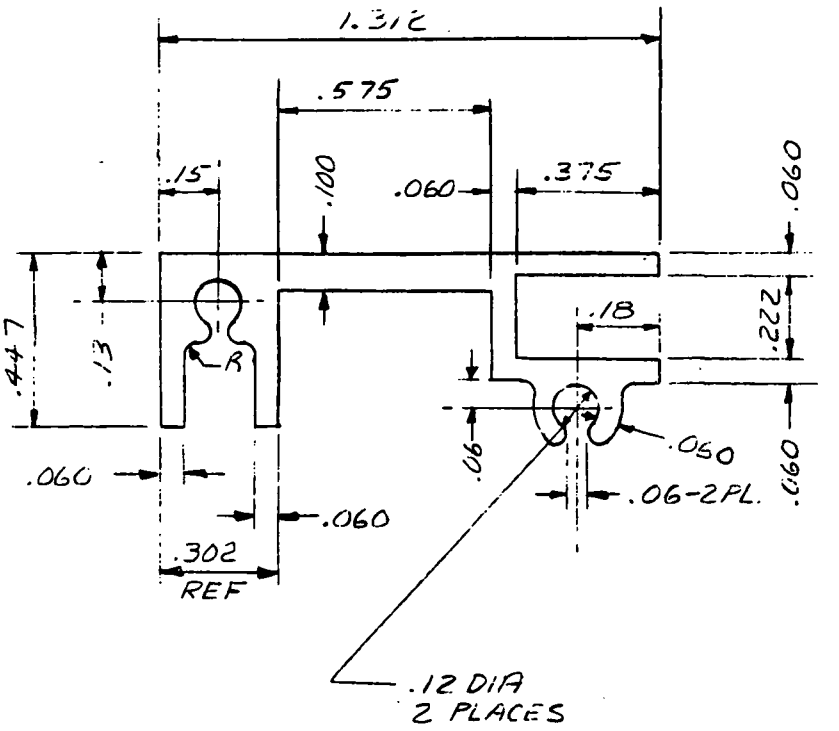

Figure 17. Extrusion - Single Glass

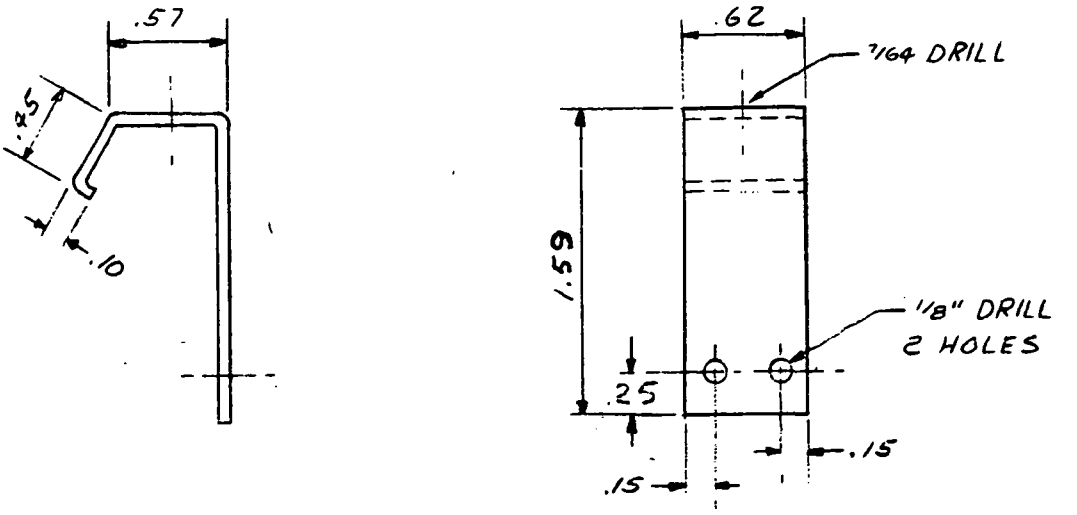

Figure 18. Absorber Bracket Extender - Single Glass

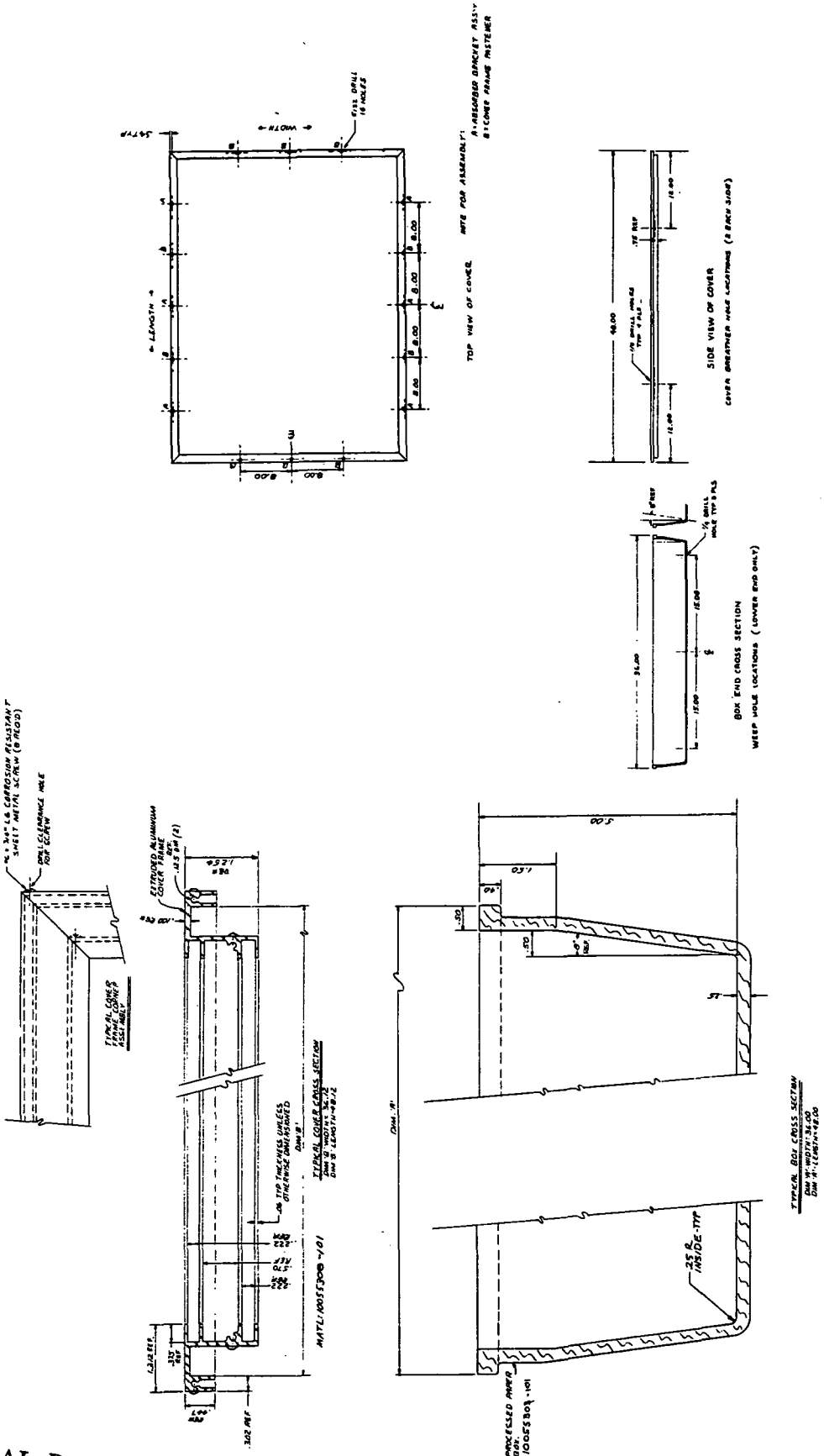

Figure 19. Box and Extruded Frame -- Double-Glass

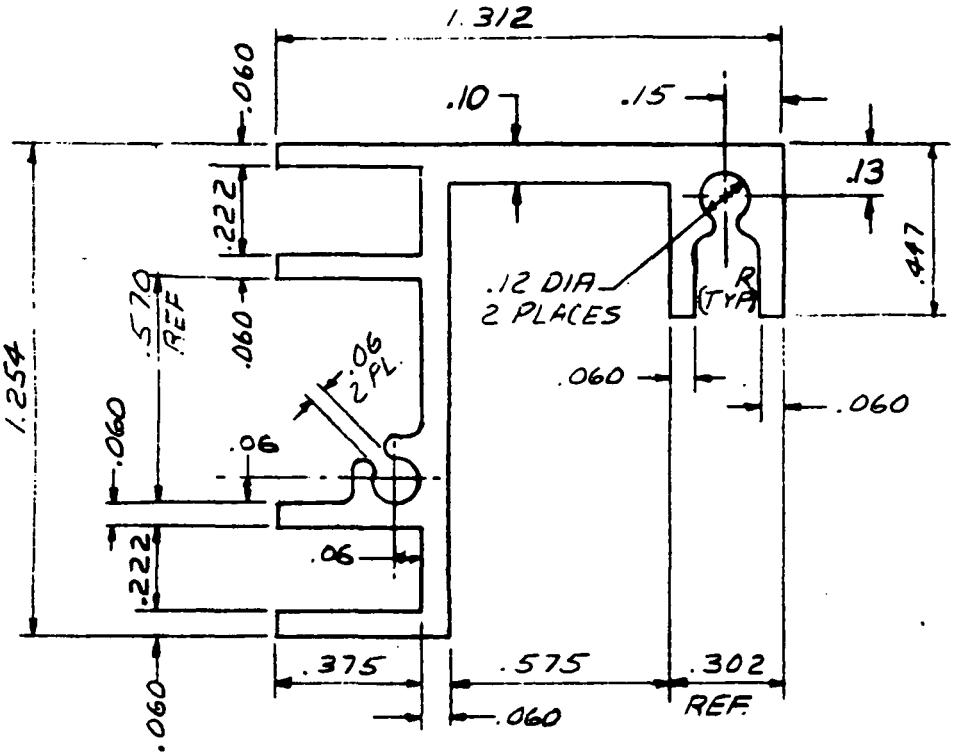

Figure 20. Extrusion - Double Glass

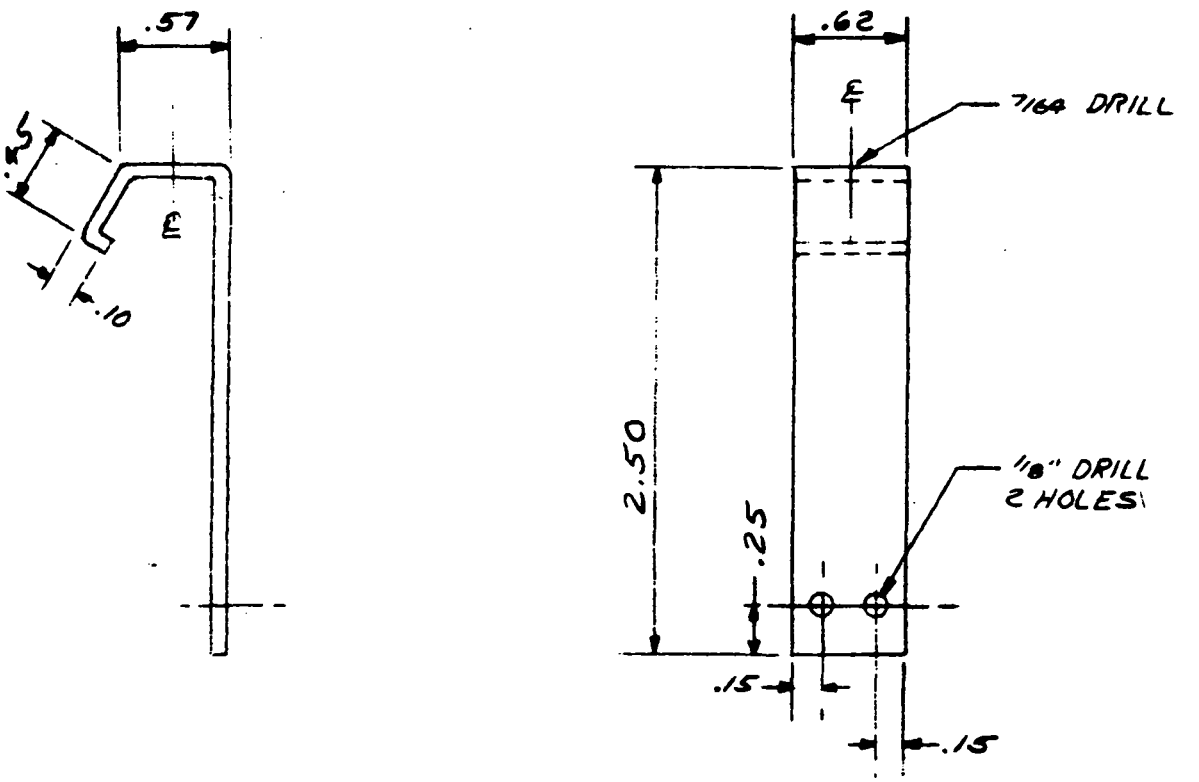

Figure 21. Absorber Bracket Extender - Double Glass

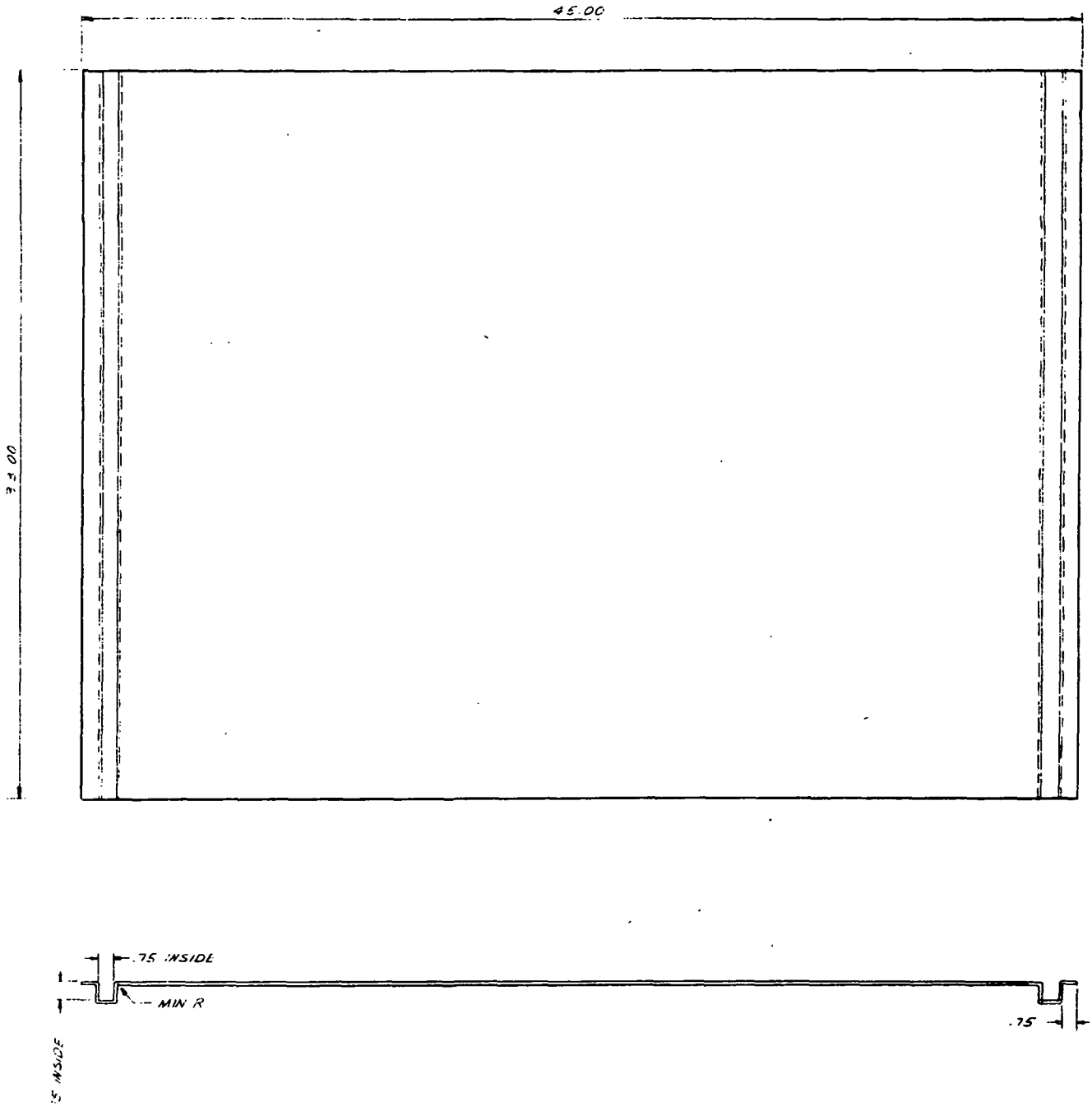

Figure 22. Panel "A" -- Absorber

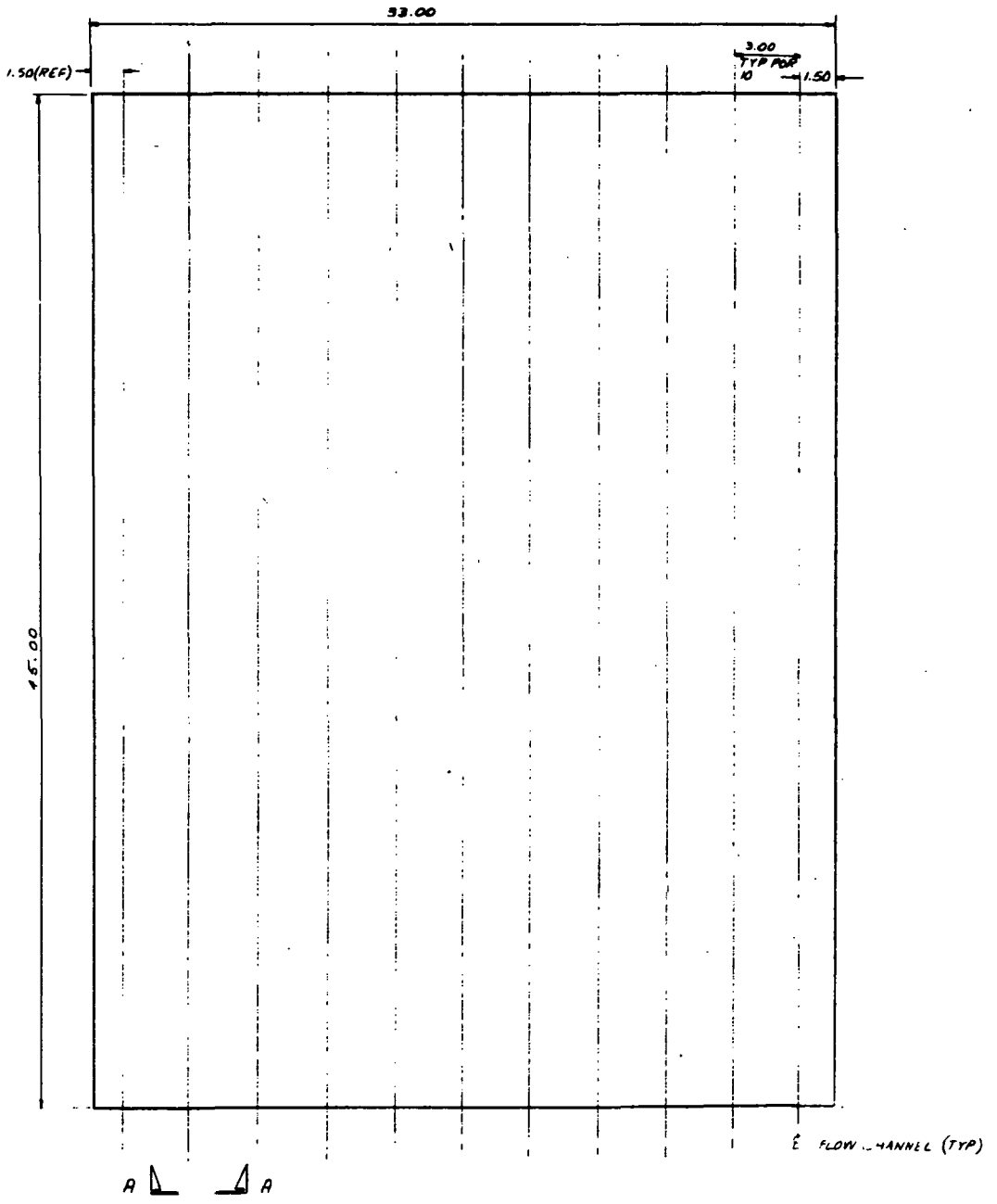

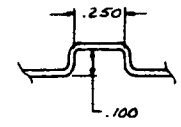

SECTION A-A
TYP FOR 11 FLOW CHANNELS
TWICE ACTUAL SIZE

Figure 23. Panel "B" -- Absorber

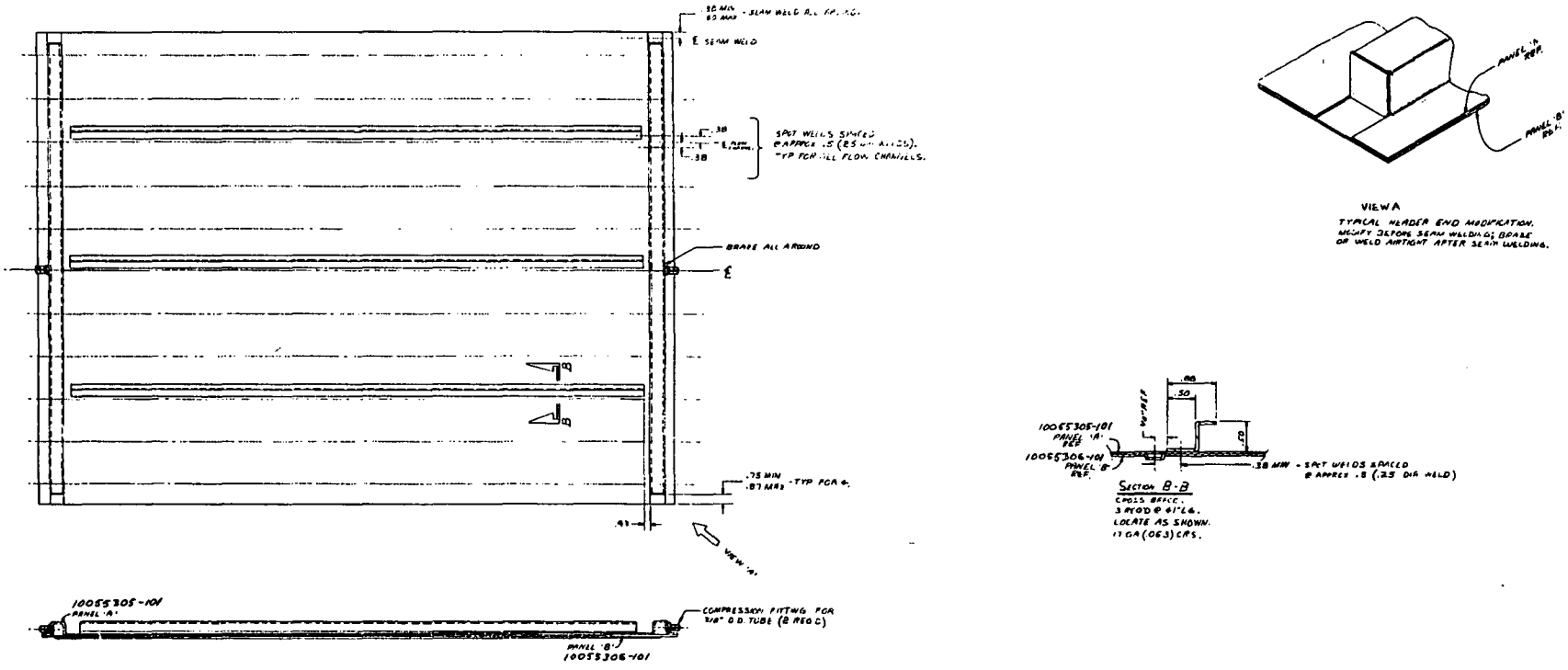

Figure 24. Absorber Assembly

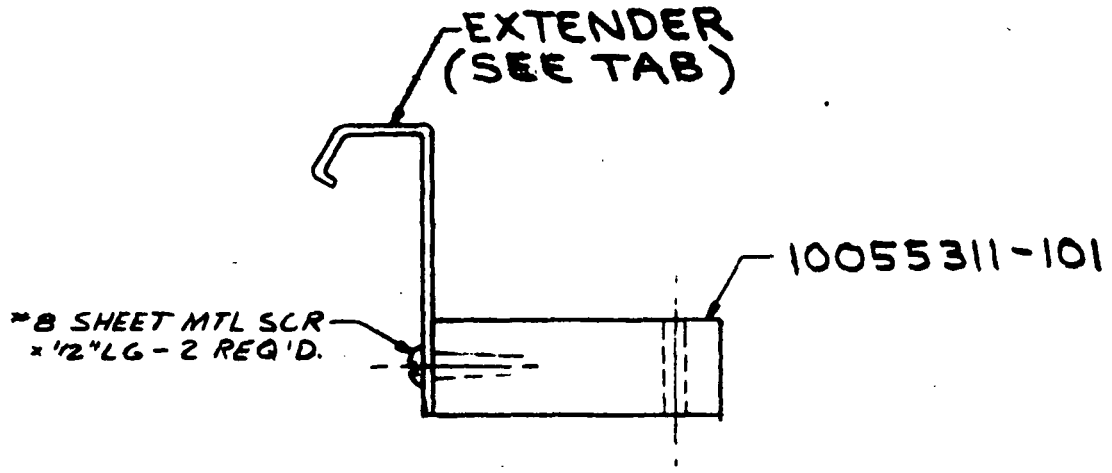

Figure 25. Absorber Bracket Assembly - Typical

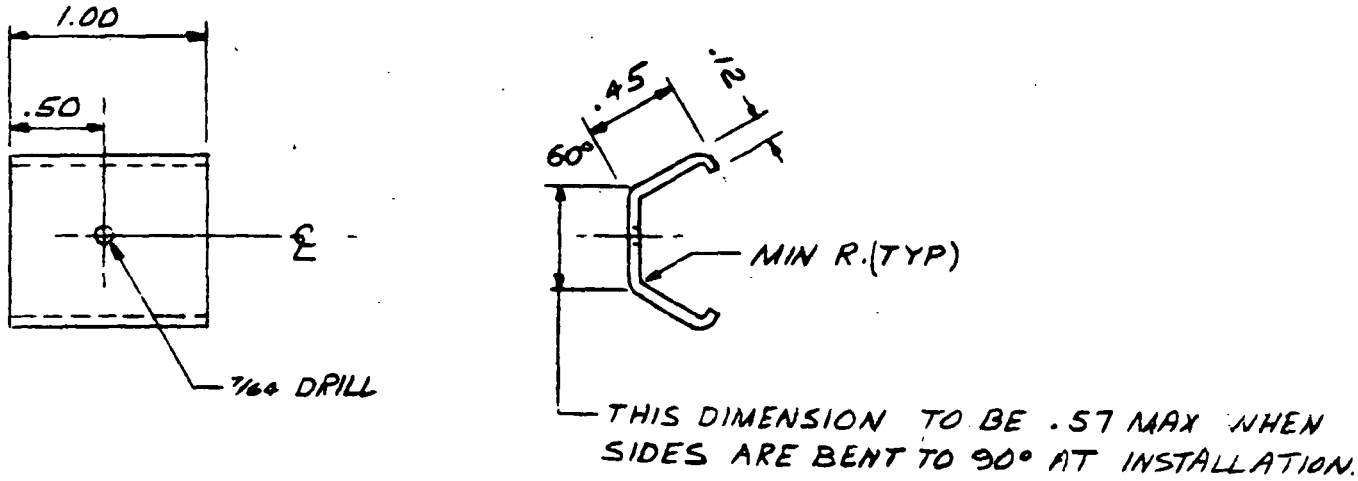

Figure 26. Cover Frame Fastener

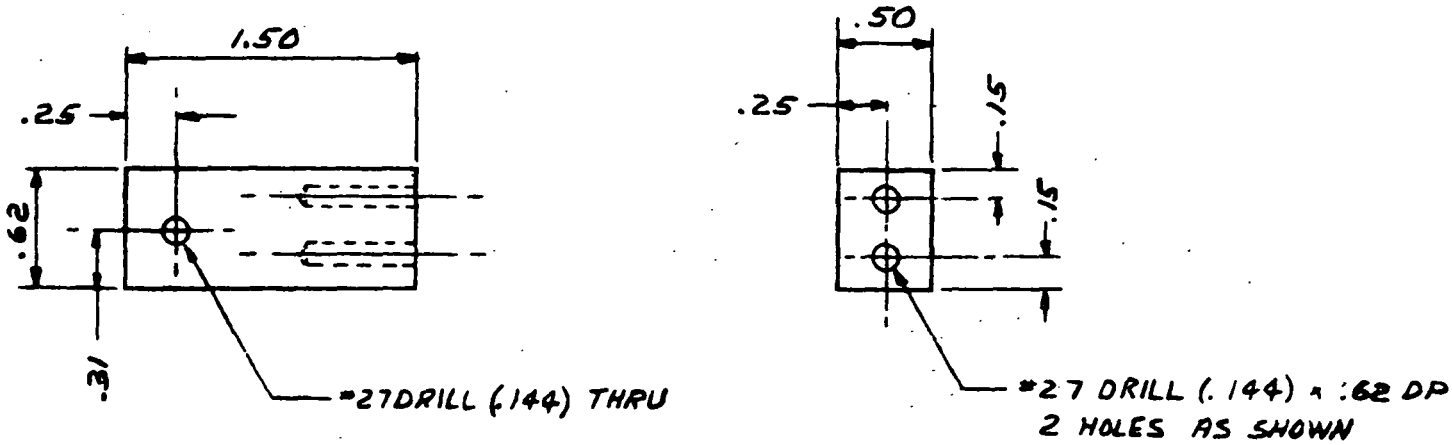

Figure 27. Absorber Bracket Base - Single and Double Glass

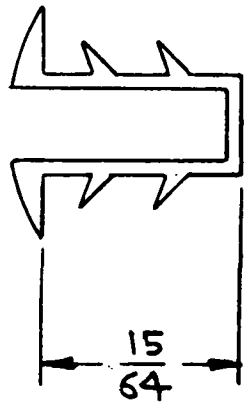

Figure 28. Glazing Seal

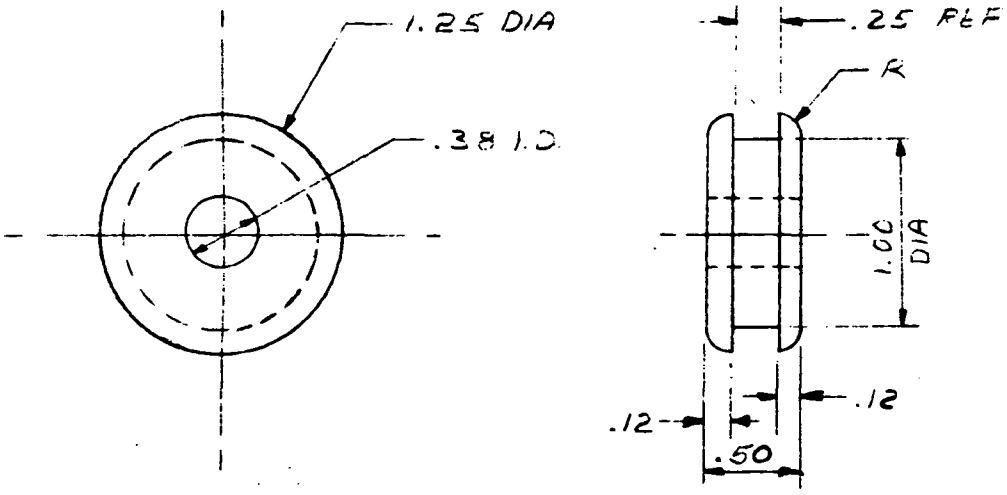

Figure 29. Connect Tube Grommet

PROCUREMENT, FABRICATION AND ASSEMBLY

Parts List

The solar collector parts lists are given in Tables 10 and 11. None of the parts require any high technology fabrication processes or highly accurate machining. Several of the piece parts for the collector have been procured from outside vendors. These are listed below along with a brief description and manufacturer and/or supplier.

Procured Piece Part	Description	Mfg/Supplier
Molded paper housing	3 ft. x 4 ft x 5 ft depth x 1/4 in. nominal thickness	Format Containers, Inc. Wisconsin
Cover frame aluminum extrusion	One or two channel extrusion to hold cover glass	Alexandria, Extrusions, Inc. Alexandria, MN
Fiberglass insulation	1 1/2 in. bats of OC703 semirigid fiberglass board	Owens Corning Fiberglass
Grommets	3/8 in. ID x 1 1/4 in. OD x 1/2 in. thick black silicone rubber	Honeywell Plastics Lab
Glazing seal	1/8 in. x 3/8 in. PVC window weather stripping GC-460	Alco Supply Co. Minneapolis, MN
Glass	Double strength FOURCO Clearlite low iron	Northwestern Glass Co. Minneapolis, MN
Screws	1/2 in. No. 6 sheet metal 3/4 in. No. 7 sheet metal	---

TABLE 10. - SOLAR COLLECTOR PARTS LIST -- SINGLE COVER COLLECTOR

Qty	Item	Description
1	Housing	Brown molded paper pan, 3 ft x 4 ft x 4 1/4 in. deep x 1/4 in. thick (nom.)
2	45-deg mitred end cover frame extrusion	Single channel 36 in. long, OD blue anodized
2	45-deg. mitred side cover frame extrusion	Single channel 48 in. long. OD blue anodized
Approx 37 bd ft	Insulation	OC-703 1 1/2 in. thick semi-rigid fiberglass boards
2	Interconnect grommets	3/8 in. ID, 1 1/4 in. OD, 1/2 in. thick black silicon rubber
14 ft	Glazing seal	1/8 in. x 3/8 in. PVC window weather stripping
1 lite	Glass	34 1/2 in. x 45 1/2 in. double strength FOURCO Clearlite low iron
2 dz	Screws	3/4 in. No. 7 self tapping sheet metal screws
1 dz	Screws	1/2 in. No. 6 self tapping sheet metal screws
1	Absorber	33 in. x 45 in. spot and seam welded sheet steel absorber with iron oxide coating and organic overcoat
2	Interconnect tube	3/8 in. copper tubing, 5 in. long
2	Compression fitting	3/8 in. compression fitting nuts with nylon
6	Absorber bracket insulation	Nylon blocks
6	Absorber bracket clips	0.050 in. aluminum clips, single cover
10	Cover frame clips	0.050 in. aluminum clips

TABLE 11. - SOLAR COLLECTOR PARTS LIST
DOUBLE COVER COLLECTOR

Qty	Item	Description
1	Housing	Brown molded paper pan, 3 ft x 4 ft x 4 1/4 in. deep x 1/4 in. thick (nom.)
2	45-deg mitred end cover frame extrusion	Double channel 36 in. long, OD blue anodized
2	45-deg mitred side cover frame extrusion	Double channel 48 in. long, OD blue anodized
Approx 37 bd ft	Insulation	OC-703 1 1/2 in. thick semi-rigid fiberglass boards
2	Interconnect grommets	3/8 in. ID, 1 1/4 in. OD, 1/2 in. thick black silicon rubber
28 ft	Glazing seal	1/8 in. x 3/8 in. PCV window weather stripping
2 lites	Glass	34 1/2 in. x 46 1/2 in. double-strength FOURCO Clearlite low iron
2 dz	Screws	3/4 in. No. 7 self-tapping sheet metal screws
1 dz	Screws	1/2 in. No. 6 self-tapping sheet metal screws
1	Absorber	33 in. x 45 in. spot and seam welded sheet steel absorber with iron oxide coating and organic overcoat
2	Interconnect tube	3/8 in. copper tubing, 5 in. long
2	Compression fitting	3/8 in. compression fitting nuts with nylon
6	Absorber bracket insulation	Nylon blocks
6	Absorber bracket clips	0.050 in. aluminum clips, double cover
10	Cover frame clips	0.050 in. aluminum clips

Fabrication

The methods used to fabricate the collector housing, absorber, coating, and brackets are described in the following paragraphs:

Housing

The process used for the manufacture of the paper boxes requires a tightly knit brass screen form. This form is lowered into a paper mache slurry and suction is applied within the screen mold, causing layers of paper to build on the mold. The time and suction pressure of the process determines the product thickness. The mold is removed from the slurry and the box is placed on a drying rack which can be run through an oven. The properties of the resulting paper product are determined by the type and rag content of paper used and by the chemical binders used in the slurry. There are numerous possibilities of binders which can be used to increase the strength, durability, and weatherability of the collector housing. Such processes may eliminate the need for a second plastic impregnation step to increase collector housing life.

Absorber

The absorber is fabricated from two sheets of sheet steel, one with formed parallel flow channels and the other with formed headers. These sheets are then spot welded together and seam welded around the periphery to make a water tight panel.

The 3/8 in. copper supply and return tubes are centered on the top and bottom sides of the absorber header using compression fittings.

Male compression fittings are welded to the headers at these points and the tubes are coupled to the absorber using the female fittings and a special socket wrench. This type of fitting allows for tubing attachment from outside the collector box. After fabrication, the absorbers are leak checked to 25 psig.

Coating

An iron oxide coating is applied to the absorbers using an Ebonal S solution from Enthone, Inc. The bath temperature is 290°F and the absorbers are left in the solution for two minutes. A standard alkaline cleaning solution is used along with an acid etch prior to coating.

The overcoat is an ethylene propylene material (EPM) which is applied to a thickness of 0.2 mil. The product used is Vistalon 606 EPM which is a product of Exxon Company.

The reflectance curve for the coating is shown in Figure 30. The uncoated surface has an absorptance of .90 and emittance of .12 (α/ϵ = 7.7). The overcoated sample has an absorptance of .92 and an emittance of .20 (α/ϵ = 4.6).

Brackets

The absorber brackets are fabricated from 1.3 mm (0.050 in.) aluminum clips and nylon blocks. Self tapping screws are used to attach the nylon insulator to the aluminum clip. The cover frame clips are also made from 1.3 mm (0.050 in.) aluminum. The absorber brackets maintain the position of the absorber within the box by attachment to the cover frame. Both absorber brackets and cover frame clips are used to hold the housing to the cover assembly. See Figure 31 for anchor clip and absorber bracket sketches.

Cover Frame Assembly

The cover frames are assembled as follows:

One-Cover Frame

1. Four strips of spline are cut to length.
2. A length of PVC is placed over the glass edge and the frame side is tapped into place. Subsequent sides are tapped into place in the same manner.
3. Two screws are used in each corner to secure the cover frame assembly.

Two-Cover Frame

1. Eight strips of spline area are cut to length.
2. Two sheets of glass are cleaned on one side and then placed on edge with clean sides facing each other.
3. Two pieces of spline are placed on the top edges and the first side is tapped onto the two lites.
4. The two ends are then fitted in the same manner without rotating the lites.

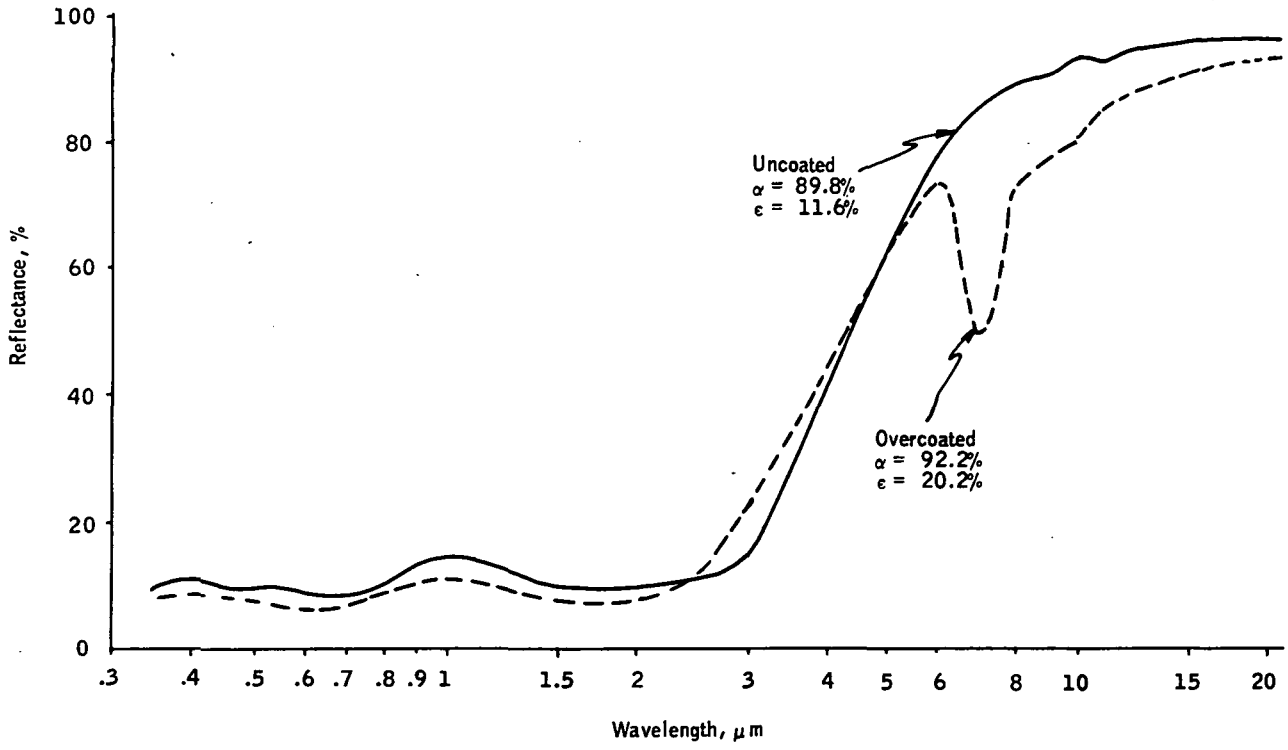

Figure 30. Reflectance Curves for Iron Oxide Coating with and without Organic Overcoat

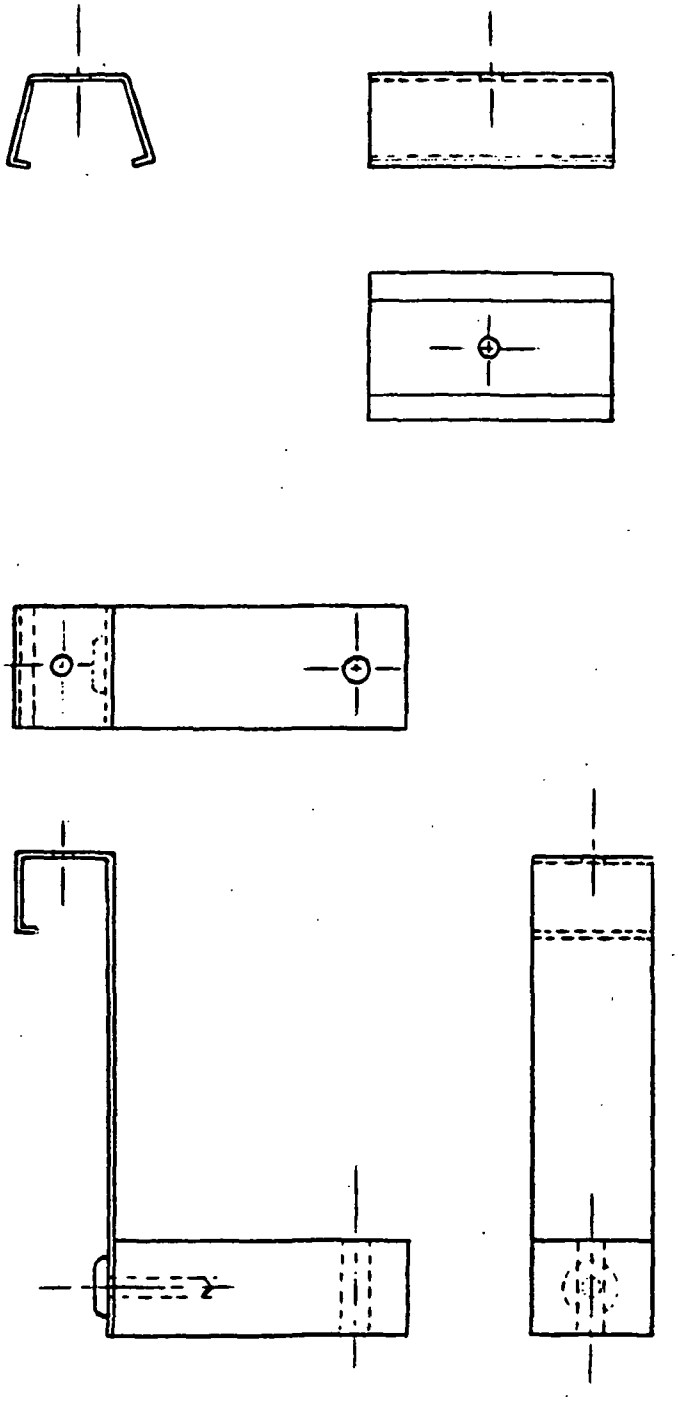

Figure 31. Anchor Clip and Absorber Bracket Detail

5. Four sheet metal screws are used to attach these three sides together.

6. The assembly is rotated, the fourth side is fitted with the spline, and then the fourth frame side is tapped into position. The frame is completed by securing these two corners with four more sheet metal screws (Figures 32 & 33).

Collector Assembly

The collectors are assembled in the following steps:

1. Weep holes are drilled in the housing along the intersection of the box back and bottom. (Figure 34)

2. The insulation is fitted in 2.5 cm x 10.2 cm (1 in. x 4 in.) strips around the edge, and the bottom is filled in with 7.6 cm (3 in.) of semirigid fiberglass. A black polyester fabric is used to cover the yellow edge insulation. The material is tested in an oven at 204°C (400° F) for shape change or degradation. For a production collector, black insulation should be used. (Figure 35)

3. The absorber brackets and cover frame anchor clips are placed in position on the box edge and squeezed into the box material. The edge fiberglass is trimmed to make room for these brackets. (Figures 36, 37 and 38)

4. The absorber is instrumented and placed in position without tubes connected. The absorber is fastened to the nylon absorber brackets using self tapping sheet metal screws. (Figures 39 and 40)

5. Holes 2.5 cm (1 in.) in diameter are drilled in the box ends and fiberglass in line with the header tube outlets. The tubes are attached from the outside using a 5/8 in. socket wrench with a hollow handle. Rubber grommets are slid onto the tube and into the hole in the housing. (Figure 41)

6. The inside glass of the cover assembly is cleaned and then the cover assembly is placed in position. Holes are drilled in the appropriate positions, and sheet metal screws are used to attach the cover frame to the absorber brackets and anchor clips. (Figures 42 and 43)

7. Thermocouples are installed on the two collectors at the appropriate assembly steps according to the sketch provided by MSFC. Figure 44 shows the location of these thermocouples.

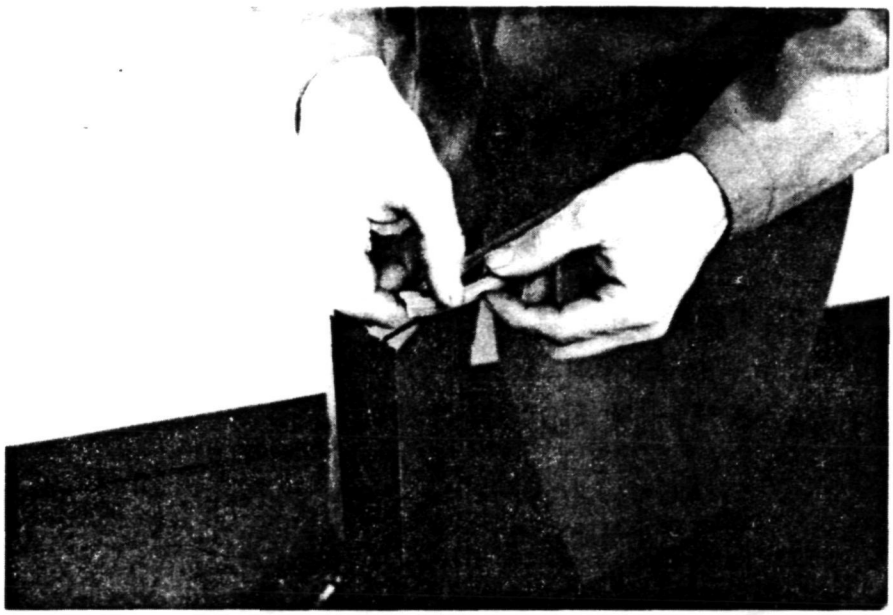

Figure 32. Glazing Spline is Fitted on Glass

Figure 33. Frame is Secured with Sheet Metal Screws

Figure 34. Weep Holes are Drilled in Housing

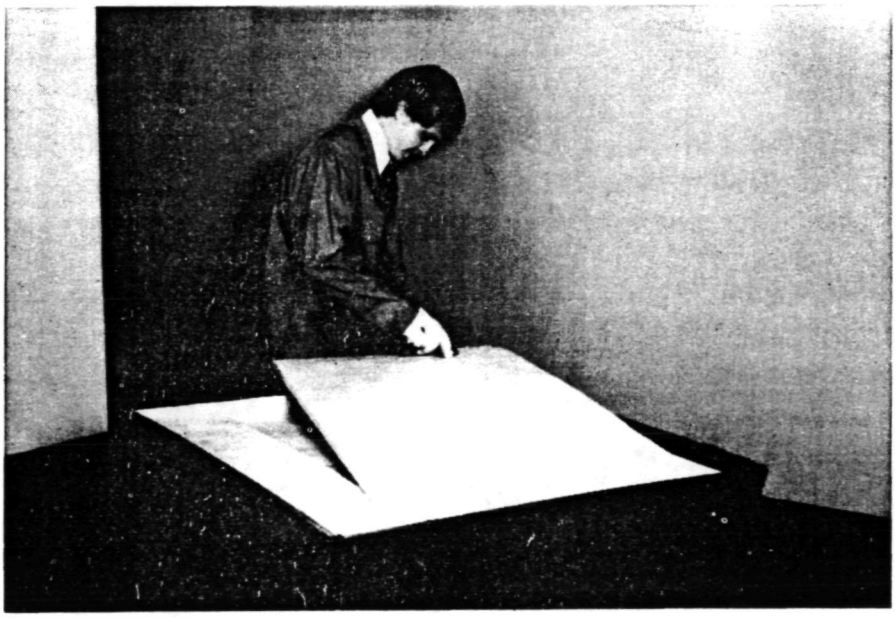

Figure 35. Insulation is Cut for Housing

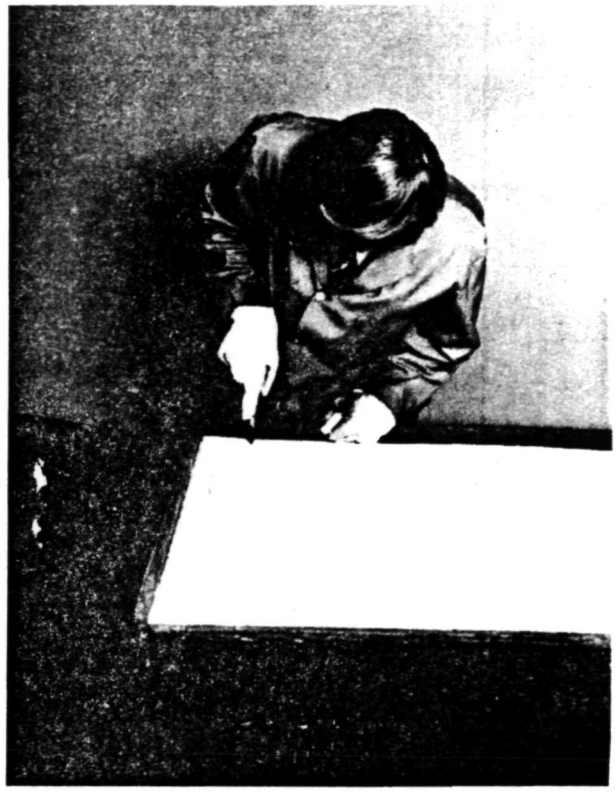

Figure 36. Insulation is Cut to Allow for Absorber Bracket

Figure 37. Absorber Bracket is Snapped into Place

Figure 38. Bracket is Clamped Securely to Housing

Figure 39. Absorber Panel is Placed in Housing

Figure 40. Absorber is Fastened to Nylon Brackets

Figure 41. Rubber Grommets are Placed in Position

Figure 42. Holes are Drilled Over Brackets

Figure 43. Cover Frame is Screwed to Housing

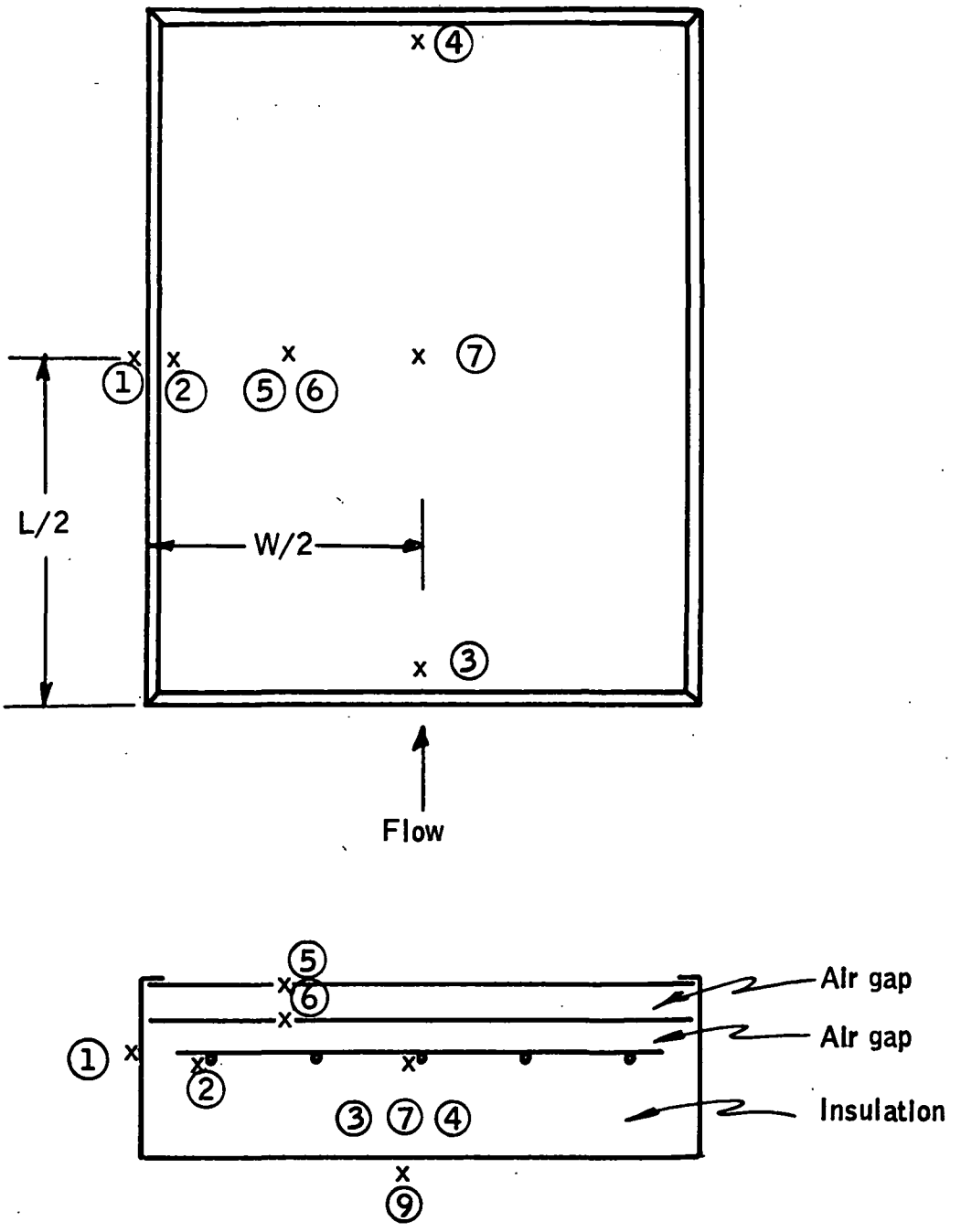

Figure 44. Thermocouple Locations (Iron Constantan)

The assembled collector is a rigid unit. It is not necessarily water tight as there is no weather stripping between the cover frame and box. This could easily be changed with the addition of a butyl rubber sealer along the box edge.

COLLECTOR PERFORMANCE

Test Plan

The tests conducted on the two collector configurations investigated the effects of variations in fluid inlet temperature and incident flux level. The test data were used to generate steady state performance curves for the one and two cover collector configurations.

Leak Test

The absorber panels were pressure tested to 25 psig for leaks. This test was made prior to application of the absorber coating.

Indoor Test Facility

The collector tests are conducted in an indoor test facility that uses a solar simulator to provide the incident flux. The solar simulator generates a range of flux levels that closely approximates the distribution of the solar spectrum at air mass 2. The simulator consists of 143 projection lamps evenly spaced in a 1.83 m (6 ft) square array containing 14 rows and 11 columns. The output from each lamp is collimated by a 15 cm (6 in.) diameter plastic Fresnel lens set in an array 23 cm (9 in) in front of the lamp array. Using the Fresnel lenses results in a flux output that is essentially 100 percent direct radiation.

The solar simulator is powered by a three phase, 208 volt "wye" configuration circuit capable of providing 43,000 volt amperes of power. Each phase of the circuit is monitored by an SCR power controller which restricts the power output from zero to full scale, dependent on an operator supplied control signal. The full-scale output from the solar simulator is 1010 W/m^2 (320 $Btu/hr\text{-}ft^2$) at a distance of 4.57 m (15 ft) from the lens array.

This solar simulator is similar in design to that at the NASA Lewis Research Center, Cleveland, Ohio. A detailed discussion of solar simulator design and operation may be found in NASA Technical Memorandum TMX-3059, "Low Cost Air Mass 2 Solar Simulator".

The collector test loop is presented diagrammatically in Figure 45. System operation is as follows:

The glycol/water mixture is pumped from the reservoir to a 4.57 m (15 ft) constant head tank. An overflow line to return fluid to the reservoir maintains a constant pressure head. This pressure head drives fluid to a conventional hot water heater and then through a constant temperature bath. From there, the fluid goes through the flow-

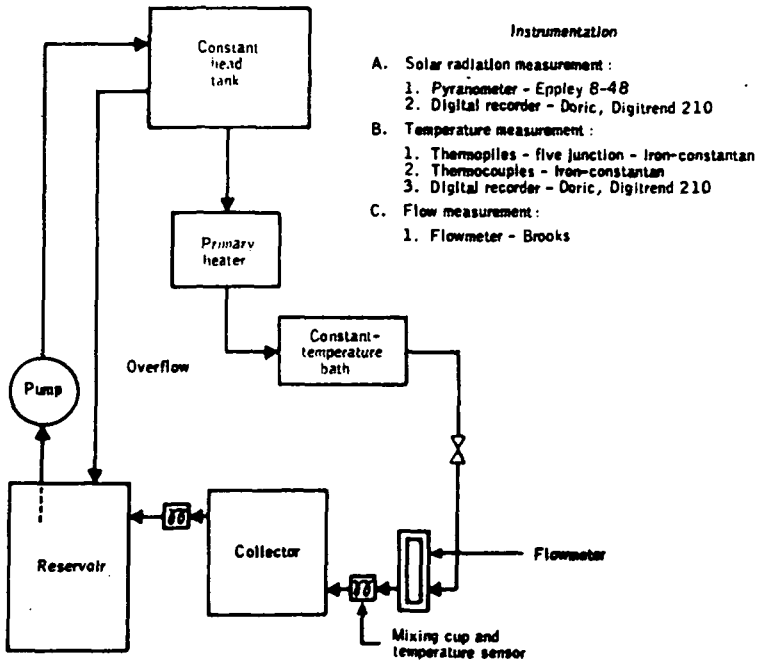

Figure 45. Diagram of Indoor Collector Test Loop

meter and to the collector. The outlet from the collector returns fluid to the reservoir and completes the cycle. The valve placed between the constant temperature bath and the flowmeter regulates the flow.

Mixing cups, each containing a five junction thermo-pile and a thermocouple, are inserted at the inlet and outlet of the collector. From these, the fluid temperature difference across the panel and fluid inlet and outlet temperatures can be measured. Another thermo-couple placed behind the collector stand measures the ambient temperature. These temperatures are recorded on a digital recorder. Iron constantan thermocouple wire is used for these measurements.

The flow rate is determined by using a calibrated flowmeter. As the system approaches steady state, the flow rate is maintained at a constant value. This flow rate is also periodically checked by measuring the time for the return fluid to fill a 1000 ml graduated cylinder.

The flux from the simulator is determined using an Eppley pyranometer. A 16 point flux map at the collector surface is made and recorded for each experimental run. The average value is used as the effective incident radiation level.

Test Matrix

Each performance test is run with a 48.9 kg/hr m^2 (10 lbm/hr-ft^2) flow rate of nominally 50/50 water/ethylene glycol solution. The collector is tilted at an angle of 34 degrees with respect to horizontal and with a zero effective wind velocity across the face of the collector. The test matrix for each collector is shown in Table 12.

TABLE 12.- TEST MATRIX

Ambient temperature = 21° C (70° C)
Wind velocity = 0 kph (0 mph)
Collector tilt angle = 34°
Mass flow rate = 48.9 kg/hr-m^2 (10 lbm/hr-ft^2)

Flux, W/m^2 (Btu/hr-ft^2)	Test parameter	Inlet temperture 27° C (80° F)	49° C (120° F)	71° C (160° F)	93° C (200° F)
473 (150)	$\dot{m}$, lb/hr-ft^2 C_p, Btu/lb-°F ΔT, °F Q_{col}, Btu/hr-ft^2 Q_{inc}, Btu/hr-ft^2 η				
789 (250)	$\dot{m}$, lb/hr-ft^2 C_p, Btu/lb-°F ΔT, °F Q_{col}, Btu/hr-ft^2 Q_{inc}, Btu/hr-ft^2 η				
1010 (320)	$\dot{m}$, lb/hr-ft^2 C_p, Btu/lb-°F ΔT, °F Q_{col}, Btu/hr-ft^2 Q_{inc}, Btu/hr-ft^2 η				

A test cycle consists of preheating the fluid reservoir to the desired inlet temperature, 27°C (80°F), 49°C (120°F), 71°C (160°F), or 93°C (200°F), allowing flow through the collector to maintain inlet temperature equilibrium throughout the system. Once the desired inlet temperature is attained, the primary heater is shut off, the flow rate is adjusted to 48.9 kg/hr-m^2 (10 lbm/hr-m^2), and the inlet temperature is trimmed and maintained by the constant temperature bath.

After firing up the solar simulator, the flux map for the intended incident flux level is measured, and the illuminated collector is allowed to run until equilibrium is observed for the fluid temperature rise across the collector. Values for the inlet temperature, fluid temperature rise, fluid mass flow rate, and incident flux level are then recorded. The actual measurement process takes approximately thirty minutes, once initial fluid inlet temperature equilibrium has been achieved.

The measurement process is then repeated for the next incident flux level, without altering the flow rate or fluid inlet temperature.

Data Reduction

The data are reduced using a Hewlett-Packard programmable calculator which calculates the thermal efficiency for each test run and provides a linear curve fit of the data points on a graph of efficiency, η, versus the parameter $[(T_{inlet} - T_{ambient})/Q_{incident}]$. From these performance curves a heat removal efficiency factor, F_R, and an overall heat loss coefficient, U_L, can be found from the following equation:

$$\eta = F_R\left[\alpha\tau_e - U_L\left(\frac{T_{in} - T_{amb}}{Q_{inc}}\right)\right]$$

Here α is the measured plate absorptance and τ_e is the effective transmittance of the cover system. These F_R and U_L factors may then be compared with those of other conventional flat plate solar collectors which have been tested on the same solar simulator. A discussion of the above equation and results of similar testing can be found in NASA CR-134804, "Development of Flat Plate Solar Collectors for the Heating and Cooling of Buildings," by J.W. Ramsey, J.T. Borzoni and T. H. Holland.

Performance Test Results

The one and two cover versions of the solar collector were tested using the contractor's solar simulator. Test results and performance curves for each of the two solar collectors are shown in Tables 13 and 14 and Figures 46 and 47 respectively.

TABLE 13.- COLLECTOR TEST DATA FOR MSFC SOLAR COLLECTOR WITH ONE GLASS COVER

Ambient temperature = 21°C (70°F)
Wind velocity = 0 kph (0 mph)
Collector tilt angle = 40°
Mass flow rate = 53.8 kg/hr-m^2 (11 lbm/hr-ft^2)

Diffuse/direct ratio = 0
Percent ethylene glycol in heat transfer fluid = 57%

Note: All English units

Flux, W/m^2 (Btu/hr-ft^2)	Test parameter[a]	Inlet temperature			
		27°C (80°F)	49°C (120°F)	71°C (160°F)	93°C (200°F)
473 (150)	$\dot{m}$	7.34	11.49	11.25	11.26
	C_p	.7900	.8109	.8331	.8553
	ΔT	13.33	8.87	5.07	1.07
	Q_{col}	77.3	82.6	47.5	10.3
	Q_{inc}	134.0	147.4	134.3	138.6
	η	.577	.560	.354	.074
631 (200)	$\dot{m}$	7.55	11.48	11.50	11.17
	C_p	.7900	.8124	.8337	.8561
	ΔT	17.46	14.00	7.00	3.73
	Q_{col}	104.2	130.6	67.1	35.7
	Q_{inc}	168.3	223.1	166.6	166.2
	η	.618	.585	.403	.215
789 (250)	$\dot{m}$	11.89	11.48	11.24	11.16
	C_p	.7896	.8131	.8336	.8568
	ΔT	13.80	16.33	8.87	6.27
	Q_{col}	129.6	152.4	83.1	59.9
	Q_{inc}	203.7	262.9	204.1	199.6
	η	.636	.580	.407	.300

[a]See Table 12 for test parameter units.

TABLE 14.- COLLECTOR TEST DATA FOR MSFC SOLAR COLLECTOR WITH TWO GLASS COVERS

Ambient temperature = 21°C (70°F)
Wind velocity = 0 kph (0 mph)
Collector tilt angle = 40°
Mass flow rate = 53.8 kg/hr-m^2
(11 lbm/hr-ft^2)

Diffuse/direct ratio = 0
Percent ethylene glycol in heat transfer fluid = 57%

Note: All English units

Flux, W/m^2 (Btu/hr-ft^2)	Test parameter[a]	Inlet temperature			
		27°C (80°F)	49°C (120°F)	71°C (160°F)	93°C (200°F)
473 (150)	$\dot{m}$	11.99	11.49	11.78	11.42
	C_p	.7990	.8115	.8336	.8564
	ΔT	10.00	7.07	6.67	4.80
	Q_{col}	95.80	65.9	65.5	46.9
	Q_{inc}	161.9	134.6	154.5	142.3
	η	.592	.490	.424	.330
631 (200)	$\dot{m}$	11.67	11.46	11.78	11.24
	C_p	.8009	.8143	.8351	.8580
	ΔT	14.67	12.53	12.00	10.40
	Q_{col}	137.1	117.0	118.1	100.3
	Q_{inc}	228.3	214.5	215.1	219.7
	η	.600	.545	.549	.457
789 (250)	$\dot{m}$	11.80	11.53	11.38	11.16
	C_p	.7908	.8162	.8380	.8581
	ΔT	16.60	14.93	11.73	12.87
	Q_{col}	154.9	140.5	111.9	123.2
	Q_{inc}	253.6	264.6	257.7	265.3
	η	.611	.531	.434	.464

[a]See Table 12 for test parameter units.

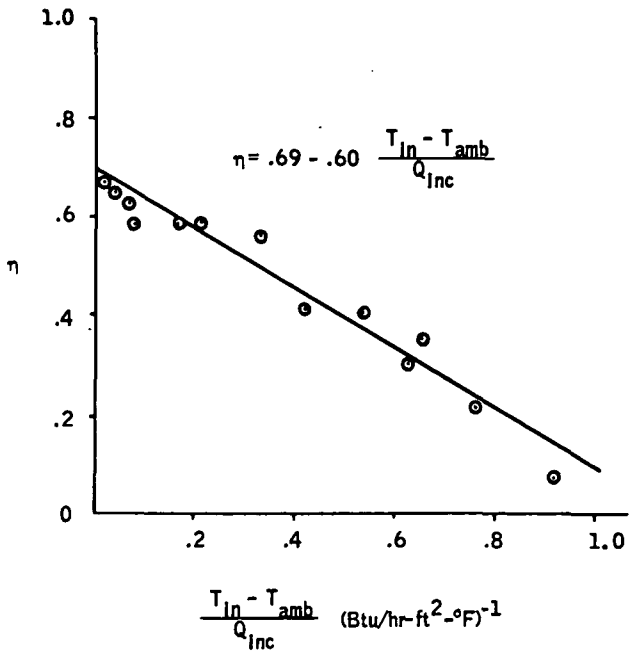

Figure 46. Performance Curve for Single-Cover MSFC Solar Collector

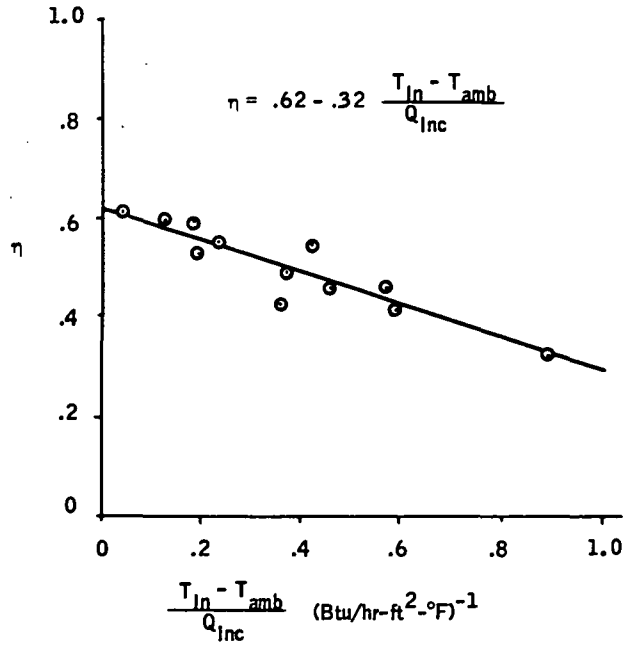

Figure 47. Performance Curve for Two-Cover Solar MSFC Collector

The equations of the performance curves shown in Figures 46 and 47 were generated by a linear regression curve fit of the test points. These resulting performance equations are as follows:

One-cover NASA MSFC solar collector:

$$\eta = .69 - .60 \frac{(T_{in} - T_{amb})}{Q_{inc}}$$

Two-cover NASA MSFC solar collector:

$$\eta = .62 - .32 \frac{(T_{in} - T_{amb})}{Q_{inc}}$$

For purposes of evaluation, the results are compared with those of a well designed conventional solar collector* which has been tested under identical conditions. Two-cover configurations for both collector types are compared in Figure 48.

For a typical air conditioning application, an ambient temperature of 80°F and a collector inlet temperature of 200°F, an average solar flux of 250 Btu/hr-ft^2 would generate the following collector efficiencies:

Collector configuration	Collector efficiency for typical cooling application
MSFC with one cover	40 percent
MSFC with two covers	47 percent
Black paint collector with one cover	27 percent
Black paint collector with two covers	33 percent

The MSFC one and two cover collectors are 48 and 42 percent better, respectively, than the corresponding black painted collectors.

*This collector has a nonselective black painted Roll Bond aluminum absorber in a steel box with glass covers and fiberglass insulation.

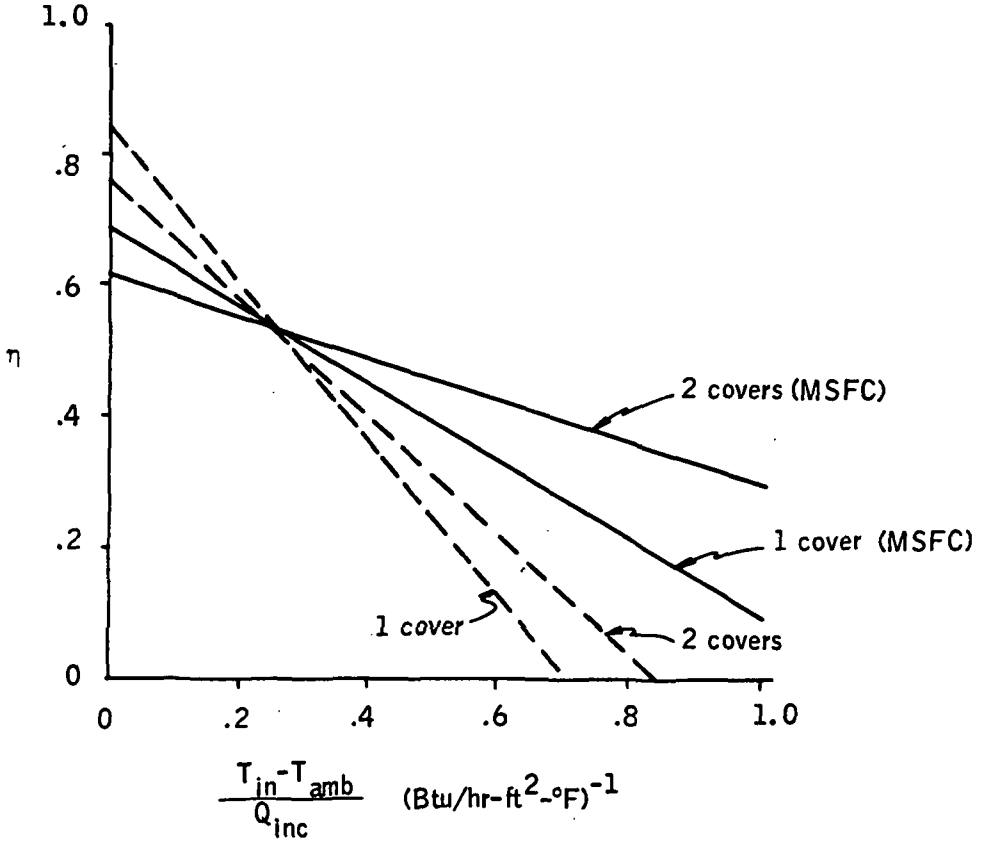

NASA MSFC Solar Collector

1-Cover : $\eta = .69 - .60 \frac{(T_{In} - T_{amb})}{Q_{inc}}$

2-Cover : $\eta = .62 - .32 \frac{(T_{In} - T_{amb})}{Q_{inc}}$

Well-Designed Black Paint Solar Collector

1-Cover : $\eta = .84 = 1.19 \frac{(T_{In} - T_{amb})}{Q_{inc}}$

2-Cover : $\eta = .75 - .89 \frac{(T_{In} - T_{amb})}{Q_{inc}}$

Figure 48. Comparison of MSFC and Well-Designed Flat-Plate Solar Collectors

For a typical heating application (i.e., an ambient temperature of 40° F and a collector inlet temperature of 120°F), a 250 Btu/hr-ft^2 insolation level would generate the following collector performance efficiencies:

Collector configuration	Collector efficiency for typical heating application
MSFC with one cover	50 percent
MSFC with two covers	52 percent
Black paint collector with one cover	46 percent
Black paint collector with two covers	47 percent

The one-cover MSFC collector is 6 percent better than the two-cover black painted collector. The one- and two-cover MSFC collectors are 9 and 11 percent better, respectively, than the corresponding black painted collectors.

Utilization

Daily collection values for typical heating and cooling conditions have been obtained empirically using the performance equations given in Figure 48 and ASHRAE calculated solar insolation for a clear day in the appropriate season. These curves are shown in Figures 49 and 50 for summer cooling (June) and winter heating (December), respectively. The results are summarized in Table 15.

TABLE 15. - DAILY COLLECTOR PERFORMANCE SUMMARY

Collector configuration		Daily collector efficiency	
		Summer cooling	Winter heating
		T_{amb} = 80°F T_{inlet}=200°F	T_{amb} = 40°F T_{inlet}=120°F
MSFC	1 cover	33.1	45.9
	2 covers	41.2	49.9
Black paint	1 cover	21.2	40.0
	2 covers	25.6	42.1

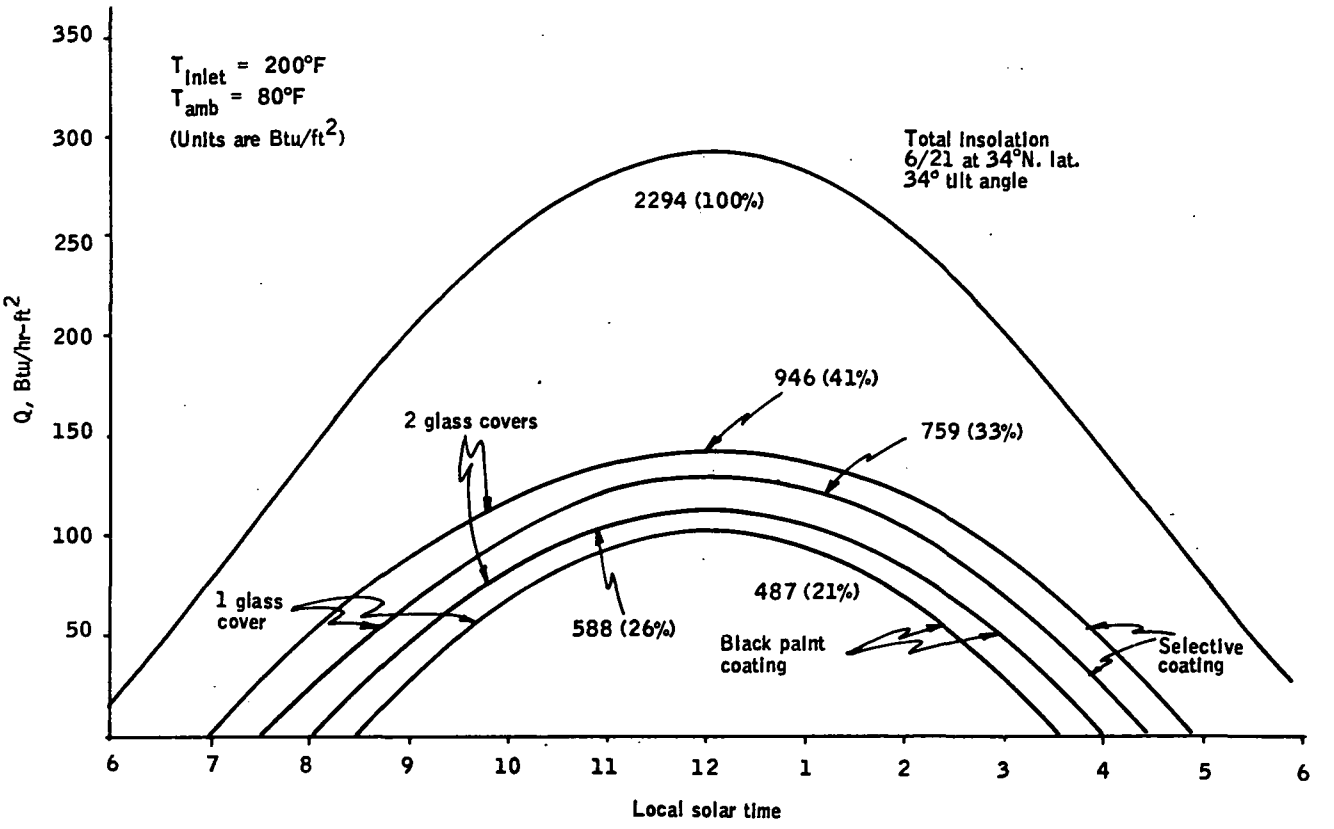

Figure 49. Daily Collection Curve for Summer Cooling

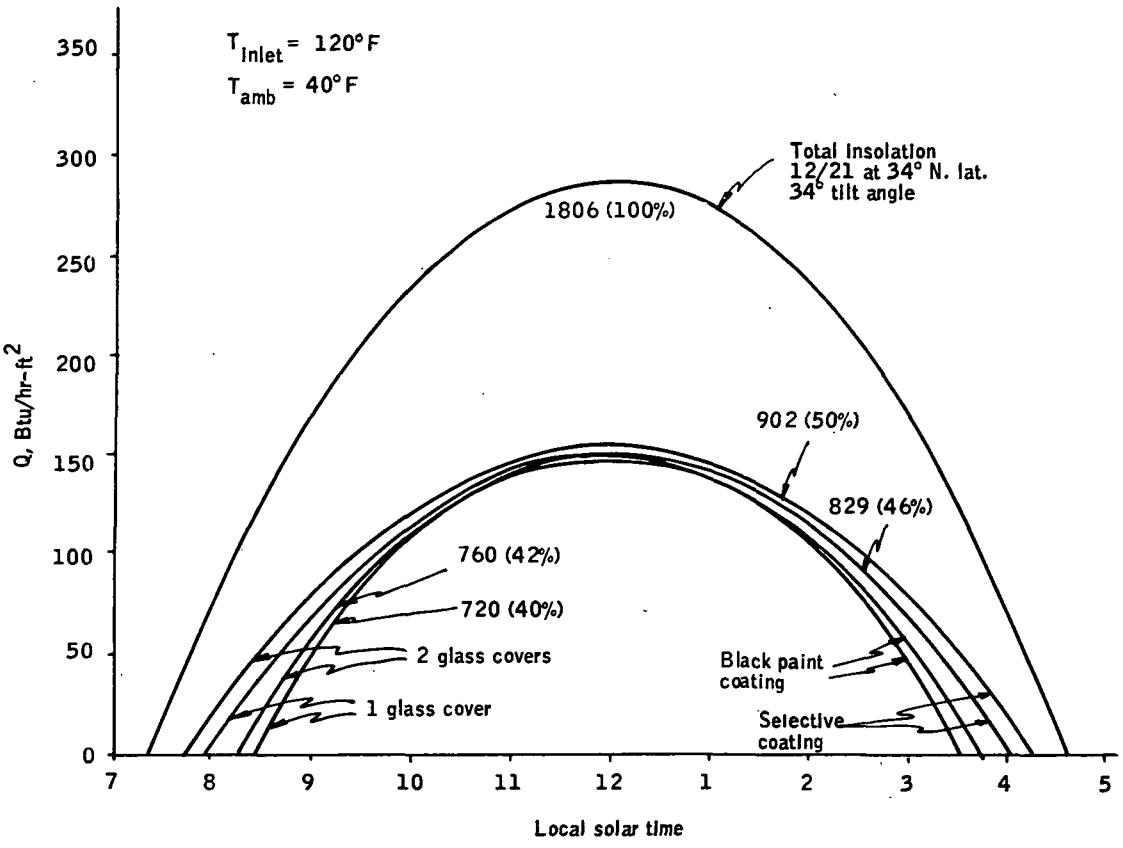

Figure 50. Daily Collection Curve for Winter Heating

Table 16 summarizes the percentage increase due to the additional cover and also compares the MSFC collector with the well designed black painted collector.

TABLE 16. - ENERGY COLLECTION INCREASE COMPARISON BETWEEN SEVERAL COLLECTOR CONFIGURATIONS

Collector configuration comparison		Percentage increase	
Increase from	To	Summer	Winter
MSFC 1 cover	MSFC 2 cover	24.5	8.7
BLPT 1 cover	BLPT 2 cover	20.8	5.2
BLPT 1 cover	MSFC 1 cover	56.1	14.8
BLPT 2 cover	MSFC 2 cover	60.9	18.5

In all cases, the MSFC collector is superior to the conventional black painted collector. The MSFC collector is significantly better than the black painted collector for heating, and especially so for cooling. This is due to the selective coating and also the increase in insulation due to the box material itself.

OUTDOOR TESTING AT MARSHALL SPACE FLIGHT CENTER

Two assembled collector units (1 each of one and two cover units) were delivered to NASA MSFC on 24 October 1975 for testing. They were instrumented with iron constantan thermocouple wire (Type J). The thermocouples were installed using metalized silicone rubber cement and aluminum foil tape in the locations specified by NASA MSFC. External thermocouples were not attached but were delivered with the collectors.

The collectors were mounted on an outdoor test rack during January, 1976 by NASA personnel. Shortly thereafter, two conditions were noted by the NASA technicians: the inner glass had cracked on the two cover collector, and a film had collected on the inner glass surface.

The contract monitor called on 27 January 1976 to indicate that he had removed the two cover collector from the test rack because of a cracked inner cover. He further indicated that both the one and two cover collectors had condensation partially obscuring the cover glass(es) and also that both collectors were holding some water from a rain storm. The contract monitor's intent was to replace the broken cover glass and resume testing; however, he did not have a set of collector drawings and was reluctant to disassemble the collector without them.

It was subsequently agreed that the contractor's engineers would visit the facility to evaluate the condition of the collectors. Upon arrival at MSFC, the engineers examined the two cover collector and made the following observations:

- The inner cover had a series of cracks around its periphery, similar to those previously observed at the contractor's plant, resulting from no flow operation with a nonselective absorber coating.
- Both cover glasses were coated with some outgassing by-product, having an odor similar to that of Krylon.
- Deposits of a brown fluid were noted on the sides of the cover frame near the top edge of the collector.
- Approximately one quart of fluid, apparently water, drained from the box beneath the absorber when it was tipped to a vertical position.

- A white granular deposit, probably a mineral deposit, was noted on the bottom outside surface of the box and also on sections of the insulation covering within the box.

- The overcoat had apparently evaporated off of the top one-third of the panel. The middle third seemed quite thick and was sticky to the touch.

Operating data were obtained from the technician who installed the collector on the test rack. He indicated that the inner cover glass had cracked during test set-up after approximately three hours of no-flow operation. The outgassing byproduct occurred during this no-flow operation period. This operating period was followed by 2 days of rain on the exposed collector and another period of no-flow operation, during which additional cracking of the inner cover glass occurred.

The glass failure was apparently due to the thermal stresses in the second (inner) glass cover. The failure could be due to the higher stagnation temperature resulting from the superior insulation qualities of the housing or due to insufficient selectivity of the iron oxide coating ($\alpha \sim .90$, $\epsilon \sim .20$).

The overcoat evaporization is believed to have been due to the high stagnation temperature reached. The collector had not been connected to the instrumentation prior to failure so the stagnation temperature remains unknown.

The overcoat evaporization and deposition on the glass were also evident on the single cover collector which was still on the test rack. This collector had been instrumented but stagnation temperature readings were not available.

Corrective action taken while at MSFC included the following:

- The cover frame was removed and the broken inner cover glass replaced.

- Breathing holes were drilled through the sides of the cover frame between the glass layers. Vent holes were also drilled in the sides of the box.

- Three weep holes were drilled in the bottom edge of the box and fitted with rivets secured by tinnerman fasteners.

Several additional corrective actions were proposed, to be taken by both the contractor and MSFC.

The proposed contractor actions included the following tasks:

- Procure tempered cover glass for installation by MSFC.
- Provide an additional absorber plate with a selective black chrome coating.
- Evaluate the need for additional condensation protection, and, if necessary, provide a desiccant system.

For its part of the corrective action program, MSFC would:

- Add weep holes to one-cover collector.
- Return two-cover collector to test rack for additional no-flow operation.
- Test the effect of breathing holes on the condensation problem.
- Provide no-flow operating temperature data for the one-cover collector.
- Test a two-cover collector with the black chrome absorber coating and tempered glass.

CONCLUSIONS AND RECOMMENDATIONS

The collector design developed during the course of this program was intended to provide good collection efficiency with a low production cost in high volume. Three significant design features were employed to achieve the cost/performance objective: an extruded aluminum cover system similar to conventional storm window glazing; oxidation coating on the steel absorber; and an insulation material for the collector housing.

As was evidenced by the performance test results, the use of a nonmetallic housing significantly reduces U_L in both the one-cover and two-cover collector models. Couple this performance improvement with the potential low cost of manufacturing (approximately $\$.30/ft^2$ of finished collector in the 3' x 4' size delivered) and the use of a processed-paper collector housing appears to have considerable promise. Certainly more investigation should be performed to further qualify the material in terms of durability and expected lifetime. The scope of this program did not permit extensive life testing nor did it provide for adequate examination of possible additives to improve the durability and physical characteristics of the material. In light of the potential advantages to be derived from the use of the processed-paper housing, further development activity, particularly in the areas of determining useful life and additives for extending useful life, is recommended.

The iron-oxide absorber coating, while less effective than the more common black-nickel or black-chrome electroplate coatings, offers hope of a low-cost selective absorber coating. The difficulty observed during testing at Marshall Space Flight Center was a weakness in the particular organic overcoat applied to the iron oxide, rather than a fault of the oxide coating itself. Since the iron-oxide coating requires an overcoat to raise its absorptance into the .90 plus range, it is strongly recommended that additional effort be expended on the determination of a suitable organic material that will increase the absorptance without raising the emittance to unacceptable levels, and yet still not degrade at high temperature. This, of course, was the failure mode noted during operation at Marshall Space Flight Center: the organic overcoat evaporated from the absorber and condensed on the cover glass while the collector was left under no-flow conditions. While the plate temperature was not measured during the no-flow operating period, it is expected that plate temperatures in excess of 400°F were experienced.

The physical design of the collector, particularly that of the cover system, proved to be easy to both manufacture and assemble. It fastens rapidly to the collector housing and provides a weather seal without the use of adhesives or sealants. This enables the collector to be easily serviced when installed on a roof. One disappointing aspect of the cover design was the failure of the inner cover glass under no-flow conditions. The failure

observed at Marshall Space Flight Center was one of thermal stress on the inner cover glass. Substitution of tempered glass will eliminate this failure mode, but it will also increase the material cost of the collector. A second solution is to substitute a lower-emissivity coating on the absorber, thereby reducing the reradiation to tolerable levels. In view of the present difficulties observed with the iron-oxide coating, the cost of substituting a black-chrome or black-nickel coating might be offset by avoiding the need for tempered glass. A study of this possibility is recommended.

Since the use of a processed-paper box significantly reduces the slope of the collector performance curve, the analysis performed early in the program to compare the performance of the one- and two-cover versions of the same collector should be reexamined. It may well appear that the two-cover collector does not make economic sense for most applications with this collector design. This conclusion was drawn for the case of an Atlanta installation early in the program, but it was not obvious if the one-cover collector performance was superior for more severe climatic applications, such as heating in Minneapolis. It is recommended that a study of application in key cities around the country be performed to resolve this question. Obviously, the applicability of the one-cover collector provides a distinct cost savings to the would-be user.

APPENDIX A
THERMAL DESIGN ANALYSIS

Analysis and tests have indicated that a flat plate absorber with parallel flow passages is an effective design in transferring the energy absorbed on the surface to the liquid passing through the collector. In general, the key question is: What is the average plate temperature compared with the average fluid temperature in the collector? The difference in these two temperatures is due to the thermal resistance between the absorber surface and the fluid. The resistance is comprised of the conduction path in the plate and the thermal boundary layer in the fluid. The contractor has a computer program which has been effectively used to evaluate these effects for many different flow patterns and passage designs.

The thermal relationships that govern flat plate collector performance are fairly well understood and are readily available in the literature. To evaluate the performance impact of various collector configuration changes, it is necessary to search the literature, assemble the necessary analytic relationships, and actually calculate the thermal performance for each case of interest.

The following paragraphs present an analysis of two areas of interest: thermal and flow considerations for sizing and spacing of absorber flow tubes, and spacing between the absorber and cover or covers.

Absorber Flow Tube Size and Spacing Considerations

In this section, the overall thermal efficiency is determined for changes in certain design parameters of a typical flat plate collector. Specifically, the parameters varied were cross tube dimensions, intertube spacing, absorber material, material thickness, flow rate, and absorber header size. The typical flat plate collector considered has the following characteristics:

- Width -- 76.2 cm (30 in.)
- Length -- 114.3 cm (45 in.)
- Working fluid -- Water
- Tube geometry -- Circular

Factors Influencing Collector Thermal Efficiency

The rate of useful heat collection is given by the rate of incident solar radiation minus heat losses:

$$q_u = \left[q_a - U_L \left(T - T_a\right)\right] \tag{A1}$$

where

q_u = useful heat collected, W (Btu/hr)

q_a = incident solar flux on absorber surface, W (Btu/hr)

U_L = a lumped loss term, W/°C (Btu/hr-°F)

T = collector temperature, °C (°F)

T_a = ambient temperature, °C (°F)

Since q_a is fixed, the collector rate is optimized by making $(T - T_a)$ as small as possible while still maintaining a net heat flux to the working fluid (i. e., make $T - T_{w-o}$ small, where T_{w-o} is the temperature of the incoming fluid).

A thermal efficiency factor, F_R, is defined by Bliss[A1] as:

$$F_R = \frac{\text{actual heat collection rate}}{\text{heat collected if collector were at incoming fluid temperature}}$$

and an auxiliary efficiency factor, F':

$$F' = \frac{\text{actual heat collector rate}}{\text{heat collected if collector were at average fluid temperature}}$$

Using the above definitions, Equation (A1) can be written in the form:

$$q_u = F_R \left[q_a - U_L \left(T_{w-o} - T_a\right)\right] \tag{A2}$$

where U_L = overall heat loss coefficient.

The expression for F_R in terms of F', U_L, and flow rate per unit collector area, kg/hr-m^2 (lb/hr-ft^2), G, was derived by Bliss[A1]:

$$F_R = \frac{GC_p}{U_L}\left[1 - e^{-\left(F'U_L/C_pG\right)}\right] \tag{A3}$$

A1 Bliss, Raymond W., The Derivation of Several "Plate Efficiency Factors" Useful in the Design of Flat-Plate Solar Heat Collectors. Solar Energy 3, 55 (1959).

where C_p = specific heat of fluid, J/kg-°C (Btu/lb-°F), and

$$F' = \frac{1}{\frac{w\,U_L}{\pi d h_c} + \frac{1}{\frac{d}{w} + \left[\frac{w\,U_L}{d\,U_c} + \frac{1}{(1 - d/w)F}\right]^{-1}}} \tag{A4}$$

and

$$F = \frac{\tanh U_L (w - d)/2\,k\,M}{U_L (w - d)/1\,k\,M} \tag{A5}$$

where

k = conductivity of absorber material, W/m-°C (Btu/hr-ft-°F)

d = tube diameter, m (ft)

w = tube spacing, m (ft)

M = absorber material thickness, m (ft)

h_c = heat transfer coefficient, W/m^2-°C (Btu/hr-ft^2-°F)

U_c = bond conductance between tube and panel, W/°C (Btu/hr-°F)

The heat transfer coefficient for flow in the cross tubes of the absorber panel was calculated assuming developing laminar flow. The correlation by Rohsenow[A2] is given as:

$$Nu_x = \frac{h_c d}{k_f} = 4.36 + \frac{.023\,(d/x)\,Re\,Pr}{1 + .0012\,(d/x)\,Re\,Pr} \tag{A6}$$

where

Nu = Nusselt number

x = Distance along tube

Pr = Prandtl number = 0.72 for water

Re = Reynolds number = $4\theta/\pi d\nu$

[A2] Rohsenow, W.M. and H. Choi, Heat, Mass and Momentum Transfer. Prentice-Hall (1961), p. 142.

C-2

and

θ = flow rate per tube, kg/hr (lb/hr)

ν = dynamic viscosity, $N \cdot s/m^2$ ($lbf \cdot s/ft^2$)

The average heat transfer coefficient for each tube is:

$$\overline{h_c} = \frac{k_f}{dL} \int_0^L Nu_x \, dx$$

Results of Computations

The efficiencies F_R, F', F, and the heat transfer coefficient, h_c, were computed for different tube diameters and spacings (Tables A1 and A2), absorber materials and thicknesses (Tables A3 and A4), and flow rates (Table A5), assuming a loss rate of $U_L = 1.2$. Previous analysis has shown that U_L is constant to within 1 percent over the ranges of the variables presented here.

TABLE A1. - EFFECT OF TUBE DIAMETER

[Steel, M = 1.5mm (0.060 in.)
w = 5.1 cm (2.0 in.)
θ = 4.5 kg/hr (10 lb/hr)]

d, in.	F	F′	F_R
0.1	.9804	.9479	.9186
0.2	.9824	.9505	.9210
0.3	.9843	.9528	.9232
0.4	.9860	.9548	.9251
0.5	.9877	.9567	.9268

TABLE A2. - EFFECT OF TUBE SPACING

[Steel, M = 1.5 mm (0.060 in.)
d = 2.5 mm (0.1 in.)
θ = 4.5 kg/hr (10 lb/hr)]

Tube spacing, w, in.	h_c, Btu/hr-ft^2-°F	F	F′	F_R
2.0	212	.9804	.9479	.9186
2.5	212	.9691	.9298	.8947
3.0	212	.9558	.9102	.8700
3.5	212	.9404	.8893	.8448
4.0	212	.9233	.8674	.8192
4.5	212	.9047	.8449	.7935

TABLE A3. - EFFECT OF ABSORBER MATERIAL

[M = 1.0 mm (0.040 in.)
θ = 4.5 kg/hr (10 lb/hr)
d = 2.5 mm (0.1 in.)
w = 5.1 cm (2.0 in.)]

Material	F	F′	F_R
Steel	.9710	.9395	.9107
Aluminum	.9939	.9598	.9297
Copper	.9966	.9962	.9321

TABLE A4. - EFFECT OF ABSORBER THICKNESS

[Steel, d = 2.5 mm (0.1 in.)
w = 5.1 cm (2.0 in.)
θ = 4.5 kg/hr (10 lb/hr)]

M, in.	F	F′	F_R
.060	.9804	.9479	.9186
.040	.9710	.9395	.9107

TABLE A5. - EFFECT OF FLOW RATE PER TUBE

[Steel, M = 1.5 mm (0.060 in.)
d = 2.5 mm (0.1 in.)
w = 5.1 cm (2.0 in.)]

θ, lb/hr	h_c, Btu/hr-ft^2-°F	F	F′	F_R
10	212.4	.9804	.9479	.9186
20	223.5	.9804	.9495	.9347
50	250.8	.9804	.9529	.9469

The results give an indication of the influence of the principal design parameter on the thermal efficiency, F_R. The efficiencies were computed for tube sizes between 0.25 cm and 1.3 cm (0.1 and 0.5 in.) and spacings between 5.1 cm and 11.4 cm (2 and 4.5 in.). Over this range it was found that the tube diameter has only a slight effect on F_R, as seen in Table A1. Efficiency decreases roughly 3 percent for each 1.3-cm (0.5-in.) increase in spacing, as shown in Table A2. Physically, an increase in the spacing results in fewer tubes per collector and, for a given cross-tube flow rate, this means a reduction in the flow rate per unit area of collector. It also results in an effectively longer and, therefore, less efficient fin (i.e., less efficient heat transfer between collector and the cross tube).

Increasing the cross-tube diameter has the result of slightly increasing the efficiency. This is somewhat surprising in view of the large decrease in h_c entailed by an increase in tube size. However, it can be seen from Equation (A4) that the d dependence of h_c is neutralized in F' and, in addition, a large tube size allows more incident solar radiation to hit the tubes directly. Therefore, this slight increase in F_R seems reasonable.

Absorber material enters into the total efficiency through the fin efficiency, F. As can be seen in Table A3, the most drastic change in materials (from steel to copper) produces only a 2- or 3-percent change in F_R.

A decrease in the absorber thickness appears to decrease F_R by about 0.1 percent or less, as shown in Table A4. From the expression for fin efficiency, F, one can see that tube spacing and tube diameter will have an effect on this, but in the thickness range 1.0 mm to 1.5 mm (0.04 to 0.060 in.), F differs only slightly.

Finally, the flow rate per tube determines how effectively heat can be transferred to the fluid by the absorber. Table A5 indicates about a 3-percent increase in F_R for a fivefold increase in flow rate.

Effects of Cross-Tube Geometry and Header Size

Previous considerations of the flow problem indicate a more efficient transfer of heat from the absorber if the flow is uniformly distributed through the cross tubes. Since the flow through each tube is dependent on the pressure change between the entrance and exit, this change should be kept as uniform as possible. Considering the sketch of a collector that follows, an expression for the change in pressure along the supply header can be written as:*

$$(\Delta p)_{supply} = 4f\left(\frac{X}{D}\right)\rho\ \frac{V^2}{2}\ (X) - d\left(K\rho\frac{V^2}{2}\right) \qquad (A8)$$

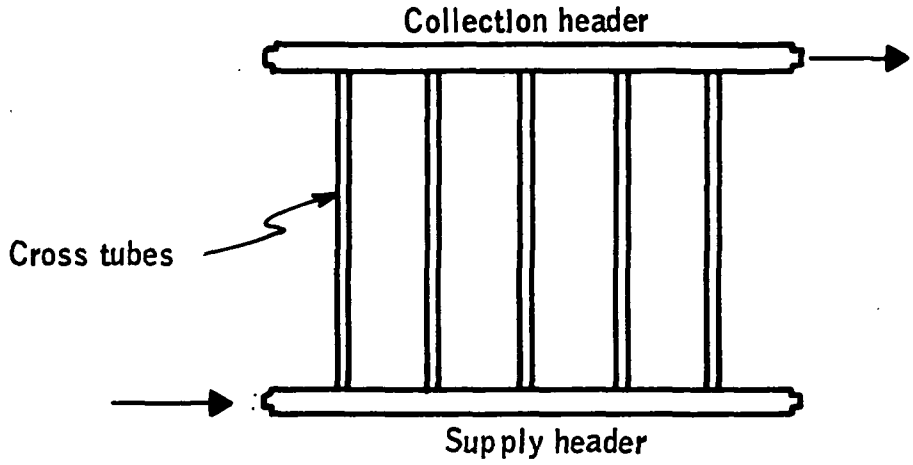

The first term is the pressure drop due to viscosity and the second represents the pressure gain due to the loss of momentum to the cross tubes. In the equation, K is some constant factor depending on the tube entrance conditions. A similar expression for the pressure change along the collection header can be written as:

$$(\Delta p)_{coll} = 4f\left(\frac{X}{D_H}\right)\rho V_c^2 + d(K\rho V_c^2) \qquad (A9)$$

*See Table A6 for definition of symbols applicable to Equations (A8) through (A20).

TABLE A6. - LIST OF SYMBOLS

Symbol	Description
f_H	Friction factor (header)
X	Distance along heater, m (ft)
V	Velocity along header, m/hr (ft/hr)
K	Entrance loss coefficient
D	Header diameter, m (ft)
ρ	Density, kg/m^3 (lbm/ft^3)
$(\Delta p)_{coll}$	Pressure change along collection header, kg/m^2 (psig)
V_c	Velocity along collection header, m/hr (ft/hr)
n	Number of cross-tube station (measure from entrance)
N	Total number of cross tubes
L	Length of header, m (ft)
V_s	Velocity along supply header, m/hr (ft/hr)
c	Velocity in cross tubes, m/hr (ft/hr)
q	Flow rate per tube, kg/hr (lbm/hr)
$\overline{\Delta p}$	Average pressure change across two headers, kg/m^2 (psig)
θ	Total flow rate, kg/hr (lbm/hr)
f_t	Friction factor (tubes)
ℓ	Length of cross tubes, m (ft)
z_1	Width of rectangular tube, m (ft)
z_2	Height of rectangular tube, m (ft)
$\tilde{f}$	Friction factor corrected for rectangular tube

Since the collector consists of a finite number of cross tubes, the equivalent discrete equations for the n^{th} cross-tube station can be written as:

$$(\Delta p)_{supply} = \frac{4fn}{N}\left(\frac{L}{D}\right)\rho V_s^2 - nK\rho c^2 \tag{A10}$$

$$(\Delta p)_{coll} = \frac{4fn}{N}\left(\frac{L}{D}\right)\rho V_c^2 + nK\rho c^2 \tag{A11}$$

where L is the total length of the header, N is the total number of cross tubes, and c is some appropriate mean cross-tube velocity. In terms of the overall flow rate, Q, and flow rate per tube, q, we can write the above equations in the form:

$$(\Delta p)_s = \frac{64fn}{N}(Q - nq)^2\left(\frac{L}{D}\right)\frac{1}{\rho\pi^2 D^4} - \frac{16nK\,q^2}{\pi^2\rho d^4} \tag{A12}$$

$$(\Delta p)_{coll} = \frac{64n^2q^2}{\rho\pi D^4}\left(\frac{L}{D}\right)\frac{fn}{N} + \frac{16nKq^2}{\pi^2\rho d^4} \tag{A13}$$

Thus,

$$(\Delta p)_s - (\Delta p)_c = \overline{\Delta p} = \frac{64fn}{\rho\pi^2 N D^4}\left(\frac{L}{D}\right)(Q^2 - 2nqQ) - \frac{-32nKq^2}{\pi^2\rho d^4}$$

or, since $q = Q/N$, we have:

$$(\Delta p) = \frac{64fn}{\rho\pi^2 N D^4}\left(\frac{L}{D}\right)\left(\frac{Q^2 - 2nQ^2}{N}\right) - \frac{32nKQ^2}{N^2\pi^2\rho d^4} \tag{A14}$$

Notice that the pressure difference varies roughly parabolically down the length of the header. Now, if this fluctuation in pressure is small compared with the cross-tube viscous pressure drop, then we can assume the flow will be reasonably uniform. The cross-tube pressure drop is

$$(\Delta p)_t = 4f\left(\frac{\ell}{d}\right)\rho c^2 = 4f_t\left(\frac{\ell}{d}\right)\frac{16q^2}{\rho\pi^2 d^4}$$

where ℓ is the cross-tube length.

Therefore,

$$(\Delta p)_t = 64 f_t \left(\frac{\ell}{d}\right) \frac{q^2}{\pi^2 d^4 \rho} \tag{A15}$$

and the largest Δp from Equation (A7) is roughly

$$(\Delta p)_{max} = \frac{64f}{\rho\pi^2 N D^4} \left(\frac{L}{D}\right) Q^2 - \frac{32nKQ^2}{N^2\pi^2\rho d^4} \tag{A16}$$

We therefore require

$$\frac{64f_H}{\rho\pi^2 N D^4} \left(\frac{L}{D}\right) Q^2 - \frac{32KQ^2}{N^2\pi^2\rho d^4} L << 64 f_t \left(\frac{\ell}{d}\right) \frac{Q^2}{N^2 \rho\pi^2 d^4} \tag{A17}$$

or

$$\frac{f_H}{ND^4} \left(\frac{L}{D}\right) - \frac{K}{2N^2 d^4} << f_t \left(\frac{\ell}{d}\right) \frac{1}{N^2 d^4}$$

or

$$\frac{\ell}{d^4} \left[f_t \left(\frac{\ell}{d}\right) + \frac{K}{2}\right] >> f_H \frac{N}{D^4} \left(\frac{L}{D}\right)$$

Thus,

$$\frac{D^4}{d^4} >> \frac{N f_H (L/D)}{f_t \left(\frac{\ell}{d}\right) + \frac{K}{2}} \tag{A18}$$

for a noncircular cross section. According to Rohsenow and Choi, D may be interpreted as an equivalent diameter given by:

$$D_e = \left[2\left(\frac{z_1 + z_2}{z_1 z_2}\right)\right]^{-1} \tag{A19}$$

and a correction function, ϕ, is introduced so that

$$\tilde{f} = 16/Re_{d_e} \phi \tag{A20}$$

Although rather crude, Equation (A18) gives some indication of the necessary relationship between cross tubes and header size. A small L/D would tend to increase the required D/d ratio (i.e., smaller tubes or larger header), or a large number of cross tubes would require a larger D/d ratio.

Summary

To summarize, we have found that for reasonably small variations in the design parameters of a flat-plate solar collector, the overall thermal efficiency as given by the Bliss formulation is altered only slightly. For tube diameters between 2.5 mm and 12.7 mm (0.1 and 0.5 in.), a less than 3 percent change in F_R per every 2.5 mm (0.1 in.) of variation can be expected. For tube spacing in the range 5.1 cm to 11.4 cm (2.0 to 4.5 in.), a similar 3 percent change for each 1.3 cm (0.5 in.) is found. The significant material change produced only about a 2 or 3 percent change in the efficiency. In the thickness range of 1.0 mm to 1.5 mm (0.040 to 0.060 in.), a change of less than 1 percent is found, and, finally, for flow rates in the range from 4.5 to 22.7 kg/hr tube (10 to 50 lb/hr tube), there is less than a 5 percent effect on F_R. The flow uniformity seems to depend primarily on a reasonably high ratio header to cross tube size, so that variations in the pressure between supply and collection headers is bounded by the viscous pressure drop across the tubes.

Collector Cover to Absorber Panel Spacing Considerations

Heat is lost from the absorber panel by conduction through the bottom and sides of the collector assembly insulation and by convection and radiation through the top cover. The convection heat transfer between the absorber panel and cover or between covers is dependent upon the air gap spacing. The following analysis was performed to assess the importance of absorber to cover spacing.

Free convection between parallel surfaces has been studied for some time and a number of correlations exist between the heat transfer coefficient and the product of the Grashof and Prandtl numbers. This product (the Rayleigh number) is a measure of the relative importance of bouyant forces and can be written as the product of the following quantities:

$$Ra = g\beta \, d^3 \, \frac{\Delta T \, Pr}{\nu^2} \qquad \text{(A21)}$$

where

Ra = Rayleigh number

g = acceleration of gravity, m/sec^2 (ft/sec^2)

β = coefficient of thermal expansion, $°C^{-1}$ ($°F^{-1}$)

ΔT = temperature difference between two surfaces, °C (°F)

d = spacing between surfaces, m (ft)

ν = kinematic viscosity, m^2/sec (ft^2/sec)

Pr = Prandtl number = ν/α

α = coefficient of thermal diffusivity, m^2/sec (ft^2/sec)

The relationship between the Rayleigh number and the convective heat transfer coefficient, h_c, has the form:

$$Nu \equiv \frac{h_c d}{k_{air}} = C(Ra)^n \tag{A22}$$

where Nu is the Nusselt number, c and n are empirically determined constants, and k_{air} is the thermal conductivity of air in W/m-°C (Btu/hr-ft^2-°F).

Tabor[A3] expressed the Rayleigh number in the following way:

$$Ra = a\, d^3\, \Delta T \tag{A23}$$

where

$$a = g \beta \rho^2\ Cp/\mu\, k_{air}$$

Using Equation (A23), we may rewrite Equation (A22) in the form:

$$h_c = C(k_{air}\, a^n) \left(\frac{\Delta T^n}{d^{1-3n}} \right) \tag{A24}$$

As can be seen, for fixed ΔT, h_c decreases with increasing gap distance. However, as d increases so does the Rayleigh number, and experiments indicate that the coefficient, C, and the exponent, n, will be altered. Tabor recommends the following correlations between h_c and Ra for typical flat-plate collectors at various orientations:

[A3] Tabor, H., Radiation, Convection and Conduction Coefficients in Solar Collectors. Bull, Res. Council of Israel, Vol. 6C, pp. 155-176 (1958).

- Horizontal planes, heat flow upwards:

$$Nu = 0.168\,(Ra)^{0.281} \text{ for } 10^4 < Ra < 10^7$$

- 45-degree inclination, heat flow upwards:

$$Nu = 0.102\,(Ra)^{0.310} \text{ for } 10^4 < Ra < 10^7$$

- Vertical planes:

$$Nu = 0.0685\,(Ra)^{0.327} \text{ for } 1.5 \times 10^5 < Ra < 10^7$$

For most collectors the Rayleigh number falls between 10^4 to 10^7 so that the functional dependence of h_c on the gap distance can be seen immediately from Equation (A24). For a collector tilted at 45 degrees:

$$h_c \sim \frac{1}{d^{0.07}} \tag{A25}$$

Therefore, doubling the distance between the cover and absorber decreases the convective heat transfer by about 5 percent.

The energy transfer between the absorber panel and the first cover is exactly the same as between any other two adjacent glass covers and is also equal to the energy lost to the surroundings from the top cover. The heat transfer equations that describe the energy transfer are:

$$q/A = h_{c1}\,(T_c - T_{g1}) + \epsilon_{c1}\sigma\left[T_c^{\,4} - T_{g1}^{\,4}\right] + K(T_c - T_{g1})/d_1 \tag{A26}$$

$$q/A = h_{c2}\,(T_{g1} - T_{g2}) + \epsilon_{12}\sigma\left[T_{g1}^{\,4} - T_{g2}^{\,4}\right] + K(T_{g1} - T_{g2})/d_2 \tag{A27}$$

$$q/A = h_{cij}\,(T_{gi} - T_{gj}) + \epsilon_{ij}\sigma\left[T_{gi}^{\,4} - T_{gj}^{\,4}\right] + K(T_{gi} - T_{gj})/d_{ij} \tag{A28}$$

$$\vdots$$

$$q/A = h_w\,(T_{gn} - T_a) + \epsilon_{na}\,\sigma\left[T_{gn}^{\,4} - T_a^{\,4}\right] \tag{A29}$$

where

q/A = heat loss in Btu/hr-ft^2

h_{cij} = convection heat transfer coefficient between i^{th} and j^{th} covers

T_c = absorber temperature

T_{gi} = i^{th} cover temperature

ϵ_{ij} = effective emissivity between i^{th} and j^{th} covers

σ = Boltzmann constant

K = conductivity of air

d_{ij} = spacing between i^{th} and j^{th} covers

h_w = convective heat transfer coefficient for outer cover = 4 to 5 Btu/hr-ft^2-°F

T_a = ambient temperature

n = number of covers

a = ambient

It is assumed that the effective sky temperature is equal to the ambient temperature.

Each equation represents the heat flux from one cover to the next via convection, radiation, and conduction, the last equation is the heat flux from the n^{th} cover to the environment. The equations were solved for both a single-cover and a two-cover collector. The thermal conductivity, viscosity, and Prandtl number for air were assumed constant. For Rayleigh numbers less than 10^4, it was assumed that

$$Nu = 1 \quad \text{or} \quad h_c = K/d \tag{A30}$$

The results of computations are shown graphically in Figure A1 for a two-cover collector. The total heat loss to the environment is plotted versus the outer cover spacing for three different inner-cover spacings. The break in the graph represents the regime where the Rayleigh number is near 10 000 and a good correlation was unavailable. Below an outer spacing of about 1.9 cm (0.75 in.) the Rayleigh number is below 10 000 and the convection and conduction losses are assumed equal. Above 2.2 cm (0.875 in.) the correlation introduced by Tabor was used for the convected heat loss.

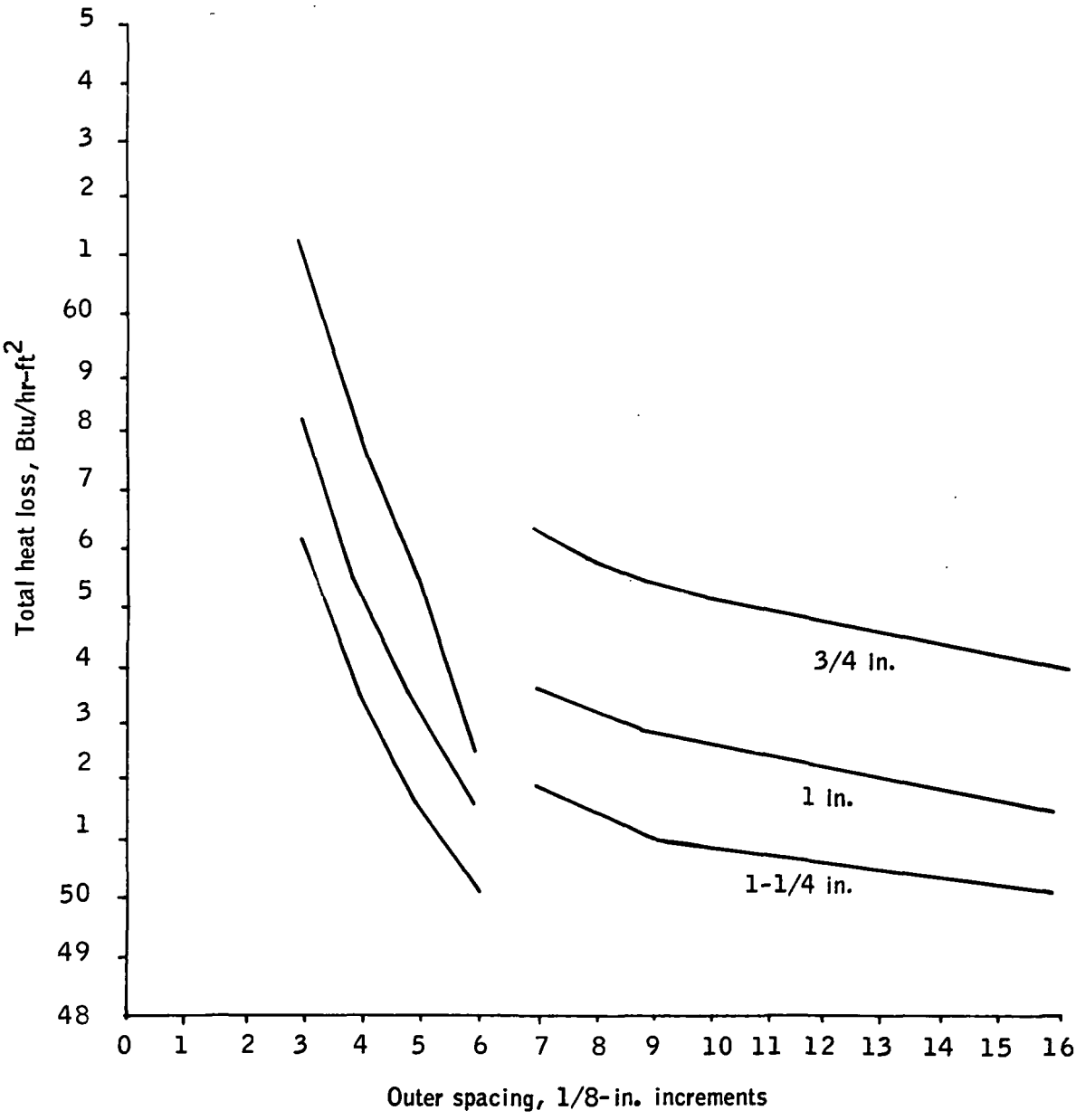

Figure A1. Heat Loss versus Cover Spacing

APPENDIX B
SELECTIVE ABSORBER COATING ANALYSIS

For a heating and cooling system, the primary requirements for the absorber coating are high optical efficiency (high solar absorptance, α, and low infrared emittance, ϵ), low cost, and satisfactory environmental durability. These properties are discussed in this appendix for:

- Black nickel
- Black chrome
- Copper oxide
- Substrates
- Iron oxide coatings on steel
- Organic overcoats

Following the discussion of these coating materials is a supplementary discussion of iron oxide and organic overcoating.

Coating Description

Black Nickel

Black nickel is a nickel-zinc-sulfur complex which can be applied to many substrates by an electroplating process. This coating achieves high solar absorption through the combined effects of interference and absorption and is transparent in the infrared (2 to 20 μm), so that a low-emittance metal substrate will show through in that region.

The contractor's preliminary durability tests on black nickel indicated it could withstand 1 week in air at approximately 550°F, approximately 1/3 sun years of ultraviolet, and the equivalent of 40 years of thermal cycles from room temperature to ~104°C (~220°F). Therefore, a program to improve the optical efficiency of the coating was initiated in which the effects of bath composition, temperature, and pH and plating current densities and times were evaluated. It was found that the composition could be altered so that the maximum effect of a natural absorption of the coating in the solar wavelengths and an optical interference effect could be obtained. These studies enabled us to improve the coating absorption from approximately 86 percent (typical of industrial plating job shops) up to approximately 96 percent while achieving an emittance of 7 percent at 200°F. The spectral reflectance of such a coating is shown in Figure B1.

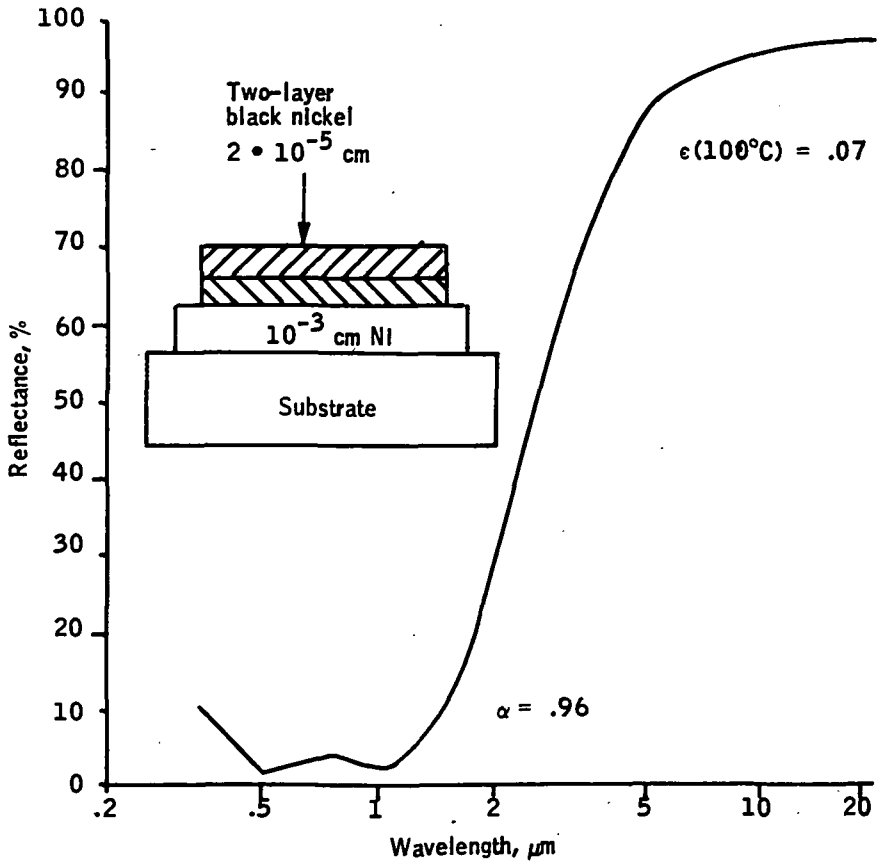

Figure B1. Spectral Reflectance of Black Nickel Selective Coating

The contractor's investigation of black nickel coatings included process scale-up to 3 x 4 ft panels, evaluation of long-term bath degradation, and optical reproducibility. The scale-up was successful except for a tendency for color fringes to form near the edges of large panels due to optical interference effects. This problem does not significantly affect performance and can be minimized with careful placement of the panel and anodes during the electroplating. The bath itself was found to be remarkably stable over 5 months of use during which approximately 150 panels were plated. Under constant use, it was necessary only to adjust pH every other day and maintain a critical thiocyanate ion concentration every week or two.

All panels that were measured (approximately 15) had ≥94 percent solar absorptance with emittance less than 10 percent at 200°F.

There were, however, variations in panel resistance to the combined effect of thermal and humidity cycling. A test regularly used follows the procedure of MIL-STD-810B, Method 507, Procedure I. This test consists of a thermal

and humidity cycle, from room temperature to 71°C (160°F) at 95-percent RH and from 71°C to room temperature at >85-percent RH, over a 24-hour period. This is a very severe, accelerated environmental test. The test conditions impose a vapor pressure on the panels which constitutes the major force behind moisture migration and penetration. Some coated panels survived over 1 week under this test, while others completely corroded after 1 day. Some coating parameters which may be important to humidity resistance include:

- Low thiocyanate concentration
- "Old" (oxidized) bright nickel substrates
- Pitted nickel substrate (galvanic cell problems)

There may be other parameters not yet identified.

A possible solution to the humidity-induced corrosion problem might be the use of humidity-resistant, silicone-based coatings which can be applied over the solar absorber coating. These coatings have high-temperature stability, do not greatly increase the overall emittance values, and in most cases increase the solar absorptivity due to their low refractive index. These coatings provide a degree of corrosion protection, but it is not known if they lead to a significant long-term improvement.

Black Chrome

Black chrome is a commercial electroplated chrome-oxide coating with diffuse reflectance properties. Manufacturer's data indicate that the coating remains black to temperatures of 900°F in air. Significantly, a black chrome coating developed by the contractor showed no change in optical properties after 1 week in the MIL-STD-810B humidity test.

We have briefly studied the effects of current density, bath temperature, and plating times on the optical performance of black chrome. Our best black chrome coating had an α of 96 percent with ϵ (200°F) of 12 percent (on nickel substrate).

Copper Oxide

Our experience with CuO coatings is rather limited, since the performance achieved in early studies could not greatly improve upon literature values of $\alpha = .90$ and $\epsilon = .20$. More work with this chemical-dip-type coating is justified, due to its relatively low cost; however, it does require a copper substrate or copper absorber plate.

Substrates

The primary optical requirement of the substrate* is to provide a surface with low infrared emittance. The material also must not easily corrode since the thin black absorber coating provides little protection.

Aluminum, zinc (galvanized steel), and copper provide substrates somewhat stable to corrosion when oxidized but have fairly high emittance under those conditions (greater than 10 percent). Nickel has often been used, since it forms a stable coating for several metals and results in a low emittance ($\sim .07$) substrate.

The Contractor's experience has been primarily with nickel-coated steel substrates. Steel was selected because of its low cost, high strength, ease of fabrication, and compatibility with electroplated nickel. The requirements for nickel layer are quite severe, since any pores or pinholes through the nickel will quickly lead to corrosion of the steel (due to galvanic coupling) and subsequent failure of the panel circulation system. A straightforward solution to the problem (i.e., using very thick nickel layers, greater than 2-mil, leads to cost penalties ($8¢/mil\text{-}ft^2$ for nickel alone).

A most important, and poorly understood, requirement for the absorber coating is the long-term durability. Candidate coatings should possess durability with respect to all reasonable environmental degradation mechanisms expected for about a 15-year life. Thermal runaway conditions of 400°F, humidity, and thermal cycling must be withstood. Long-term corrosion due to combined effects of humidity, 220°F temperatures, and dissolved carbon-dioxide and sulphur-dioxide gases must be minimal. The question of absorbing coating durability must be answered. The selection of tests to evaluate coating durability must be carefully made in order to allow meaningful extrapolation of short-term accelerated test results to predict long-term lifetimes.

The cost and optical efficiency must be tied together in analysis. Although the use of selective coatings is justified for 200°F flat-plate collectors, their cost is a significant consideration, and decisions concerning candidate coatings must be based on cost-efficiency. Examples of cost-efficiency questions which should be addressed include:

- What is the minimum nickel-coating thickness for acceptable durability?
- Is the higher emittance of coatings deposited on zinc or copper justified by the lower cost of such coatings?
- Can absorption values be further improved?

*Substrate here refers to the surface on which the absorber coating is deposited. It can be the same as the bulk substrate material or it can be a thin layer of material plated onto the bulk substrate.

Coating substrate systems which have been investigated are given in the following sketch:

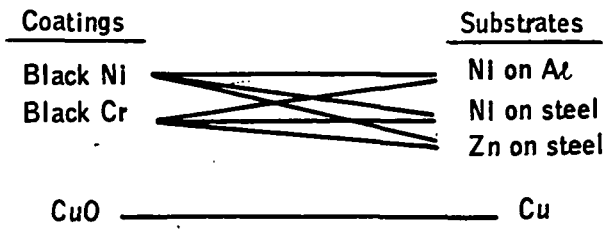

Some preliminary estimates of large-scale coating-substrates costs are shown in Figure B2. Each item is followed, in parentheses, by the estimated cost in dollars/ft^2. These costs are based on the present industrial rates and/or our estimate of the process. The estimated cost of a particular candidate coating-substrate combination can be found by adding the component costs on the diagram. For example, the estimated cost of a black Cr (0.15) coated galvanized (0.08) steel collector panel (0.30 + 0.70) would be \$1.23/ft^2.

The use of Cu as a basic panel would seem to be unlikely due to high material cost; hence, Cu may also be considered as an intermediate coating for a cheaper metal substrate, i.e., like Ni and Zn.

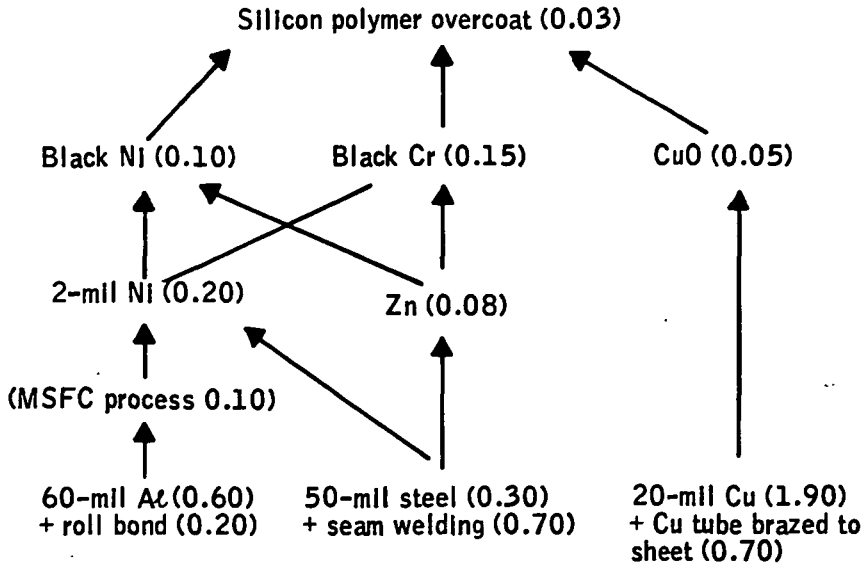

Figure B2. Preliminary Cost Estimate for Large-Scale Coating Substrates

Iron Oxide Coatings on Steel

A selective iron oxide coating (presuming a steel absorber panel), when augmented by an organic overcoat, has solar performance capability nearly equal to selective black nickel with significantly greater apparent durability and humidity resistance. The initial materials investigation for this coating is complete and the results are presented in the following paragraphs.

Iron oxide coating can be applied to steel substrates by a number of chemical and thermal processes. We have investigated primarily the Ebonol S process of Enthone, Inc. In this process the iron oxide coating is produced by immersing a steel part into the caustic Ebonol S solution, which is heated to just under the boiling point (~295°F). Auger analysis of the Ebonol coatings show that the coating is ~48 percent iron and 52 percent oxygen. Auger analysis cannot determine the compound form of the iron oxide but two possibilities are 60 percent Fe_3O_4 + 40 percent free Fe or the 90 percent FeO and 10 percent Fe_3O_4. The manufacturer claims the coating is Fe_3O_4, but apparently the composition can be changed by varying the bath temperature and concentration. The sputter-auger depth profile of the coating in Figure B3 shows a constant composition and a fairly large coating thickness.

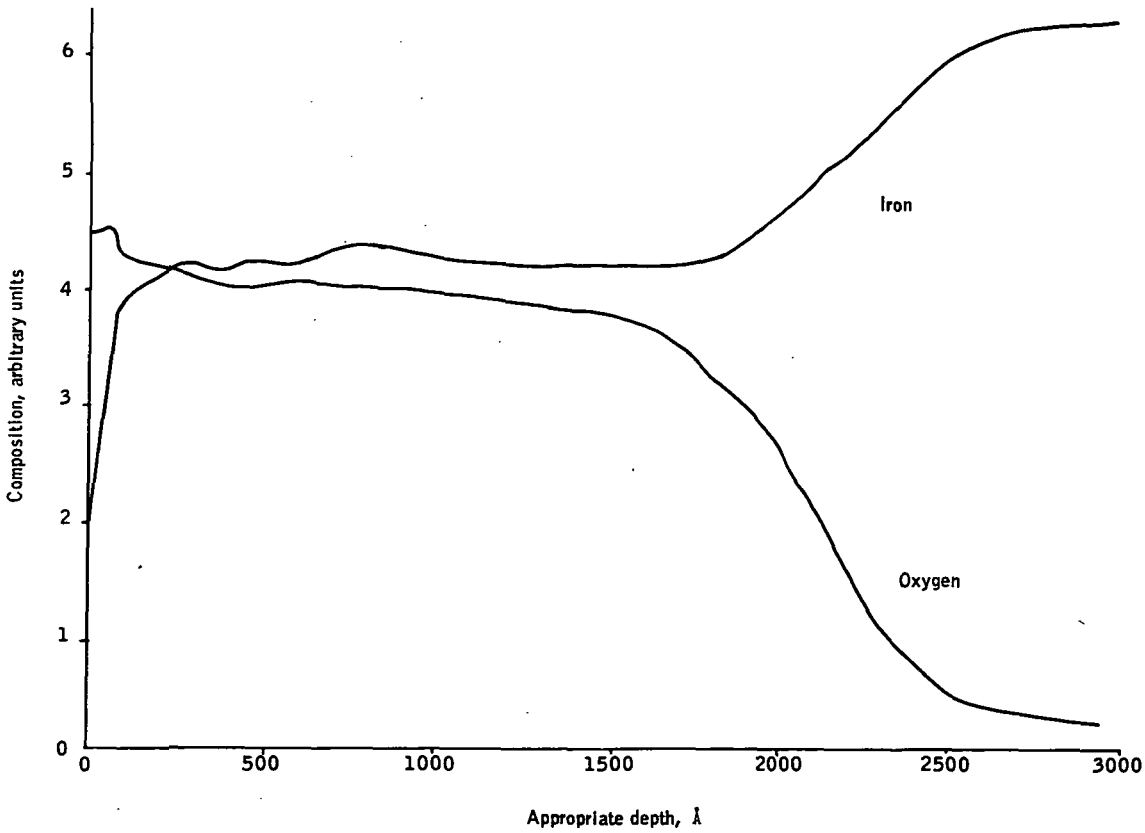

Figure B3. Sputter Auger Depth Profile of Black Iron on Steel

About 30 iron-oxide coatings were prepared during our study. The steel surface was prepared by immersion for ~10 seconds in diluted hydrochloric acid. The steel was a cold-rolled low-carbon variety which, according to Enthone, should lead to better corrosion resistance. The effect of immersion time on the spectral reflectance is shown in Figure B4. Note that the cutoff can be altered by changing the immersion time. The oscillations in reflectance for the shorter coating times are indicative of optical interference effects. This effect cannot be used to increase the average absorption over the broad solar spectral region, and coating times shorter than 2 minutes generally greatly decrease the overall absorption. The fundamental limitation is the high refractive index for the iron compounds (Fe_3O_4: 2.42, FeO: 2.32), which cause a large reflection off the front surface of the coating. As with the copper-oxide coatings, the best performance achieved, $\alpha \approx 85$ percent and $\epsilon \approx 10$ percent, is marginal, but may be improved with organic overcoats.

One steel sample with a 1-μm-thick iron-oxide coating was given the 160°F humidity test and survived with only a few points of rust. It remains to be seen whether thinner coatings of iron oxide will have sufficient humidity protection value.

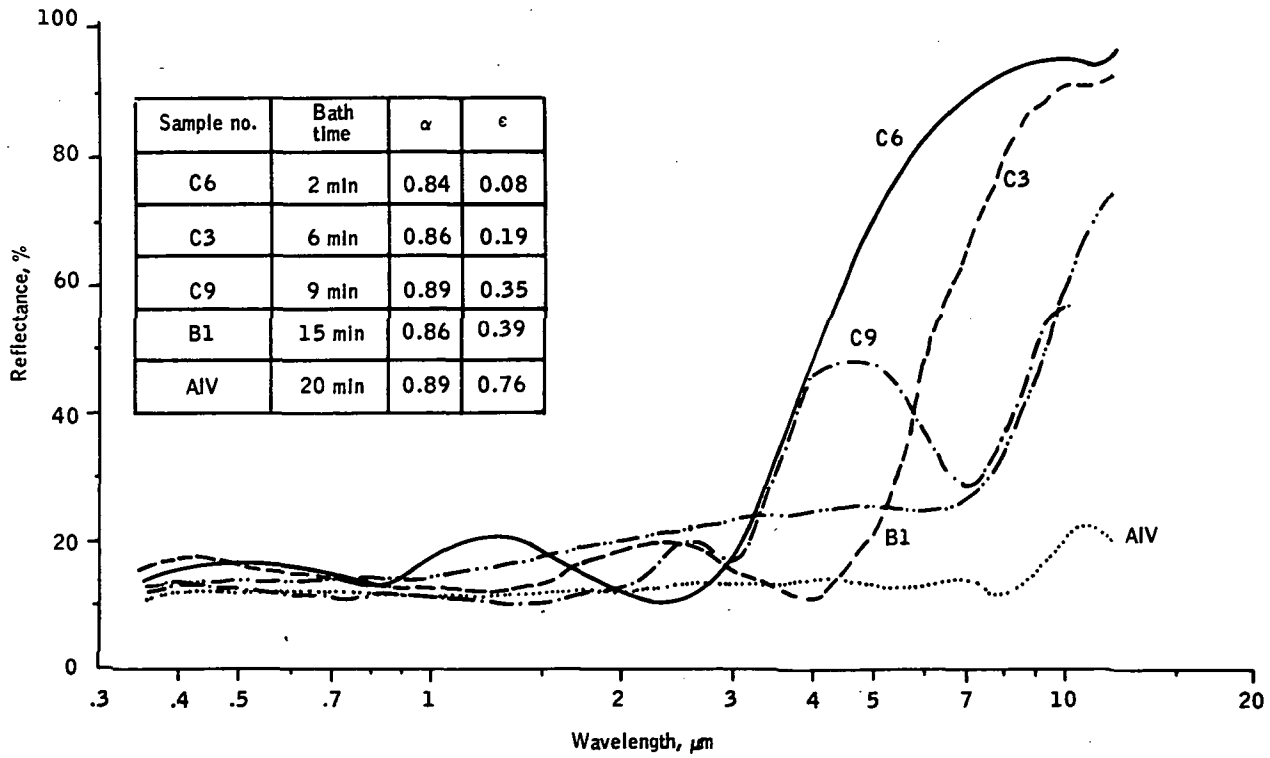

Figure B4. Effect of Immersion Time on the Spectral Reflectance of Black Iron Coating

Organic Overcoats

Overcoating solar absorbers with polymeric organic materials was originally considered as a possible means of increasing the humidity corrosion resistance of several coatings. It was later found that such coatings, in many cases, had the additional desirable effect of greatly increasing solar absorptance by reducing the mismatch in refractive index between the solar absorbing coating and air. For example, a thick organic coating with a refractive index of 1.5 could reduce the front surface reflectance of iron oxide ($n \sim 2.4$) from ~16 percent to ~9 percent.

Most polymeric organic coating materials have the disadvantage of being strongly absorbing in the 5- to 20-μm wavelength region and hence will greatly increase the emittance when coated on a selective solar absorber. Therefore, about 10 organic materials were coated onto solar absorber surfaces in thicknesses from ~0.05 mil to ~2 mil and checked for infrared absorption. Preliminary tests showed that all three of these materials completely prevent rust from the MIL-STD humidity test on iron-oxide absorber coatings in thicknesses of only 0.05 to 0.01 mil. At those thicknesses the organic overcoat has no effect on the solar coating emittance. These materials should be stable to 400°F or more.

Supplementary Discussion

Iron Oxide

The black iron-oxide test sample had an absorptance of .94 and an emittance of .17. The sample was left in the solution for 4 minutes, which was the timing determined from earlier tests to give an optimal coating. The graph of reflectance versus wavelength for this sample iron-oxide coating is shown in Figure B5.

Organic Overcoat

The organic overcoat is not only necessary to protect the iron-oxide surface, but it also improves the selectivity of the absorber coating. The two materials tested for use as an overcoat were:

- Vistalon 606 EPM, Product of Exxon Company
- XR-6-2205 Silicone, Product of Dow Corning

The material used was the EPM. This was chosen over silicone materials because of its superior durability, ease of application, and superior optical properties and clarity.

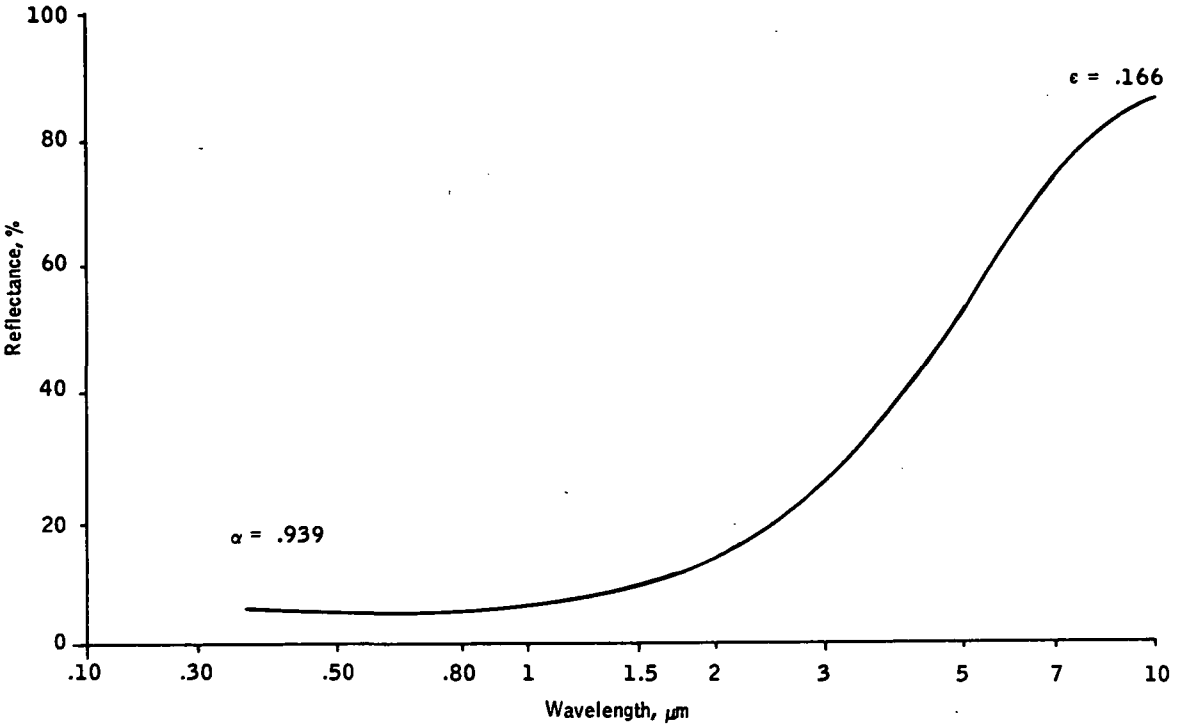

Figure B5. Spectral Reflectance of Uncoated Iron Oxide Selective Surface

The application of this material requires 20 to 30 spray coats during an 8-hour period. This is necessary to get the proper uniform thickness of 0.2 to 0.3 mil. Thicker films reduce the selectivity of the surface and thinner coatings are not as protective. MIL-STD humidity tests on the EPM-overcoated samples show no significant performance degradation to the selective surface.

Difficulties were encountered in producing a uniform iron-oxide coating on the absorber panels. The black iron coating without an organic overcoat has acceptable performance but durability requires an organic overcoat, and the overcoat tends to drive the emittance to an unacceptable level (.39). Different coating thicknesses were examined to find the optimal coating performance (i.e., highest α/ϵ). Figure B6 demonstrates the effect of immersion time. As time decreases, absorptance and emittance decrease due to the thinner coating. The organic overcoat tends to increase absorptance and emittance as shown in Figure B7. The dips in the curves in the 7-μm range are due to absorption by the organic overcoat material.

Table B1 summarizes the results for these three selective-coating reflectance curves.

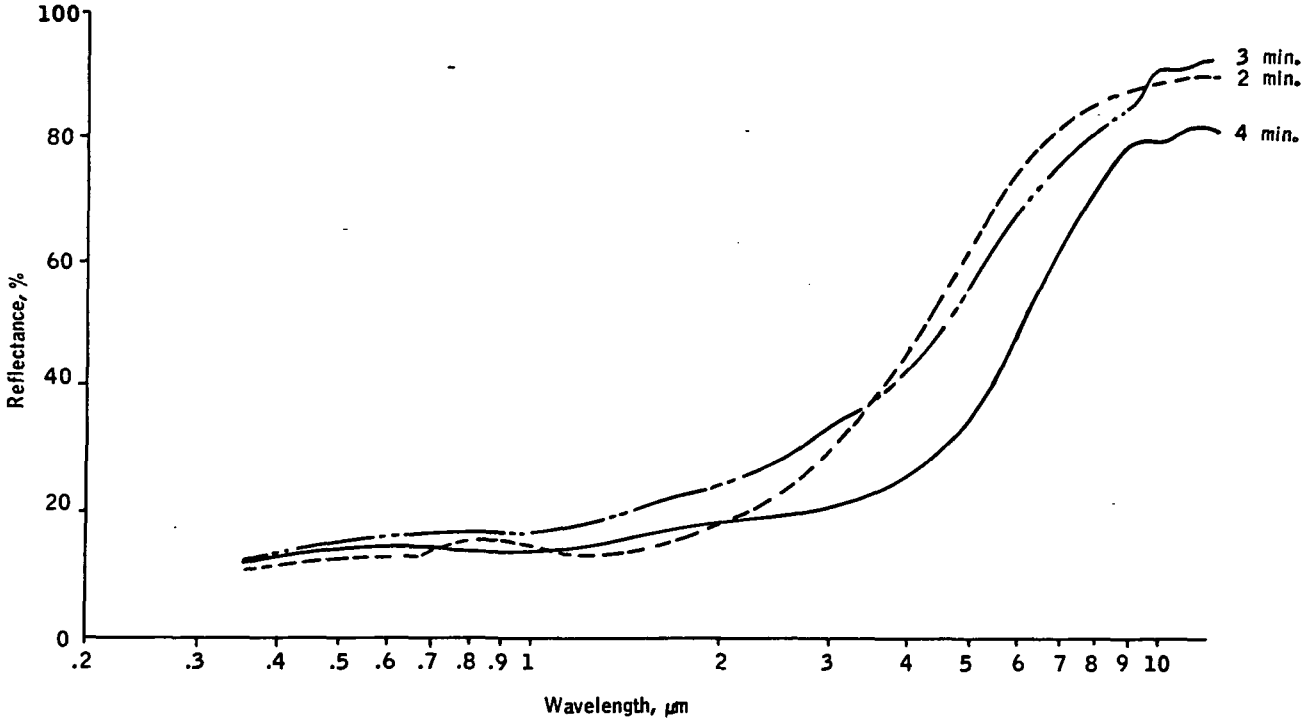

Figure B6. Reflectance of Iron Oxide Samples for 2, 3, and 4-Minute Coatings

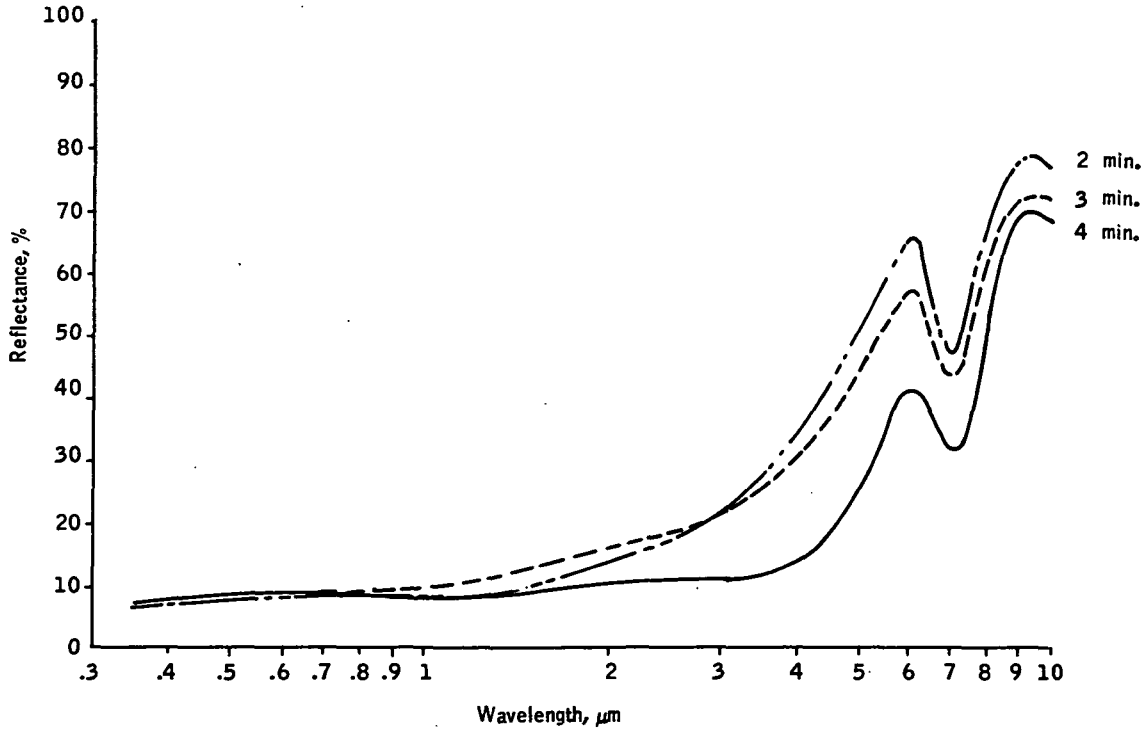

Figure B7. Reflectance of Iron Oxide Samples with Organic Overcoat for 2, 3, and 4-Minute Coatings

TABLE B1.- TEST RESULTS

Immersion time, min.	No overcoat			With overcoat		
	α	ϵ	α/ϵ	α	ϵ	α/ϵ
2	.862	.134	6.4	.912	.244	3.7
3	.859	.146	5.9	.905	.299	3.0
4	.836	.264	3.2	.916	.400	2.3

The selectivity of the 2-minute coating was the best of the test samples but was not satisfactory. A coating with an α of .90 and an ϵ of .16 was expected. To achieve this goal, a new chemical bath was mixed to ensure a clean solution and increase coating uniformity. (Prolonged boiling tends to burn solution chemicals which deposit on panels.)

Previously obtained test results have provided coatings with an α of .84 and an ϵ of .08 (α/ϵ = 10.5) before overcoating and an α of .90 and an ϵ of .16 (α/ϵ = 5.6) with a 0.3-mil overcoat.

APPENDIX C
TRADEOFF STUDIES

To more accurately evaluate some of the major design choices, such as whether to use a selective absorber coating or a nonselective absorber coating, and the choice of one cover or two collector covers, utilization curves were generated to compare the performance of the various collector types when operated for both heating and cooling for a typical year. The utilization curves indicate the expected improvement in yearly collection efficiency that can be realized from adding the more costly design features, such as a second cover. As long as the cost increase resulting from the addition of these design features is less than the performance improvement realized, the design features will be considered as viable possibilities. Utilization curves for the evaluation of a selective versus nonselective absorber coating, and the evaluation of one cover versus two collector covers are presented in this appendix.

Absorber Coating

The choice of absorber coatings will obviously be influenced by the material ultimately used for the absorber panel itself, assuming of course that a selective absorber coating is recommended for the preferred collector design. The determination of whether or not to use a selective absorber coating must be based on the cost effectiveness of each type of coating, either selective or nonselective. Application of black paint will generally be less costly than the application of either an electroplated or electroless dip process, as required by the selective absorber coatings; however, the selective absorber coatings are capable of capturing and retaining a significantly larger fraction of the incident flux, and as long as the increased application cost is less than the increased absorber performance, the selective absorber coatings will deliver more heat flux per dollar of collector cost. Furthermore, for a given energy level required to be satisfied by a solar installation, the use of selective absorber coatings will enable the use of a smaller collector array, thereby eliminating some installation cost.

To provide a guideline for determining the maximum additional cost of application that will still maintain the superior cost effectiveness of a selective absorber coating, an analysis was performed to compare the performance of a collector array over a typical calendar year of actual weather conditions, considering both a selective and a nonselective absorber coating. The results of the analysis are presented as Figure C1. The installation considered in this analysis is a 121-m^2 (1300-ft^2) array of collectors with a tilt angle of 25 degrees with respect to horizontal. The collectors have two glass covers and both edge and back insulation around the absorber panel. The nonselective absorber coating considered here is 3M Black Velvet, which has a

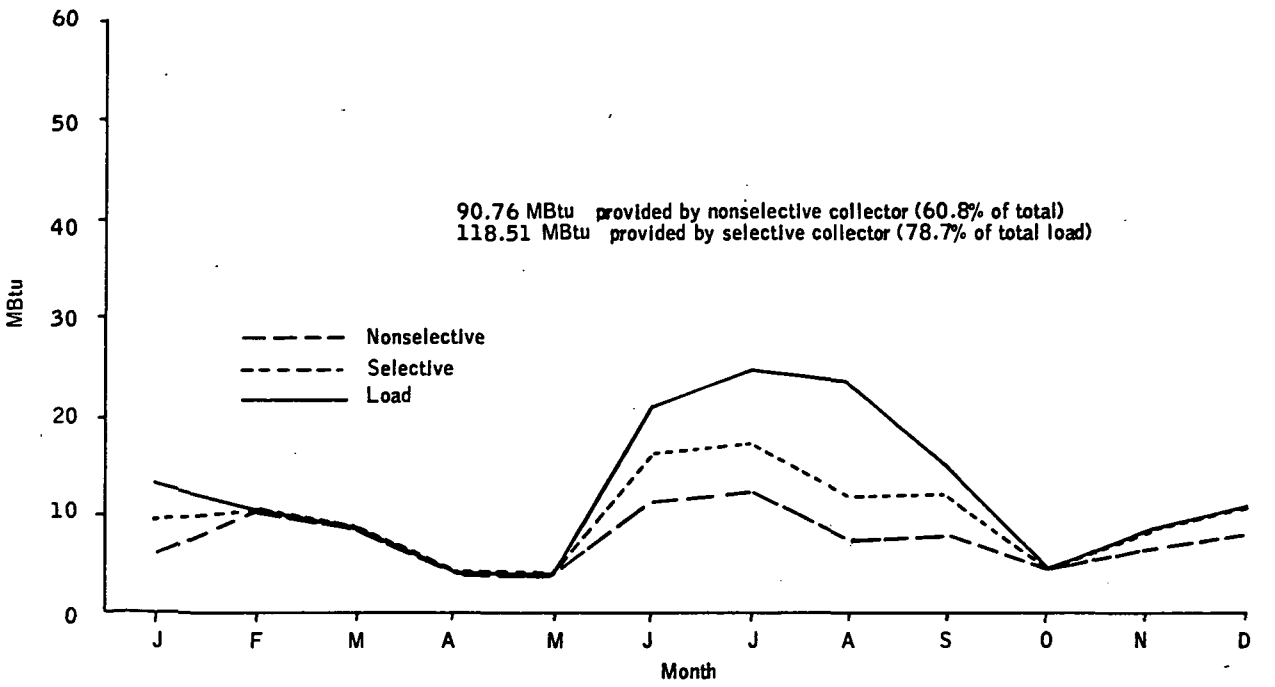

Figure C1. Comparative Performance of Selective versus Nonselective Two-Cover Collector

solar absorptivity of .95 and an emissivity of .90. The selective absorber coating considered here is black nickel, having a solar absorptivity of .94 and an emissivity of .07. The design load used for the analysis is a 232-m^2 (2500-ft^2) house of conventional construction located in Atlanta, Georgia. The load levels are derived from degree day data obtained from the U.S. Weather Bureau. The cooling load also includes the effect of humidity levels. Collector performance is calculated from an hourly analysis of weather data provided for a typical year in Atlanta, including both ambient temperature and insolation level, considering cloud cover. The load levels and collector performance levels have been summarized on a monthly basis and are presented as Table C1. Collector operation is assumed to be fixed at 60°C (140°F) for those months having no cooling load. Operation is assumed fixed at 93°C (200°F) for months having a cooling load. For months having both heating and cooling loads, operation is assumed fixed at 93°C (200°F) and the cooling load is satisfied first. In determining how much of the cooling load can be satisfied by the collector array, a coefficient of performance (COP) of .6 has been applied to the energy level supplied by the collectors. The efficiency for solar heating is assumed to be 1.0. Finally, sufficient storage is assumed to absorb the daily collected energy levels, but no energy is accrued from month to month.

TABLE C1.- ATLANTA LOAD ANALYSIS

Month	Heating load, MBtu	Cooling load, MBtu	Total load, MBtu
1	12.7	0	12.7
2	10.5	0	10.5
3	8.7	0	8.7
4	3.3	0.7	4.0
5	0.5	3.3	3.8
6	0	20.9	20.9
7	0	24.9	24.9
8	0	23.5	23.5
9	0.4	14.4	14.8
10	2.5	1.9	4.4
11	8.2	0.2	8.4
12	12.4	0.1	12.5
Total	59.2	90.0	149.2

As can be seen from Figure C1, the collector array can provide 60.8 percent of the total load requirement if it has a nonselective absorber coating, and 78.7 percent of the total load requirement if it has a selective absorber coating. This is a 17-point increase in performance directly attributable to the selective absorber coating. This is the upper limit for additional collector cost due to application of the selective coating. With this guideline in mind, it appears reasonable to conclude that a selective absorber coating will be included in the recommended collector design.

The coatings presently considered most promising are black chrome and iron oxide. They both appear significantly more durable than the black nickel coatings presently available. Black chrome samples also appear to have equivalent performance to black nickel; however, iron oxide has a lower solar absorptivity (.85) and will require an organic overcoat to raise that value above .9. This is not considered a major detriment, since iron oxide is an electroless dip process and would still be relatively inexpensive even with an organic overcoat. Iron oxide does, however, limit the choice of absorber materials to steel, while black chrome may be electroplated to steel, aluminum, or copper, assuming appropriate processing.

Cover System

The investigation of the cover system candidates required the resolution of one primary question: Should the recommended collector design have one or two covers? An analysis (Figure C2) was performed to compare the performance of both a one- and two-cover collector array. As this analysis is similar to that performed for the absorber coating evaluation, details of the approach are not repeated here. The reader may refer to the preceding absorber coating discussion to review the derivation of the figure. Tables C2 through C7 present the monthly summaries of the collection levels. The one-cover collector array can provide 71.7 percent of the heating and cooling load requirement, while the two-cover collector array can provide 78.7 percent of the load requirements. This is 7-point improvement in performance directly attributable to the addition of the second collector cover. This is the guideline for the additional cost of designing a two-cover collector. The use of a second cover not only adds the cost of more cover material, but also requires the use of a cover spacer and larger collector housing. These additional costs may well be in excess of the benefits derived from the second cover. Additional detailed cost analysis is still required in order to firmly substantiate that conclusion. It should be noted that this analysis assumes the use of a selective absorber coating for both the one- and two-cover collector configurations. A similar analysis using a nonselective absorber coating would reveal a much greater improvement to be realized by the use of a two-cover system. The additional costs of the second cover may be more justifiable.

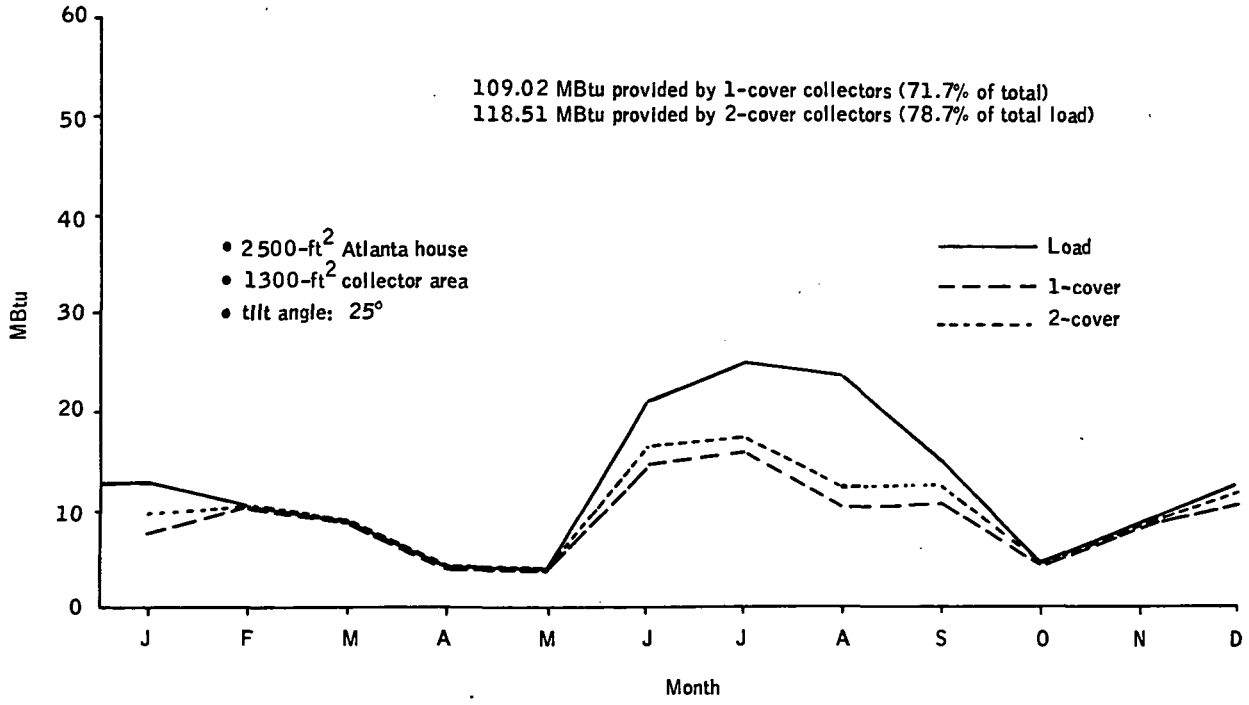

Figure C2. Comparative Performance of One versus Two Covers

TABLE C2.- ENERGY SUPPLIED BY COLLECTORS-- ONE COVER, SELECTIVE ABSORBER

Month	Energy/ft^2 of collector, Btu		Energy supplied by 1300-ft^2 array, MBtu	
	At 140°F	At 200°F	At 140°F	At 200°F
1	6191	2486	8.05	3.23
2	10 861	6115	14.12	7.95
3	20 743	12 074	26.97	15.70
4	25 349	15 298	32.95	19.89
5	27 131	16 086	35.27	20.91
6	30 078	18 616	39.10	24.20
7	31 937	20 261	41.52	26.34
8	23 081	13 093	30.01	17.02
9	22 947	13 506	29.83	17.56
10	24 377	14 877	31.69	19.34
11	12 966	7175	16.86	9.33
12	7737	3473	10.06	4.51

TABLE C3.- ENERGY SUPPLIED BY COLLECTORS-- TWO COVERS, NONSELECTIVE ABSORBER

Month	Energy/ft^2 of collector, Btu		Energy supplied by 1300-ft^2 array, MBtu	
	At 140°F	At 200°F	At 140°F	At 200°F
1	4732	1272	6.15	1.65
2	8994	4270	11.69	5.55
3	17 519	8834	22.77	11.48
4	21 892	11 515	28.46	14.97
5	23 836	12 152	30.99	15.80
6	26 998	14 493	35.10	18.84
7	28 686	15 902	37.29	20.67
8	20 254	9599	26.33	12.48
9	19 977	9988	25.97	12.98
10	21 107	10 951	27.44	14.24
11	10 882	5040	14.15	6.55
12	6002	2007	7.80	2.61

TABLE C4.- ENERGY SUPPLIED BY COLLECTORS--
TWO COVERS, SELECTIVE ABSORBER

Month	Energy/ft^2 of collector, Btu		Energy supplied by 1300-ft^2 array, MBtu	
	At 140°F	At 200°F	At 140°F	At 200°F
1	7337	3815	9.54	4.96
2	11 807	7483	15.35	9.73
3	21 565	14 647	28.03	19.04
4	25 748	17 800	33.47	23.14
5	27 210	18 656	35.37	24.25
6	29 577	20 736	38.45	26.96
7	31 352	22 156	40.76	28.80
8	23 134	15 340	30.07	19.94
9	23 228	15 661	30.20	20.36
10	24 841	17 301	32.29	22.49
11	13 707	8914	17.82	11.59
12	8739	4996	11.36	6.43

TABLE C5.- LOAD SATISFIED BY SOLAR COLLECTORS -- ONE COVER, SELECTIVE ABSORBER

Month	Operating temperature, °F	Load satisfied, MBtu
1	140	8.05
2	140	10.5
3	140	8.7
4	200	3.3 + 0.75 = 4.05
5	200	0.5 + 3.3 = 3.8
6	200	14.5
7	200	15.8
8	200	10.2
9	200	10.5
10	200	2.5 + 1.9 = 4.4
11	200	8.2 + 0.26 = 8.46
12	140	10.06
Percent of total load (Total load = 149.21 MBtu)		109.02 = 60.73 %

Note: 140°F operation assumed when there is no cooling load. 200°F operation assumed whenever there is a cooling load. A/C load satisfied first during 200°F operation. COP of .6 applied to cooling energy, 100-percent efficiency for heating energy.

TABLE C6.- LOAD SATISFIED BY SOLAR COLLECTORS -- TWO COVERS, SELECTIVE ABSORBER

Month	Operating temperature, °F	Load satisfied, MBtu
1	140	9.5
2	140	10.5
3	140	8.7
4	200	3.3 + 0.75 = 4.05
5	200	0.5 + 3.3 = 3.8
6	200	16.2
7	200	17.3
8	200	12.0
9	200	12.2
10	200	2.5 + 1.9 = 4.4
11	200	8.2 + 0.26 = 8.46
12	140	11.4
Percent of total load (Total load = 149.21 MBtu)		118.51 = 78.79%

Note: 140°F operation assumed when there is no cooling load. 200°F operation assumed whenever there is a cooling load. A/C load satisfied first during 200°F operation. COP of .6 applied to cooling energy, 100-percent efficiency heating energy.

TABLE C7.- LOAD SATISFIED BY SOLAR COLLECTORS -- TWO COVERS, NONSELECTIVE ABSORBER

Month	Operating temperature, °F	Load satisfied, MBtu
1	140	6.15
2	140	10.5
3	140	8.7
4	200	3.3 + 0.75 = 4.05
5	200	0.5 + 3.3 = 3.8
6	200	11.3
7	200	12.4
8	200	7.5
9	200	7.8
10	200	2.5 + 1.9 = 4.4
11	200	6.1 + 0.26 = 6.36
12	140	7.8
Percent of total load (Total load = 149.21 MBtu)		90.76 = 71.61%

Note: 140°F operation assumed when there is no cooling load. 200°F operation assumed whenever there is a cooling load. A/C load satisfied first during 200°F operation. COP of .6 applied to cooling energy, 100-percent efficiency heating energy.

APPENDIX D

HOUSING MATERIAL ANALYSIS

Material Test Program

During the course of the contract, certain reservations arose regarding the durability and weathering characteristics of the molded-paper-product pan. The project personnel at NASA MSFC shared this concern. Accordingly, a material test program was conducted on the molded-paper product to more accurately evaluate its potential as a collector component material. However, before discussing the test program, the following observations should be noted:

- The initial considerations for assuring acceptable physical characteristics are reviewed in the main text of this document.

- The question of flammability can apparently be resolved, at least to the extent of satisfying local building codes, by the use of additives such as powdered boron to the slurry during the pan molding process.

- The other physical characteristics of the material can be appreciably improved by impregnating it with a plasticizer. Based on initial testing and evaluation of several possible plasticizers, the most promising candidate from both a cost and performance standpoint presently appears to be EPDM (ethylene-propylene-diene material) produced by Exxon. Vacuum impregnation or dipping of this material definitely improves moisture resistance and material hardness. This process is estimated to cost $\$.65/m^2$ ($\$.06/ft^2$) and may in fact be highly cost effective.

The scope of the material test program consisted of conducting the following tests on the processed-paper box material which was used as the collector housing:

- Permeability
- Hardness
- Thermal conductivity
- Tensile strength and elongation
- Compressive strength
- Flexural strength

- Accelerated service
- Accelerated aging
- Flammability

The general nature of these tests is described below.

Permeability

Samples were impregnated with 10-, 20-, and 30-percent solids. These samples were then tested using the Contractor's Moisture Vapor Transmission Rate (MVTR) apparatus. The best level of impregnation was then determined, and the remaining tests (i.e., hardness, thermal conductivity, etc.) were performed on samples with this chosen quantity of plastic. (Several of the remaining tests are for plastic materials because the plastic-impregnated paper product is similar to plastic-impregnated glass-laminate materials.)

Other tests to determine the water resistance of paper were also considered. These methods determine the time required for water to pass through the paper-sheet material. They are ASTM D779, D1251, D895, D1276, D1008, and C355.

Hardness

The test for hardness was conducted in accordance with the requirements of ASTM D2240, which requires the use of a durometer to determine the indentation hardness of the material. This test was run for both wet and dry samples.

Thermal Conductivity

The test for determining the thermal conductivity constant was run in accordance with ASTM D2214. For this test, the sample is placed between two plates at different temperatures. The upper plate is at a constant temperature, while the temperature of the lower plate is slowly changing. The temperature difference is measured by thermocouples and the rate of heat flow is determined from the area, thickness, and temperature profile. The test was run for a dry material sample and the thermal conductivity was determined to be 0.5 Btu in/hr-ft^2-°F.

Tensile Strength and Elongation

Tensile strength was determined using ASTM Test D638 for Tensile Properties of Plastics as the guide. This test was run, for both wet and dry samples, using tensile strength testing machinery.

Compressive Strength

The modulus of elasticity was determined using test method ASTM D695. In this test, the mechanical property is found by loading the sample in compression at relatively low uniform rates. The modulus was determined for both wet and dry samples of the material.

Flexural Strength

The test method used for flexural properties was ASTM D790. In this test, a bar of rectangular cross section is tested in flexure as a simple beam, the bar resting on two supports and the load applied by means of a loading nose midway between the supports. The specimen is deflected until rupture occurs. Both wet and dry samples were tested.

Accelerated Service

The sample was tested using the MIL-STD-810B humidity test method. The test consists of temperature cycles from 82°F to 160°F and humidity cycles from 85- to 95-percent relative humidity with 24-hour cycles for 10 days.

Accelerated Aging

Tests were performed to determine the effects of light and water exposure on the sample material. The method used followed ASTM D1499 procedures for the Artificial Weathering Tests (ASTM E42).

Flammability

Tests were performed to determine the relative flammability of the plastic-impregnated paper material. Two ASTM methods were referred to for these tests. They are designated D638 and F108. The second test is a fire test for roofing materials.

The above tests are summarized in Table D1.

Material Test Program Details

The series of structural tests previously mentioned were made on the paper box material to evaluate its potential as a collector component. The box samples tested were impregnated with 10-percent Enmar plastic. This quantity of plastic was chosen as a tradeoff between material cost and comparative durability determined from humidity tests run on a series of samples having various

TABLE D1.- MATERIALS TEST MATRIX

Test	Wet	Dry	Percent solids (10, 20, 30)	ASTM standard test no.	Test title
Permeability	X		10	D779	Water resistance of paper, paperboard, and other sheet materials by the dry indicator method
Permeability	X		20	D779	
Permeability	X		30	D779	
Hardness	X			D2240	Indentation hardness of rubber and plastics by means of a durometer
Hardness		X		D2240	
Thermal conductivity	X			D2214	Thermal conductivity constant of material with Cenc-Fitch apparatus
Thermal conductivity		X		D2214	
Tensile strength and elongation	X			D638	Tensile properties of plastics
		X		D638	
Compressive strength	X			D695	Compressive properties of rigid plastics
Compressive strength		X		D695	
Flexural strength	X			D790	Flexural properties of plastics
Flexural strength		X		D790	
Accelerated service	No coating			D756	Resistance of plastics to accelerated service
Accelerated service	Painted with acrylic white			D756	
Accelerated aging	at 200°F			D1499	Operating light - and water - exposure apparatus (carbon-arc-type) for exposure of plastics
Flammability		X		D635	Flammability of self-supporting plastics
Flammability		X		E108	Fire test of roof coverings
Additional permeability tests					
1.	X			D1251	Water vapor permeability of packages
2.	X			D895	Water vapor permeability of packages
3.	X			D1276	Water vapor transmission of shipping containers
4.	X			D1008	Water vapor transmission of shipping containers
5.	X			C335	Water vapor transmission of thick materials

percentages of plastic impregnation. The plastic material used was an acrylic lacquer per MIL-L-813 produced by Enman Industrial Finishes, Wichita, Kansas.

Of initial concern was the impregnant (acrylic lacquer) and the percent of solids to be used. Solutions of 10-, 20-, and 30-percent solids were prepared using the Enmar lacquer and a suitable solvent. The samples were then impregnated as follows:

1) The samples were cut in suitable shapes and vacuum-baked at 212°F for 16 hours.

2) The samples were then cooled for a minimum of 2 hours in a dessicator.

3) The samples were next immersed in the lacquer solution, put in a vacuum chamber at room temperature, and the chamber was evacuated for 15 minutes.

4) The samples were removed from the chamber and the excess lacquer was removed.

5) The samples were air-dried at room temperature for a minimum of 4 hours.

6) The samples were then baked in an air-circulating oven at 212°F for 16 hours.

The above procedure was repeated on all lots of 10-, 20-, and 30-percent solid lacquer solution. All samples were then subjected to 10 days of temperature/humidity cycling per MIL-STD-810. At the completion of the cycling, all samples were visually inspected and a hardness reading was taken. This was done to determine the percent of solids to use in the final test series. Based on the visual inspection and hardness reading, plus the added concern of eventual high production and material costs, the 10-percent solution was selected, since in appearance and hardness there was no apparent difference in the three percentages.

Mechanical strength tests were performed on the paper-mache material. These tensile, compression, and flexural tests are all standardized and described by the American Society for Testing and Materials (ASTM) as D695, D638, and D790, respectively. ASTM Test 635 was used to test material flame resistance. In general, the ASTM procedures were followed with some modifications.

Flexural Strength Tests

Flexure strength is a measure of the force required to cause failure of a rigid material when bent (flexed). The test is performed by supporting a bar-shaped specimen (see sketch below) whose dimension has been measured at both ends and applying a steadily increasing load at the center. The specimen is flexed until it breaks. On the basis of the load required to break a specimen, the flexure strength of a material is calculated to show the force that would be required to fail a sample with cross-sectional area of 1 square inch.

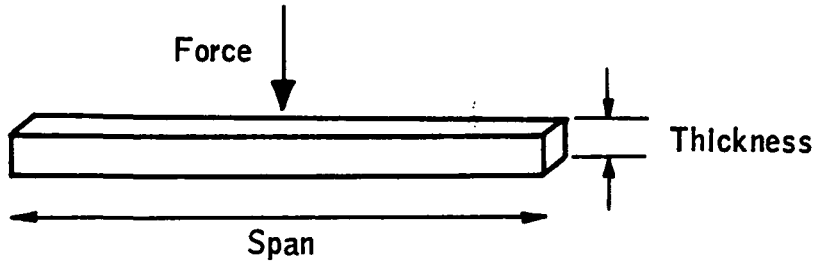

Flexure modulus is a measure of the stiffness of a material and can be determined by the formulat shown below if the amount of bending (deflection) at the center of the bar is measured.

$$\text{Flexural stress} = \frac{3}{2} \times \frac{\text{load x span}}{\text{width x thickness}^2}$$

$$\text{Flexural modulus} = \frac{(\text{span})^3 \text{ x load}}{4 \text{ width x thickness}^3 \text{ x deflection}}$$

Flexural Strength Test Results

The flexure properties of the paper box material are listed in Table D2. The flexural strength is 1640 psi which is similar to that of soft wood composition board, 34-lb/ft^3 polyethylene foam, 18 to 25-lb/ft^3 urethane foam, and low-density polyethylene. The flexural modulus of 140 000 psi implies that the material is stiffer than the above foams: more like composition board or a denser (40- to 50-lb/ft^3) foam.

The stress-strain curve for the flexural test is shown in Figure D1.

TABLE D2. - FLEXURE PROPERTIES[a]

Run	Flexural strength, psi	Flexural modulus, psi
1	1430	134 000
2	1520	
3	1740	122 000
4	1710	158 000
5	1870	155 000
6	1150	91 000
7	1560	134 000
8	1590	139 000
9	1810	160 000
10	2030	169 000
Average	1640	140 000

[a]Test notes: 4-in. span; 2-in./min. test speed; specimen dimensions 0.478 to 0.490 in. width, 0.278 to 0.348 in. thickness.

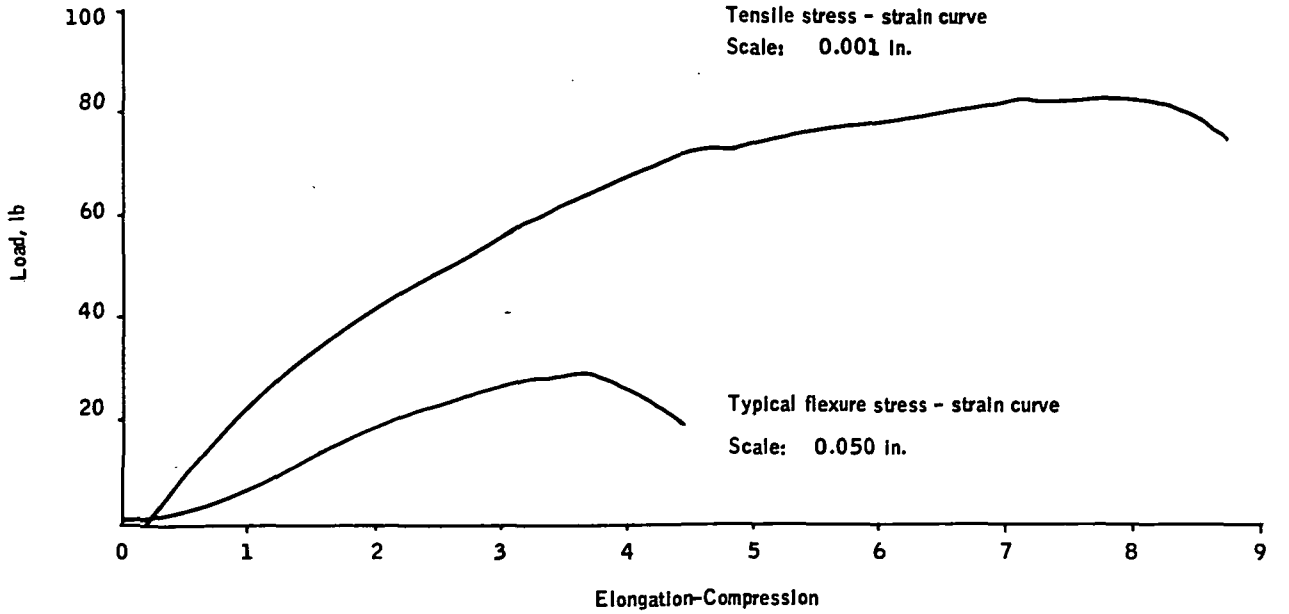

Figure D1. Tensile and Flexure Stress-Strain Curves

Tensile Tests

Tensile strength measures the force needed to pull a specimen apart. The specimen for a tensile test is generally a long, slender bar with enlarged ends to which grips for pulling are attached. The specimen for our tests did not have a special grip area but were uniform in size for their entire length.

The test is performed by measuring the cross-sectional area of the sample and pulling to failure at a designated speed. The force in pounds required to break is so calculated that tensile strength is reported as the force that would be necessary to break a specimen of the material of 1-square-inch cross-section.

The tensile modulus (stiffness) can also be determined if the amount of elongation is measured. The formula for tensile modulus is:

$$\text{Modulus} = \frac{\text{load (lb)} \times \text{specimen length}}{\text{cross-sectional area} \times \text{deflection}}$$

Tensile Strength Test Results

The test results are summarized in Table D3. The paper material has an average tensile strength of 700 psi. This is comparable to the tensile strength of the previously mentioned materials for flexural strength. Again, the modulus (145 000 psi) implies a stiffness greater than that of foams but similar to that of composition board, polypropylene, or nylon. The collector box does not encounter any tensile loading, however, so a material with high tensile strength should not be required. The tensile stress-strain curve is shown in Figure D1.

TABLE D3.- TENSILE PROPERTIES[a]

Run	Tensile strength, psi	Tensile modulus, psi
1	810	185 000
2	640	146 000
3	700	127 000
4	620	219 000
5	800	100 000
6	760	111 000
7	540	127 000
Average	700	145 000

[a]Test notes:
Specimens: Grip area same dimension as test area.
Sample size: Width 0.475 to 0.495 in.
Thickness 0.210 to 0.360 in.
Test speed: 0.050 in./min.

Compression Tests

Compression strength is a measure of the force required to push or compress a specimen until "failure" is reached. The type of "failure" may depend on the dimensions of the specimen and on the material used. Some cases will result in a shattering failure and in other cases failure will be considered as a specified deflection as the load is applied. Both of these cases were involved in the tests on the molded paper product:

- Flatwise tests -- The compressive force was applied to the thickness of the material (see sketch).

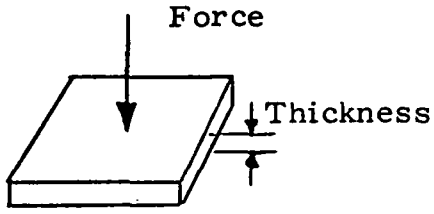

In our tests compressive strength was determined at deflections of 30 percent and 50 percent of the original thickness.

- Edgewise tests -- The compressive force was applied in a direction perpendicular to the thickness of the material of a relatively long narrow specimen (see sketch).

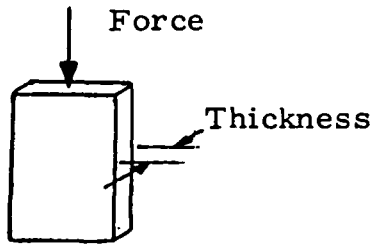

The relative stiffness (modulus) can also be determined by measuring the deflection as the load is applied:

$$\textit{Modulus} = \frac{\text{load x thickness (in direction of compressive force)}}{\text{cross-section x deflection}}$$

Compression Strength Test Results

The flatwise and edgewise compression test results are given in Tables D4 and D5, respectively. The stress-strain curves for these tests are shown in Figures D2 and D3. The compressive strength of the material is again similar to that of 34-lb/ft^3 polyethylene foam but stiffer.

An overall analysis of the material's structural integrity for use in solar collectors will be made upon completion of the entire test series. Conclusions here are limited to a comparison with other materials because the results of structural tests alone do not establish the paper product's overall durability.

Flame Test Description and Results

A 0.5-inch wide strip of the box material is cut to a length of 6 inches. The sample is held at one end and a flame is applied to the other end for 30 seconds. The flame is removed and the time required for the flame to burn to the 4-inch mark is recorded. The flame test data are summarized in Table D6.

All of the samples burned to the 4-inch mark with an average burn rate of 1.2 inches/minute. The material is therefore flammable and not self-extinguishing as many plastic materials are. Several materials with comparable burn rates are listed below:

Material	Burn Rate (inches/minute)
ABS	1.0 to 1.5
Polystyrene	1.2 to 1.5
Acrylic	1.6
Nylon	0.5

TABLE D4. - FLATWISE COMPRESSIVE PROPERTIES[d]

Run	Compressive strength, psi		Linear modulus, psi
	30% defl.[a]	50% defl.[b]	
1	470	1310	15 300
2	495	1540	15 800
3	540	1660	17 200
4	350	960	10 800
5	325	885[c]	10 200
Average	435	1270	13 900

[a]Stress-strain - linear.

[b]Beyond yield point.

[c]Very rough surface.

[d]Test notes:
Sample size = 1 in. x 1 in.
Thickness = 0.322 to 0.361 in.
Test speed = 0.050 in./min.

TABLE D5. - EDGEWISE COMPRESSIVE PROPERTIES[a]

Run	Compressive strength, psi	Modulus, psi
1	600	23 500
2	510	23 000
3	670	34 300
4	700	35 500
5	700	38 200
6	590	29 500
7	---	35 100
Average	630	31 400

[a]Test notes:

Test speed: 0.05 in./min.

Sample size: Width = 0.300 to 0.061 in.
Thickness = 0.500 ± 0.007 in.
Length = 1 in ± 0.013 in.

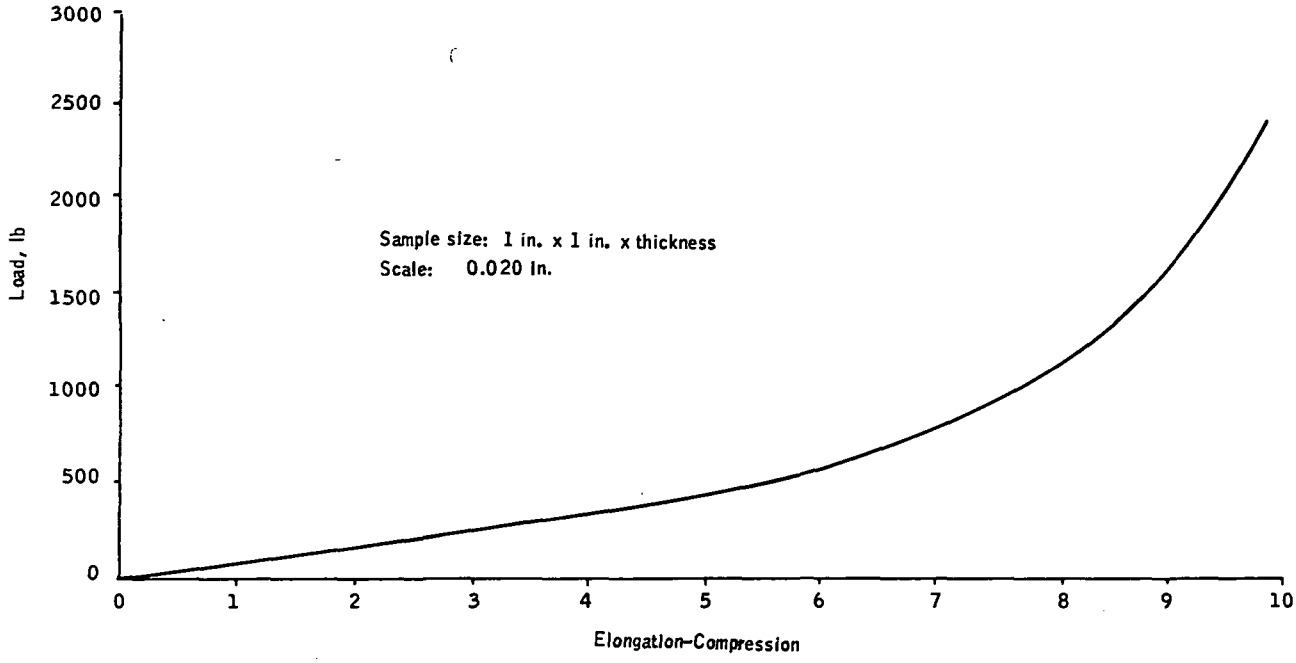

Figure D2. Stress-Strain Curve for Flatwise Compression Test

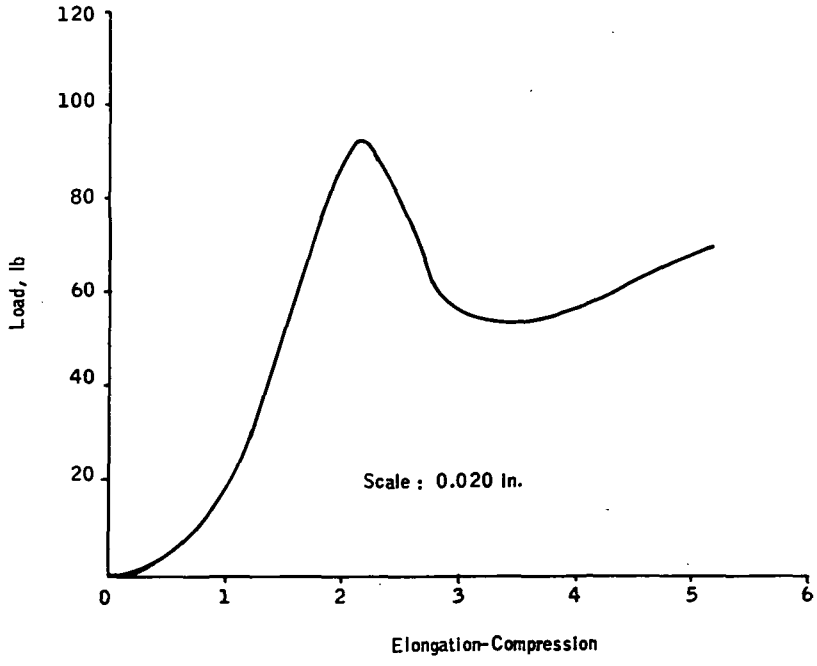

Figure D3. Stress-Strain Curve for Edgewise Compression Test

TABLE D6. -FLAME RESISTANCE[a]

Run	Seconds to burn 4 in.
1	206
2	187
3	201
4	205
5	186
Average	197

[a]Sample dimensions: 6 in. x 0.5 in. x thickness.

A flame retardant may be added to the paper slurry prior to molding. This should significantly reduce the material's flammability to be at least self-extinguishing, if not inflammable.

Box Material Analysis

The effect of MIL-STD-810 Procedure 1. accelerated humid environment, was determined by measuring the flexural and compressive strength of paper mache with and without impregnation before and after exposure. This environment was originally developed to simulate exposure to a warm, highly humid atmosphere such as is encountered in tropical areas. This is an accelerated environmental test, accomplished by continuous exposure to high relative humidity at elevated temperature. These conditions impose a vapor pressure on materials which constitutes a driving force behind the moisture and penetration. Moisture-sensitive materials may deteriorate rapidly under humid conditions. Absorption of moisture by materials may result in swelling, which destroys their functional utility and causes loss of physical strength and changes in other important mechanical properties. Insulating materials which absorb moisture may suffer degradation of their electrical and thermal properties.

The accelerated humidity environment shown in Figure D4 essentially consists of exposure where the internal chamber temperature is raised from ambient to 71°C (160°F) and 95 percent RH over 2 hours and is maintained under these conditions for 6 hours. A slow cool takes place over the next 16 hours while maintaining the chamber above 85 percent RH. The cycle repeats for a total of 10 days.

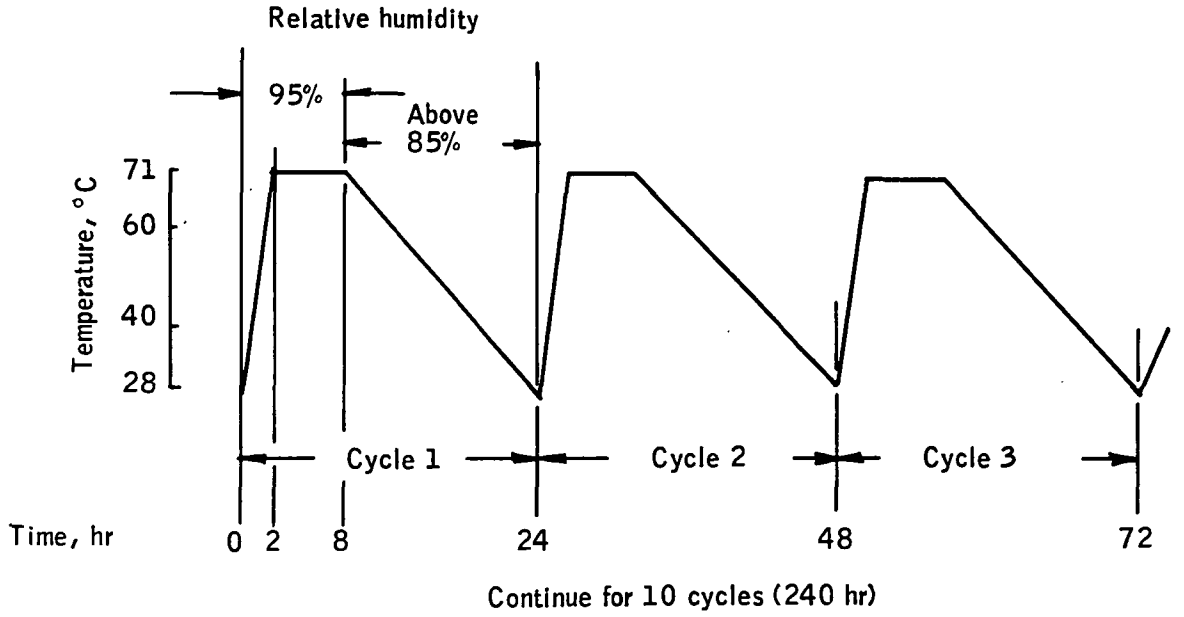

Figure D4. Humidity Cycle for Procedure I

The results of exposure to the accelerated humidity environment are summarized in Table D7. Examination of the data from Table D5 shows that impregnation has a beneficial effect in increasing the strength of the molded paper product as expected. The anomalies observed for the edgewise compressive modulus data are being rechecked. In general, impregnation increased the strength of the molded paper product by 11 percent or more before exposure and improved the relative advantage to 47 percent or more after humidity exposure. Molded paper product with and without impregnation showed significant reduction in strength after humidity exposure. As expected, unimpregnated molded paper product lost more strength as a result of humidity exposure than did the impregnated material.

TABLE D7.- RESULTS OF MIL-STD-810 HUMIDITY EXPOSURE ON MOLDED PAPER PRODUCT

Parameter	Before humidity exposure		After humidity exposure	
	No impregnation	With impregnation	No impregnation	With impregnation
Compressive strength, psi (flatwise):				
30% deflection	440	510	65	170
50% deflection	1270	1630	425	770
Compressive modulus, psi (flatwise)	1390	1580	300	440
Compressive strength, psi (edgewise), to failure	630	700	85	190
Compressive modulus, psi (edgewise)	30 800	4620	2870	8820
Flexural strength, psi	1640	1460	150	450
Flexural modulus, psi	149 000	65 000	10 900	16 500

[a]MIL-STD-810, Procedure 1.